Master of Science Thesis

Intensity Modulated Proton Therapy (IMPT) -A comparative treatment planning study

Malin Ericsson

Supervisors:
Per Nilsson and Per Engström

Department of Radiation Physics,
Lund University Hospital

Medical Radiation Physics
Clinical Sciences, Lund
Lund University, 2007

Cancerbehandling med protonstrålning – en dosplaneringsstudie

Cancer är i dagsläget en av de vanligaste dödsorsakerna i Sverige och rädslan av att drabbas finns hos många. I massmedia avlöser nya rön varandra. Det som igår skulle motverka uppkomsten av en cancertyp anses idag vara orsaken till en annan. Förvirringen som uppstår av alla råd och begränsningar gör oss rädda, rädda för ett öde vi inte kan styra. Sökande efter nya och bättre metoder att bota eller lindra sjukdomen görs på många ställen i världen. Detta arbete är en jämförande studie mellan befintliga strålbehandlingstekniker och en, för Norden, ny kommande strålbehandlingsteknik.

Personer som drabbats av cancer kan behandlas på flera olika sätt. Den vanligaste metoden är kirurgi, där den sjuka vävnaden avlägsnas, kompletterat med antingen strålbehandling (radioterapi) eller cellgifter. Strålbehandling utförs normalt med energirika röntgenstrålar, en tät ström av så kallade fotoner. Den höga energin krävs för att fotonerna ska kunna ta sig in i kroppen och slå ut tumörcellerna. Oftast används flera strålar från olika vinklar, och energi avlämnas längs hela strålvägen genom kroppen. Mest energi deponeras precis i början, efter bara någon centimeter in i kroppen. Efter det avtar energin som deponeras per längdenhet med djupet. En större deponerad energimängd innebär en större sannolikhet för celldöd, oavsett om det är friska eller sjuka celler. Då en strålbehandling planeras är den viktigaste uppgiften att koncentrera energideponeringen till själva tumören och välja vinklar på så sätt att strålkänsliga organ undviks.

För bara något år sedan började en ny teknik inom strålterapin med fotoner användas på Lunds Universitetssjukhus, **I**ntensitets**M**odulerad **R**adio**T**erapi (**IMRT)**. Varje strålfält delas upp i många mindre fält. För varje litet fält anpassas intensiteten (intensitetsmodulering) beroende på hur sträckan genom frisk vävnad fram till tumören ser ut, m.a.o. hur djupt det är till tumören i just den vinkeln och huruvida tumören är täckt av ett strålkänsligt organ eller ej. Genom att göra detta för alla strålar i alla vinklar kommer mindre energi att deponeras till strålkänsliga organ samtidigt som tumören får den stråldos som föreskrivits. Många bieffekter, så som muntorrhet vid bestrålning i huvud-hals området, kan på så vis minskas eller undvikas helt.

Det är inte bara fotoner som används i strålbehandling, även de partiklar som bygger upp atomer (elektroner, protoner och neutroner) kan produceras med höga energier och användas i dessa sammanhang. Till år 2010/2011 kommer ett nationellt protonterapi-center i Uppsala att tas i kliniskt bruk för cancerbehandling. Då protonen kommer in i kroppen avger den relativt lite energi per längdenhet och denna deposition ökar något ju längre in i kroppen protonen når. Efter flera centimeter bromsas protonen kraftigt in och den maximala energideponeringen sker strax innan den stannar helt. Denna kraftigt ökande energi-avgivning kallas för Bragg-toppen. Vävnad belägen bakom Bragg-toppen kommer inte att påverkas av bestrålningen och vävnaden framför kommer, i de flesta fall, inte erhålla lika höga doser som vid fotonbestrålning. Syftet med detta arbetet är att jämföra proton-behandlingsplaner utförda med IMRT teknik med traditionella fotonplaner samt med fotonplaner med IMRT tekniken. Resultatet blev i alla de studerade patientfallen en minskad dosbelastning till normala vävnaden, vilket är positivt ur biverkningssynpunkt. I de flesta fallen erhölls också en bättre dosplan med protonerna med lägre doser till speciellt strålkänsliga organ s.k. riskorgan.

1 Abstract

Purpose: To study Intensity Modulated Proton Therapy (IMPT) with a new treatment planning optimization software. The aim was also to make a comparative study between existing conventional photon plans, Intensity Modulated X-ray Therapy (IMXT) plans and IMPT plans for three different cancer diagnoses.

Materials and methods: The conventional photon plans and the IMXT plans were optimized in Oncentra MasterPlan (OMP) version 1.5 by Nucletron (Nucletron B.V., The Netherlands). The IMPT plans were optimized using Orbit Workstation version 1.0 developed by RaySearch (RaySearch Laboratories, Sweden). The IMPT software in Orbit was at the time of this study not clinically released.
Three different cancer diagnoses with a total number of seven patients were used, three patients with mammary carcinoma, two with prostate cancer and two with cancer of the parotid. The optimization parameters such as number of beams and beam angles were based on trial and error attempts guided by different publications. Other settings such as number of segments and iterations had already been clinically evaluated and were therefore kept within these limits.
The evaluation and comparison of the treatment plans were performed in terms of physical quantities based on Dose Volume Histograms (DVH), target dose uniformity, Radiation Conformity Index (RCI) and Equivalent Uniform Dose (EUD) for both targets and Organs At Risk (OARs) and the Irradiated Volume (IV).

Results: In the left sided mammary carcinoma cases, with the ipsilateral lung and the heart as the primary OARs, the IMPT technique rendered the best treatment plans with improved target dose uniformity and RCI. The EUD-values for the left lung and the heart was decreased and the irradiated volume was reduced on average by 24 % compared with the conventional plans and 28 % compared with the IMXT plans.
In both prostate cases the doses to the primary OARs, the rectum and the bladder, revealed only small differences between the three treatment techniques. The EUD-values for both targets and OARs, target dose uniformity, RCI and irradiated volume differed only slightly.
In the third diagnose, cancer of the parotid, the IMPT plans were superior to both photon techniques. Target dose uniformity, RCI and irradiated volume were improved with the IMPT technique. Furthermore, all delineated OARs received a significantly lower dose and hence a lower EUD than obtained with any of the photon plans.

Conclusions: All treatment plans produced with intensity modulated protons resulted in equal or better target dose uniformity with smaller irradiated volumes compared with both the conventional and the IMXT technique. Dose reductions with the IMPT plans were clearly seen in structures located at a distance from the target and not in the primary beam track. Results from this study suggest that the IMPT technique is most suitable for tumors of the head and neck, a region with many critical structures, even though the treatment plans in the mammary carcinoma cases also were improved considerably with the IMPT technique.

2 Table of contents

3 Abbreviations

CGE	**C**obalt **G**ray **E**quivalent
CTV	**C**linical **T**arget **V**olume
DVH	**D**ose **V**olume **H**istogram
EUD	**E**quivalent **U**niform **D**ose
gEUD	**g**eneralized **E**quivalent **U**niform **D**ose
GTV	**G**ross **T**arget **V**olume
IM	**I**nternal **M**argins
IMPT	**I**ntensity **M**odulated **P**roton **T**herapy
IMRT	**I**ntensity **M**odulated **R**adiation **T**herapy
IMXT	**I**ntensity **M**odulated **X**-ray **T**herapy
MeV	**M**ega **e**lectron **V**olt
MLC	**M**ulti **L**eaf **C**ollimator
NTCP	**N**ormal **T**issue **C**omplication **P**robability
PTV	**P**lanning **T**arget **V**olume
RCI	**R**adiation **C**onformity **I**ndex
SF	**S**urviving **F**raction
SM	**S**etup **M**argins
SQP	**S**equential **Q**uadratic **P**rogramming
TCP	**T**umor **C**ontrol **P**robability

4 Introduction

There are several ways to fight abnormal growth in tissue depending on the specific type of tumor and its location. The most common treatments are surgery, radiotherapy, and chemotherapy or combinations of these methods. In Sweden 30% of all cancer cure is obtained by radiotherapy [1], and in 2001 47% of all cancer patients were treated with radiotherapy at some time during their treatment period [2]. Radiation therapy today plays an important role in both curative and in palliative tumor treatment. Several new highly complex techniques are being implemented in radiotherapy making the future role of radiotherapy increasingly important.
Medical treatments with radiation began at the end of the 19th century, only a few years after Wilhelm Conrad Roentgen's discovery of x-rays on November 8, 1895 [3]. Nowadays, in traditional radiation therapy x-rays are still used and is also the most common type of radiation in a medical context. The techniques in radiotherapy have evolved during the century and new methods have been developed, all with the same goals, i.e. to concentrate the dose to the target tissue and spare as much as possible of the healthy organs and tissues. The dose to normal tissue must be minimized while delivering a high dose to the target. Despite the new advanced technologies in radiotherapy there is still a need to improve radiation treatment methods. The persisting problem with considerable doses to the tumor surrounding tissues is due to the characteristics of the interaction process of photons in matter. Primary photons are attenuated exponentially and they do therefore not have a finite range. This is the major reason for significant doses to normal tissue, even with the most advanced delivery technique.

The advantage of protons over photons for use in radiotherapy is their well defined range and the relatively small lateral scattering. The proton is a subatomic particle with a positive charge of one fundamental unit (u). Its rest mass is $1.6726231 \cdot 10^{-27}$ kg, i.e. approximately 1800 times the mass of an electron [3]. From the depth dose curve of high energy protons it can be seen that the maximum energy from the protons is released within a certain range at the end of the track, see Figure 5.1. This absorption peak is called the Bragg peak. It is owing to these characteristics together with a relatively sharp penumbra that radiation treatments with protons have acquired high expectations, above all with consideration to the organs at risk.

In Sweden a national proton therapy center located in Uppsala is in a planning/purchase phase and it is expected to be ready for patient treatments in early 2011. This new center will be provided with electromagnetically scanned proton pencil beams with the possibility of controlling the intensity of the proton beam at every point in the patient. This modality is called Intensity Modulated Proton Therapy (IMPT) [4].
The advantage of more precise dose distributions can be seen from two perspectives. It can either be utilized for sparing the tissues outside the target volume while maintaining the probability of tumor control. It can also be used to maintain the dose to the normal tissue and increase the dose to the tumor. In most practical cases the aim is somewhere in between. Almost every conventional treatment plan has the target well covered with dose but this is at the expense of considerable doses to the healthy tissue. Therefore, for natural reasons, the main task is to spare the surrounding tissue from unnecessary

radiation while keeping, or in some cases even increasing the target dose. After all, the most serious complication is failure to cure.

To ensure an optimal dose distribution in the patient the delivery of the treatment is always preceded with a thorough treatment planning process. The aim of the present work is to compare dose distributions produced with photon and proton beams. The comparison study is performed by constructing treatment plans with intensity modulated photons and intensity modulated protons for some typical diagnoses. Quantitative comparisons between these dose distributions in the volumes of interest were compared. Both the IMPT-plan and the IMXT-plan were analyzed and compared with the existing conventional photon plan that the patients were actually treated with. Dose volume histograms (DVH) are used for this purpose condensing the physical 3D dose distribution into a 2D distribution of dose vs. volume. The DVHs give information on target dose uniformity and the dose distribution in the surrounding tissues.

An attempt to evaluate the biological effect of the produced plans was made by calculating normal tissue complication probability (NTCP) and tumor control probability (TCP). The equivalent uniform dose (EUD) [5] was also calculated in order to compare the biological effect of the different plans. The comparative study was performed on three different diagnoses: mammary carcinoma and prostate cancer, the most common types of cancer in women and men, respectively, and parotid cancers where traditional photon plans often yield non-optimal results.

5 Proton therapy

5.1 History of the proton

The proton is a subatomic particle, a nucleon, which in Greek is spelled *πρῶτον* and means “first”.
The proton was discovered by Ernest Rutherford in 1918. It was during one of his experiments, shooting alpha particles into nitrogen gas, when he discovered signs of hydrogen nuclei in the scintillation detector. The only place the nuclei could have originated from was the nitrogen gas and on that basis he made the conclusion; nitrogen must contain hydrogen nuclei.

5.2 Proton interaction with matter

When a proton penetrates through matter it ionizes particles and deposits energy along the track at the expense of its own energy. The energy of the protons is lost by interactions with the surrounding media, mainly from Coulomb interactions with electrons, but also from bremsstrahlung and nuclear interactions [6]. The absorbed dose in matter is proportional to the number of ionizations, or energy imparted per unit length (keV/μm), called the Linear Energy Transfer (LET).

LET of charged particles in a medium is hence a measure of the energy deposited per unit length and is defined as:

$$LET = \frac{dE}{dl}$$ **Equation 5.1**

where dE is the average energy locally imparted to the medium by a charged particle of specified energy in traversing a distance of dl (ICRU 1962) [7]

High LET radiation results in more cells being killed per Gy. As the energy of the proton decreases, the interaction cross section and the stopping power will increase. With no energy left of the primary protons the deposited energy is also zero. Consequently this means an increasing energy deposition with increased depth until the protons eventually stops. The entrance dose is relatively low followed by a rise to a high dose region and then a very steep dose fall-off to zero, as can bee seen in Figure 5.1. This phenomenon was first observed in 1903 by the physicist William Henry Bragg and is now referred to as the Bragg peak after its discoverer [8].

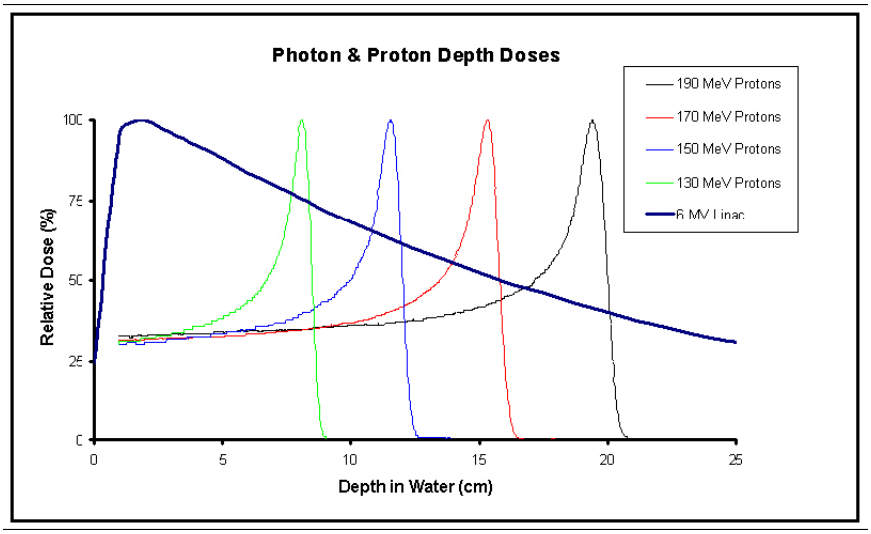

Figure 5.1 Proton depth dose curves for different energies with the characteristic Bragg peak in comparison with a 6 MV photon beam depth dose curve [9].

Due to the large mass difference between the proton and the atomic electrons, the proton proceeds through tissue in an almost straight line. With a mass of approximately 1800 times the electron, interactions with atomic electrons will only lead to small deviations from its path. Proton beams therefore have a relatively sharp penumbra in comparison to photon beams, although the penumbra increases with depth.

The depth of the Bragg peak depends on the initial energy of the proton beam, where increasing energy results in an increasing penetration depth. To manage to cover the entire depth of the target with an appropriate dose, the energy, and thus the range of the

protons, must be precisely modulated to cover a spectrum of energies. This technique is called the Spread-Out Bragg Peak (SOBP). The SOBP can be realized with e.g. a special rotating wheel with varying thickness (range modulator wheel) positioned in the proton beam that gradually slows down the protons within a specific energy range and thus modulated the initial energy of the protons [10]. These techniques are discussed in more detail in chapter 5.6

5.3 Proton therapy history

In 1929 Ernest O. Lawrence invented the cyclotron (for which he received the Nobel Prize in 1939) and made it possible to accelerate nuclear particles to very high velocities [11]. The first working cyclotron from 1929 is shown in Figure 5.2. In a scientific article from 1946, Lawrence's protégée, Professor Robert Rathbun Wilson, first proposed the theory of radiation therapy using accelerated protons [12]. Previously, cancer treatment with particles and ions had been limited due to the capacity of the accelerators, but with the new high-energy accelerators they became of therapeutic interest. Wilson discussed the advantage of concentrating high doses in the target utilizing the Bragg peak and how this could spare the surrounding healthy tissue [12].

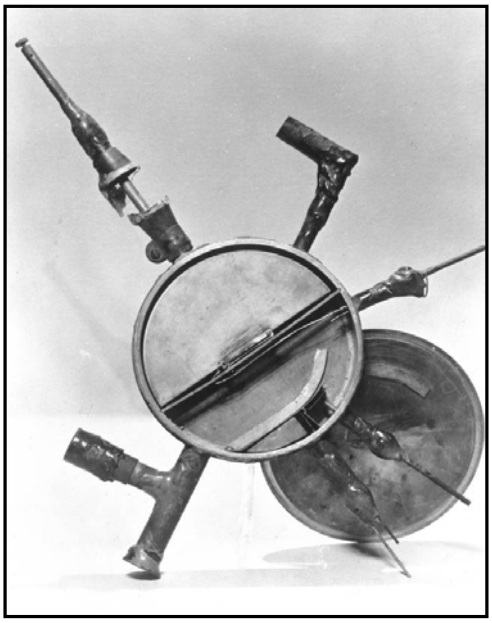

Figure 5.2 The first working cyclotron from 1929 with a diameter of 5 inches producing 80 keV protons.

These predictions made by Wilson were confirmed two years later, in 1948, by researchers at the Lawrence Berkeley Laboratory [13]. At the same laboratory the first proton therapy treatment was later performed on patients with hormone sensitive breast cancer with metastases. The purpose was to target the pituitary gland (hypophysis) and to prevent it from producing hormones stimulating the cancer growth. The reason for choosing this particular patient group was mainly the ease to resolve the structure of the pituitary gland on the x-ray films at that time.

In Sweden the first proton therapy treatment was carried out in Uppsala in 1957 using a broad beam and the spread-out Bragg peak technique.

In 1961 the Harvard Cyclotron Laboratory (HCL), in which Wilson was involved in the design, started collaboration with Massachusetts General Hospital (MGH) with the aim to pursue clinical proton therapy. It was shut down in 2002 and had by then treated 9,116 patients. The first hospital based proton therapy clinic in the United States was constructed in 1990 at Loma Linda University Medical Center (LLUMC), in Loma Linda, California [3]. A synchrotron producing 250 MeV protons were used, designed and constructed by Fermilab.

Today proton therapy is performed in several countries around the world, as can be seen in Table 5.1.

Table 5.1 An overview of all proton treatment facilities with corresponding numbers of treated patients [14].

WHO	WHERE	DATE FIRST TREATMENT	DATE LAST TREATMENT	RECENT PATIENT TOTAL	DATE OF TOTAL
Berkeley 184	CA USA	1954	— 1957	30	
Uppsala (1)	Sweden	1957	— 1976	73	
Harvard	MA USA	1961	— 2002	9116	
Dubna (1)	Russia	1967	— 1996	124	
ITEP, Moscow	Russia	1969		3833	July-05
St. Petersburg	Russia	1975		1281	May-05
Chiba	Japan	1979		145	April-06
PMRC (1), Tsukuba	Japan	1983	— 2000	700	
PSI (72 MeV)	Switzerland	1984		4182	July-05
Uppsala (2)	Sweden	1989		418	Jan-06
Clatterbridge	England	1989		1372	Dec-06
Loma Linda	CA USA	1990		10324	July-05
Louvain-la-Neuve	Belgium	1991	– 1993	21	
Nice	France	1991		2861	July-05
Orsay	France	1991		2805	Dec-06
iThemba LABS	South Africa	1993		475	May-05
MPRI (1)	IN USA	1993	– 1999	34	
UCSF - CNL	CA USA	1994		632	June-04
TRIUMF	Canada	1995		98	July-05
PSI (200 MeV)	Switzerland	1996		230	July-05
H. M. I, Berlin	Germany	1998		604	July-05
NCC, Kashiwa	Japan	1998		300	Oct-04
Dubna (2)	Russia	1999		318	July-05
HIBMC, Hyogo	Japan	2001		617	May-05
PMRC (2), Tsukuba	Japan	2001		656	June-05
NPTC, MGH	MA USA	2001		1167	July-05
INFN-LNS, Catania	Italy	2002		82	Oct-04
WERC	Japan	2002		19	Oct-04
Shizuoka	Japan	2003		195	July-05
MPRI (2)	IN USA	2004		21	July -04
(WPTC) Wanjie	China	2004		33	June-06
			TOTAL	**42766**	

5.4 Production of high energy protons

The most common isotope of hydrogen is a single proton. The protons are produced by chemical interactions often between hydrogen gas and some other substance to create a hydrogen ion, i.e. the proton. These isotopes, accelerated in cyclotrons, synchrocyclotrons or synchrotrons [15], are utilized for proton therapy treatments. Figure 5.3 shows a model of how a synchrotron can be designed. After acceleration the protons are directed into one of the treatment rooms via a beam line. A disadvantage with a cyclic accelerator is the considerable size. The implementation of a dedicated medical proton therapy clinic is a huge project which often requires new, specially adapted buildings.

Figure 5.3 A model of how a synchrotron can be designed [16]

A cyclotron uses a constant magnetic field to bend the charged particle into a circular path and a constant electric field to accelerate the particle up to about 250 MeV. In a synchrocyclotron one of these parameters, the magnetic or the electric field, is varied while in a synchrotron both parameters can be varied. In a cyclic accelerator the maximum energy that can be imparted is limited by the strength of the magnetic field and the minimum radius of the particle path. A so called isochronous cyclotron can only produce protons of constant energy since the magnetic and the electric fields are fixed, whereas the synchrotron can generate beams of varying energies.
The major differences between cyclotrons and synchrotrons are [4]:

- The cyclotron gives a continuous flow of protons while a synchrotron delivers a pulsed beam. However, this difference is probably of no significance from a clinical point of view.
- The cyclotron only produces a constant proton energy, which will be the maximal available energy. All energy modulations must therefore be performed outside the accelerator in a unit for energy degradation and will result in an undesirable production of neutrons. In contrast, the energy modulation of the synchrotron allows proton energy variation between every single pulse.

- In a cyclotron 20%-30% of the accelerated protons collide with the internal structures and results in undesirable neutron production. The synchrotron uses a magnetic beam deflector and no physical range modulator and has almost no energy loss.
- A synchrotron is larger than a cyclotron.

5.5 A modern proton center

In a proton therapy center, like the one shown in Figure 5.4, a beam-line distributes proton beams to several proton gantries in different treatment rooms. Because the preparation of the patient before the treatment takes a relative long time compared with the total treatment time it is possible to have one accelerator that delivers beam to several treatment rooms.
At the Loma Linda University Medical Center (LLUMC) Los Angeles up to 1000 patients are treated per year [17].

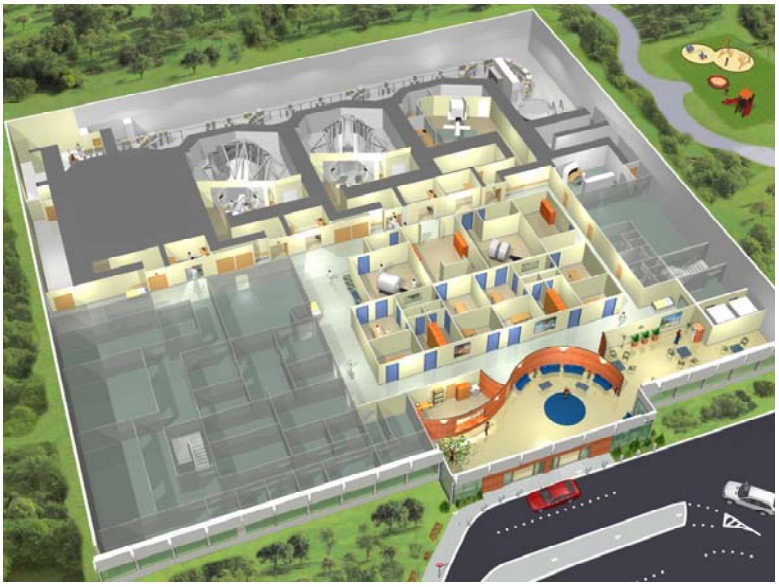

Figure 5.4 Schematic drawing of a proton therapy center (from IBA)

5.6 How to deliver a homogenous dose distribution to the target

Since the beam of monoenergetic protons mainly delivers its energy during a very narrow interval (within the Bragg peak) at the end of the track, there is a need to increase this interval in order to obtain a homogenous dose distribution encompassing the entire target. Thus the range (energy) of the protons has to be modulated. This is commonly done by inserting automatic range shifting plates into the beam [18]. The exact construction of the modulation plates differs between vendors and can consist of a rotating stepped absorber, a ridge filter or a spiral ridge filter [6]. The range shifts usually occur in discrete steps

(typically 5 mm) that will result in a Spread-Out Bragg Peak (SOBP), illustrated in Figure 5.5, in order to create a homogeneous dose to an extended volume.

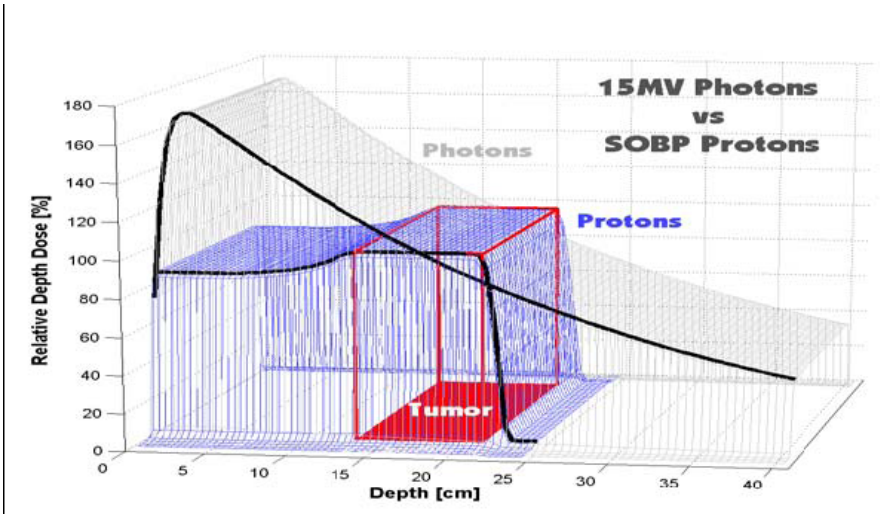

Figure 5.5 Illustration of spread out Bragg peak compared with 15 MV photon beam [8]

To cover the target in the lateral direction, the spread of the beam can be performed by either a passive scattering technique or a scanning technique. In the passive scattering method the protons are passing through high atomic scattering foils. The dose distribution shows a Gaussian fluence profile after a single scattering foil and therefore, to create a more homogeneous flux and large field sizes, a technique with double scattering foils is often used [6]. The conformation of the dose to the distal edge of the tumor is performed with customized compensators while the lateral conformation of the dose is achieved by individually shaped collimators. The main disadvantage of the passive scattering technique is that the conformation of the dose to the proximal edge of the tumor is often not optimal (see Figure 5.6)

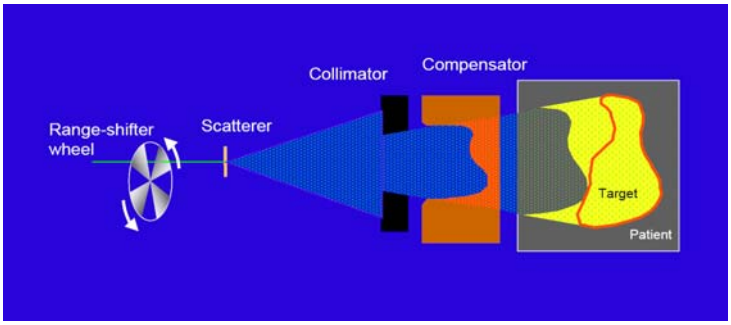

Figure 5.6 Illustration of passive scattering [Tony Lomax, AAPM summer school, 2003]

The principle of the scanning method is to scan the proton pencil beam over the target volume and is illustrated in Figure 5.7. By magnetic deflection the proton beam is swept over and conformed to the entire target. Different scanning techniques exist such as spot scanning and raster scanning.

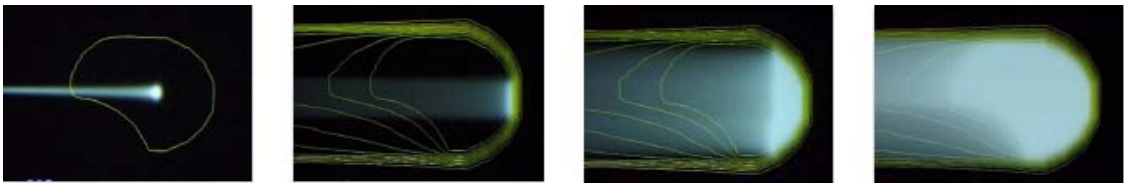

Figure 5.7 Illustration of the dose build up using spot scanning technique [4]

6 Intensity Modulated Radio Therapy

6.1 IMRT

Intensity Modulated Radiation Therapy (IMRT) is a new treatment technique being implemented worldwide. The first paper on the IMRT concept was published by Brahme et al. (1982) [19]. The clinical implementation of the technique has, however, taken a long time. IMRT is usually performed with photons but the aim is to apply it to the proton beams in the upcoming national proton center in Uppsala. When talking about intensity modulated photons the abbreviation is IMXT where the X stands for x-ray and the same theory is applied on IMPT where P stands for proton.

The superiority of IMRT compared to conventional techniques is the ability to create three dimensional high dose regions shaped to conform closely to an irregular target, especially targets with a concave surface. Structures close to or curved around the target structure can, thanks to the steep dose gradients, receive lower dose distributions compared with what would be the case with conventional treatment plans. Instead of using fixed beam intensity as in conventional radiation treatments, the beam intensity is modulated. The modulation occurs in small segments to fit the tumor structure and to avoid healthy tissue. Basically this results in an increasingly intensity for the rays that primarily reach the target and a decrease in intensity for those rays penetrating through healthy tissue. Several beams from different angles are often required to obtain a satisfactory result.

The first thing to do in IMRT planning is to select a number of beams, suitable beam angles and beam energy/energies. A number of dose limitations, i.e. objectives or constraints, are applied to the target and normal tissue structures. These functions can either be based on physical indices such as absorbed dose or radiobiological indices like TCP and NTCP. Because of lack of reliable statistics in the biological data the plans are most often made with physical indices. This is followed by an automatic optimization, which is an iterative process with algorithms searching for the most optimal solution of each beam's intensity map using inverse planning methods. The optimization is guided by the objectives and limited by the constraints. To find acceptable beam angles, several trial and error attempts must normally be made or, nowadays, a gantry angle optimization

can be used to simplify the process. The optimization will be done by determination of the best intensity map for each beam or weights of field segments. The planner must decide whether the plan is acceptable or not.

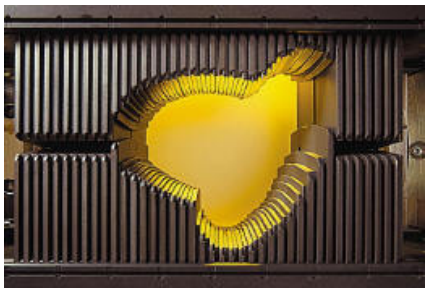

Figure 6.1 An MLC composed by several tungsten leaves. [21]

In IMXT every segment is created by a multi leaf collimator (MLC), which consists of a large number of leaves made of tungsten, a highly absorbing material [20], see Figure 6.1. Each leaf can be more or less independently positioned to create a large variety of shapes for field openings.
There are two possible ways to deliver an IMRT field using the MLC; dynamic mode or step-and-shoot technique. With the dynamic methods the leaves are moving continuously during the entire radiation process. With the step-and-shoot technique the radiations stops every time the leaves change position.
In IMPT the segments are created by the scanning method, mentioned in section 5.6 and illustrated in Figure 5.7

6.2 Optimization algorithms in general

IMRT is a very powerful tool for improving radiation therapy and where inverse planning techniques help the planner to find an optimal treatment plan with the aid of an optimization algorithm. Inverse planning requires an optimization algorithm able to best meet the many plan objectives set up by the user.

The optimization algorithm consists of two parts; first the objective function working as a link between the clinical criteria, objectives or constraints, assigning some scores to every plan. The second part is to minimize (or maximize) the objective function to find the global minima, illustrated in Figure 6.2. The functionality of the optimization algorithm is basically to measure the feasibility of a selected plan.

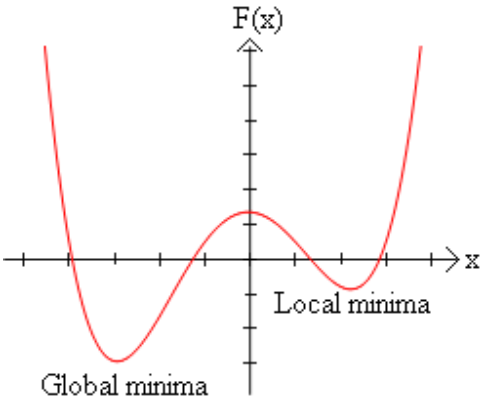

Figure 6.2 An example of an objective function, polynomial of degree 4, with the local minima at the right and the global minima at the left.

The objective function can either be based on dose-volume distribution i.e. the interaction between radiation and matter called accurate dose, or it can use radiobiological indices. The latter model is based on the biological effect from the dose distribution given to the specific tissue, in order to maximize TCP and to keep NTCP within a reasonable level. However, this is not widely implemented in clinical systems primarily due to the lack of reliable input data in the radiation-biological model. For dose-volume based optimization algorithms the objective function should consist of physical criteria; the prescribed target dose, dose homogeneity in target and maximum dose or dose-volume criteria to organs at risk.

There are mainly two types of iterative algorithms designed to calculate the global minimum of the objective function of the optimization: the stochastic and the

deterministic approach. A stochastic algorithm relies on random samplings and one method is called *simulated annealing*. This algorithm uses the theory of the gradually decreasing temperature of a thermalized system reaching the ground state.
At each iteration the ray or the weight of the beamlet is slightly changed with varying magnitude, either positive or negative. Every change is being evaluated with a point system and if the score decreases the change will be accepted. On the other hand, if the score increases, the system will not automatically reject the change, instead it will be accepted with a probability of $e^{\Delta F/kT}$ where ΔF is the change in score, k is the Boltzmann's constant and T is the parameter representing the "temperature" in this stage. This is to manage escape from local minima (see Figure 6.2), by accepting changes that actually result in a worse dose distribution the risk of getting stuck in a local minima decrease. At the beginning the "temperature" is relatively high, to provide the search after the global minima in the entire function, or find a good approximation to it. The "temperature" gradually decreases during the process and limits the search space for the solution i.e. the probability of accepting large score changes decreases.
The other optimization algorithm is the most common one. It is a deterministic iterative method based on dose differences or dose ratios. A deterministic algorithm will always behave predictable, with a given input the output will always be the same. Generally an iterative methods starts with an initial qualified "guess" and the solution will then be found by successively improved approximations. In dose planning optimization, the solution at each iteration will be updated based on the difference between the dose *achieved* and the dose *prescribed* (the objective) to each volume. This method is faster than simulated annealing but it is programmed to find the closest minimum and can not escape from a local minimum because of this. One example of this optimization algorithm is the gradient method in which the solution will be updated along the gradient of the objective function.

Apart from iterative methods and simulated annealing there are several other optimization algorithms that can be used in inverse planning systems, such as filtered backprojections, genetic algorithms, maximum likelihood approaches, linear performance etc [22]. The most common of these algorithms is, as stated before, the iterative method.

6.3 The Oncentra MasterPlan optimization algorithm for IMXT

The optimization algorithm of Oncentra MasterPlan is based on dose or dose-volume based objective functions. There are five different dose and dose/volume-based objectives associated with a relative weight factor; minimum dose, maximum dose, minimum dose-volume, maximum dose-volume and uniform dose.
The algorithm is developed by RaySearch Laboratories for solving general nonlinear problems and is a sequential quadratic programming (SQP) algorithm.
By constructing a quadratic problem using the first derivative and an estimate of the second derivative from an initial set of variables, the problem can be solved by quadratic programming and approximates the problem locally. The solution of the local problem decides in which direction a line search is to be performed. The line search in turn evaluates different step lengths to find the optimal one. For every evaluation of step lengths, a simplified 3D dose computation is required. To keep the number of evaluations

as low as possible a combination of heuristics and various polynomial approximations of the collected data points is used by the line search function.
In Knöös et al. [23] the average PTV doses in treatment plans optimized in Oncentra MasterPlan (OMP) with the pencil beam algorithm are compared with Monte Carlo (MC) calculations. In prostate cases OMP produced plans which are within ± 1% of the MC calculations. In the head and neck region OMP is 3.3% (6MV) and 3.2% (18MV) higher than the MC and for the breast cases the difference between OMP and MC are 0.9% (6 MV) and 2.3% (18MV). The differences are small and the dose distribution can be considered as fairly accurate.

6.4 The Orbit Workstation optimization algorithm for IMPT

The values of each bixel for each proton energy in each beam are the optimization parameters and they are simultaneously optimized. The value of each bixel is used as a kernel weight during optimization and the total dose is obtained by summing all weighted kernels for all energies and beams. The current dose calculation method used is a kernel based singular value decomposition algorithm (SVD) which is faster and more memory efficient than algorithms that use full kernels. The SVD dose computation algorithm may be used for heterogeneity compensation based on the CT values and their correlation to proton ranges and stopping power values. However, in the current version of Workstation heterogeneities are not accounted for. Development and implementation of a refined pencil beam dose calculation algorithm with heterogeneity corrections is presently being done.

7 Biological effects and models

7.1 RBE

Different types of radiation with equal physical dose do not result in the same biological effect. To relate biological effects from different types of radiation the *relative biological effectiveness* (RBE) is used. The RBE translates the dose for different types of radiations that give rise to the same biological effects. The unit used when the dose is weighted with the RBE factor is often CGE which is an abbreviation of "cobalt gray equivalent".

To estimate biological effects of a given dose, meaning the same damage independent of radiation type, the RBE factor is multiplied with the given dose and a dose with the unit CGE is received. The definition of RBE is:

$$RBE = \frac{dose\_of\_reference\_radiation}{dose\_of\_test\_radiation} \quad [24] \qquad \textbf{Equation 7.1}$$

where ^{60}Co is used as reference radiation.

Protons have similar biological effects as photons and much of the knowledge from photon therapy (especially fractionation) can thus be applied to proton therapy [6]. High

energy protons have a slightly higher RBE than megavoltage (MV) photon beams (having RBE=1) and an RBE value of 1.1 is typically used for clinical proton beams. The dose received from a proton beam will thus result in more damage than the same dose received from a photon beam.
Since the LET of protons increases with depth so will also the RBE factor. According to some studies the RBE value varies between 1.1 (at the entrance of the beam) and as much as 1.6 (at the Bragg peak) [6]. If this is the case, the effective range of the particles will increase by a few millimeters compared to the physical range. This may have significant effects on treatments and particularly on organs at risk close to the target structure although this effect is seldom taken into account at today's proton treatment centers.

7.2 Equivalent Uniform Dose (EUD)

Equivalent uniform dose is a radiobiologically weighted dose value. It is the single dose value calculated from an inhomogeneous dose distribution that would result in the same biological effect as if it was given uniformly to an organ or a structure [20].
The concept of EUD was introduced by Niemierko in 1997 [25]. He claimed that if the equivalent uniform dose was given uniformly to a tumor it would lead to the same cell kill in the volume as the corresponding non-uniform dose distribution. The theory is based on the knowledge that a tumor contains a large number of clonogens. During irradiation of tumor cells, the random killing of the clonogens is described by the Poisson distribution [25]. The tumor response depends on the amount of surviving clonogens. If the actual dose distribution is expected to result in the same number of surviving clonogens, the biological effect will be the same [25]. At first this was only stated for tumors volumes but was later also applied to normal tissues and called "a generalized concept of Equivalent Uniform Dose", gEUD [26].
The concept of gEUD was basically the same as in the earlier publication but "the generalization" was obviously an equation based on other parameters. In the first publication, only adapted to tumors, the equation was based on the surviving fraction (SF) and the Linear Quadratic (LQ) model. In the later and generalized form it was based on a tissue specific, unit-less parameter, $\boldsymbol{a}$. The gEUD theory is based on the knowledge of the architecture of an organ and the value of $\boldsymbol{a}$ describes whether the structure is serial, parallel or as most commonly, a combination of both types. For tumors, $\boldsymbol{a}$ is negative and for organs at risk $\boldsymbol{a}$ has a positive value.
The seriality describes the volume and dose distribution dependence of an organ.
An organ can be considered as a volume divided into small sub-volumes. In a serially arranged volume the sub-volumes act as a "chain gang" and are very dependent of each other. Just a few of these volumes need to be damaged to develop the organ injury, i.e. the organ has in this case a small volume dependence. If the organ instead is parallel all the sub-volumes are independent of each other and the organ is strongly volume dependent. A large number of the sub-volumes need to be damaged to eradicate the functionality of the organ. The concept can be resembled to electrical circuits with N components connected either in series or parallel.
For serial organs the gEUD is close to the maximum dose value in the organ while in parallel organs it corresponds more to the physical mean dose [20]
The generalized equation to calculate gEUD for both tumors and normal tissue, according to Niemierko, is:

$$EUD = \left(\frac{1}{N} \sum_i d_i^a \right)^{\frac{1}{a}}$$ **Equation 7.2**

Equation 7.2 requires evenly distributed dose calculation points.
With non-uniformly distributed dose calculation points and with voxels only partial included in a ROI, the modified equation is written as

$$EUD = \left(\sum_{i=1}^{N} v_i d_i^a \right)^{\frac{1}{a}}$$ **Equation 7.3**

where N is the number of bins (sub-volumes) in the structure of interest and $\boldsymbol{d_i}$ is the energy deposited in every bin $\boldsymbol{i}$ in the histograms. The $\boldsymbol{a}$-value is an empirical tissue-specific parameter. $\boldsymbol{v_i}$ is the volume in every bin $\boldsymbol{i}$ containing the dose $\boldsymbol{d_i}$.

THE A-VALUE
For $a < 1$, cold spots result in large effects on the gEUD i.e. lower doses are given higher weight, which hence refers to control of tumors.
For $a = 1$ hot spots and cold spots are equally weighted and the gEUD corresponds to the mean dose. a-values close to 1 are typical for parallel arranged normal organs such as liver and lung.
For $a > 1$ hot spots lead to large effects on the gEUD, higher doses are given higher weight. This corresponds to tissues of serial structures such as the spinal cord.
Illustrations of gEUD as a function of the parameter $\boldsymbol{a}$ are shown in Diagram 7.2 based on a DVH for bladder shown in Diagram 7.1.
For

$a = \infty$	gEUD is equal to the maximum dose
$a = -\infty$	gEUD is equal to the minimum dose
$a = 1$	gEUD is equal to the arithmetic mean of the dose
$a = 0$	gEUD is equal to the geometric mean of the dose

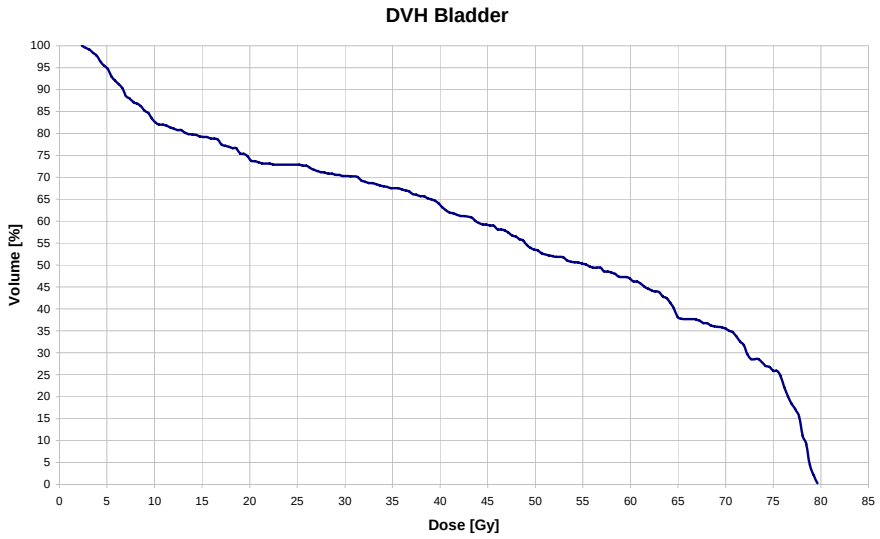

Diagram 7.1 Example of a DVH for OAR bladder used as input to a calculation of *gEUD*

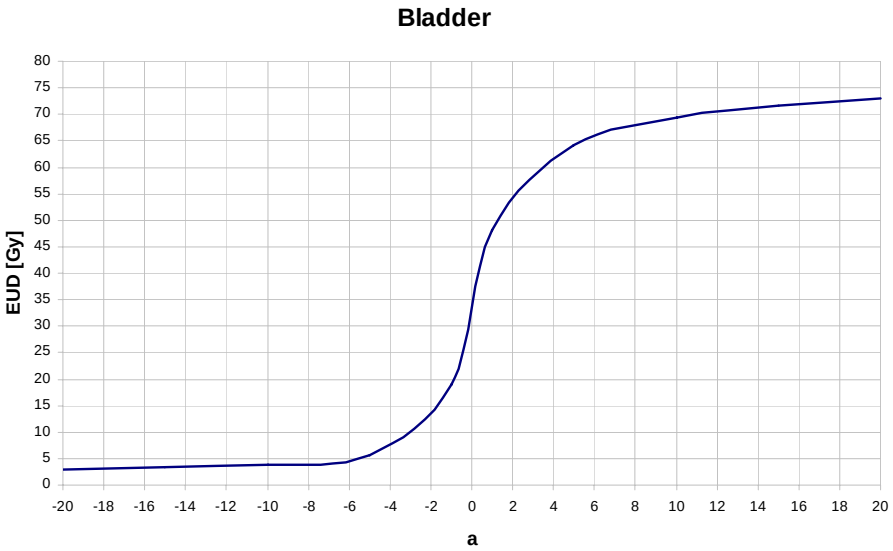

Diagram 7.2 gEUD as a function of the parameter a for the DVH in diagram 7.1

The gEUD theory is convenient to use when comparing different treatment plans and the effect of different treatment techniques. Depending on tissue type and structures, cold- and hotspots can be of crucial importance.

The input data for the model are derived for 2 Gy fraction schedules and this should be considered in the calculations by using an equivalent dose, EQD_2, derived from the Biological Effective Dose (BED) model

Equation 7.4

$$BED = D_i\left(1+\frac{d_i}{\alpha/\beta}\right)$$

where d_i is the dose per fraction and α/β is a ratio characteristic for a given type of tumor or normal tissue. The EQD_2 with the dose 2 Gy per fraction can then be described by:

Equation 7.5

$$D_i\left(1+\frac{d_i}{\alpha/\beta}\right)=EQD_2\left(1+\frac{2}{\alpha/\beta}\right)\Rightarrow EQD_2=D_i\frac{\alpha/\beta+d_i}{\alpha/\beta+2}$$

8 Basic information on the cancer diagnoses studied

8.1 Breast cancer

Breast carcinoma is the most common form of cancer in women. Approximately 25% of all cancers diagnosed in women are breast carcinoma.
In 2004 almost 7000 women in Sweden were diagnosed with breast cancer, see Diagram 8.1. This means on average, 19 women are diagnosed each day. The risk of breast cancer increases with age. Fifty percent of the women are over 64 years of age when they are diagnosed and 5% are under 40 [27]. In most cases surgery is the primary treatment form. Radiation therapy, chemotherapy or hormonal therapy can either be a complement to surgery or it can constitute the primary treatment. The prognosis of cure is dependent on the clinical stage of the breast cancer. In 1999, the 10-year relative survival rate in Sweden was estimated to be 74%.

Side effects of radiotherapy
There are several organs close to the breast that may lead to different complications as a consequence of the radiotherapy. Irradiation of the lung may induce pneumonia and secondary lung cancer. Secondary malignancies may also be induced in the contralateral breast if irradiated. Muscle stiffness and fibrosis can also develop in the chest wall and the humeral head. The risk of late cardiac complications from left-sided breast cancer radiotherapy requires that the dose to the heart is kept as low as possible.

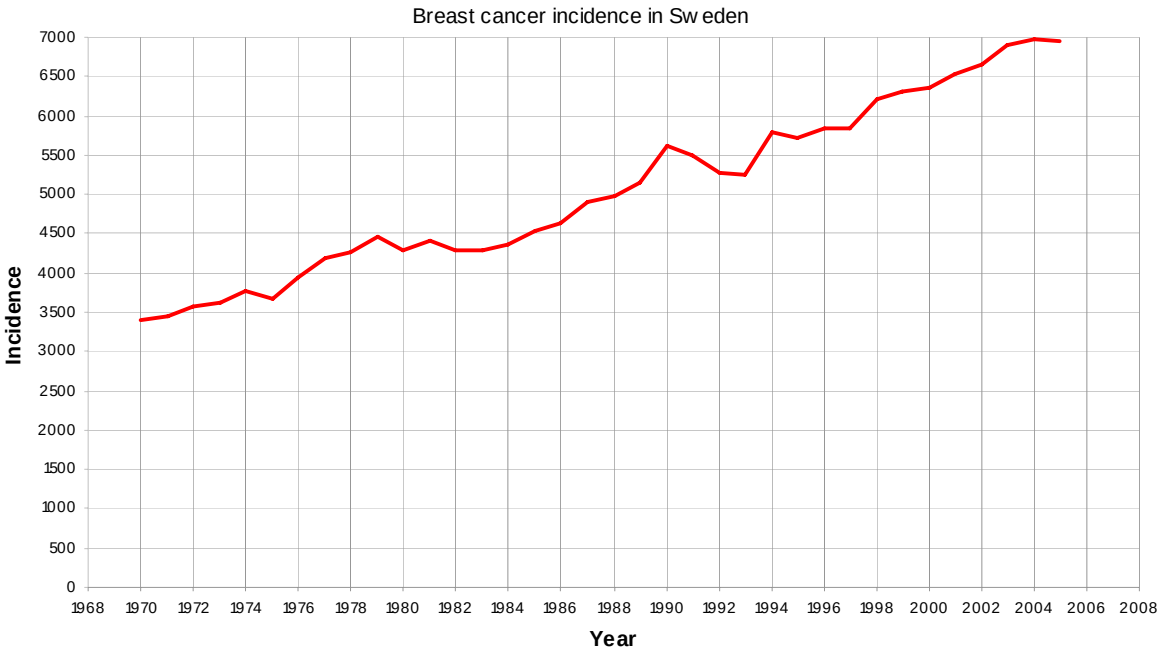

Diagram 8.1 The breast cancer incidence in Sweden from 1970 to 2004 [Swedish cancer registry, national board of health and welfare]

8.2 Prostate cancer

Prostate cancer is the most common type of cancer among men. In Sweden more than one third of all men diagnosed with cancer today have prostate cancer. The risk of getting prostate cancer increases with age and two thirds of the prostate cancer patients are over 70 years of age [28]. Diagram 8.2 shows the cancer incidence in Sweden. In 2004 almost 10 000 men were diagnosed with prostate cancer.

Prostate cancer can be treated with surgery, radiotherapy, hormone therapy, chemotherapy or combinations of these therapies. Radiotherapy can be performed with brachytherapy and/or with external beams. The choice of treatment depends on the stage of the disease, the size of the prostate and the prostate-specific antigen (PSA) value. The PSA is a protein produced by cells in the prostate gland and the value is often elevated in patients with prostate cancer or other prostate disorders.

Radiotherapy side effects

The most important organs at risk are the rectum and the urinary bladder. The known possible long term complications from conventional photon radiation therapy of the prostate are rectal bleeding, hematuria (the presence of blood in the urine), urethral stricture (internal damage to the urethra) [29].

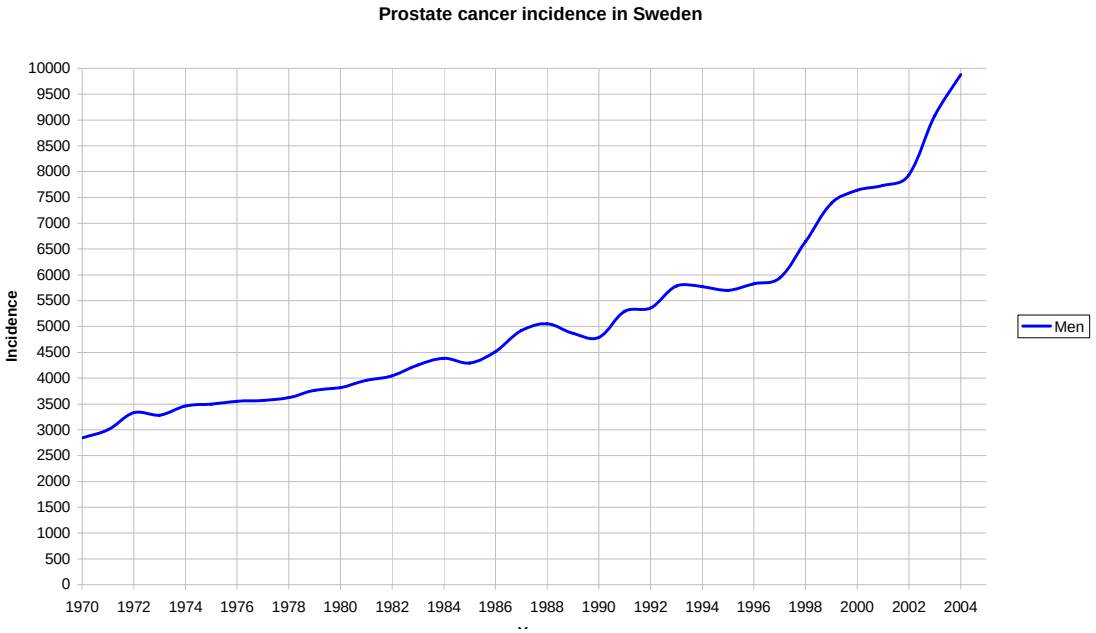

Diagram 8.2 The prostate cancer incidence in Sweden from 1970 to 2004 [Swedish cancer registry, national board of health and welfare]

8.3 Cancer of the Parotid

The parotid glands, located below and in front of the ears, are the largest of the major salivary glands. Tumors in the parotid glands are rare; the incidence each year is approximately 40 per million inhabitants with only 10 of those being malignant [30]. Approximately 90 persons in Sweden are diagnosed each year with a peak incidence between forty and fifty years of age, see Diagram 7.3.
The prognosis depends on tumor size; over four centimeter tends to have a worse prognosis than smaller lesions.
The preferred treatment of parotid tumors is a combination of surgical removal of the tumor and radiotherapy. Making a good treatment plan to parotid tumors can be hard because of all the critical structures in the head and neck region.

Side effects
The most common radiation induced side effect is permanent xerostomia, which means a temporary or permanent stop in saliva production caused by irradiation of the salivary glands. According to Emami et. al. [31] the required dose for such complication would be 32 Gy for a 5% risk when more than 50% of the volume is affected.

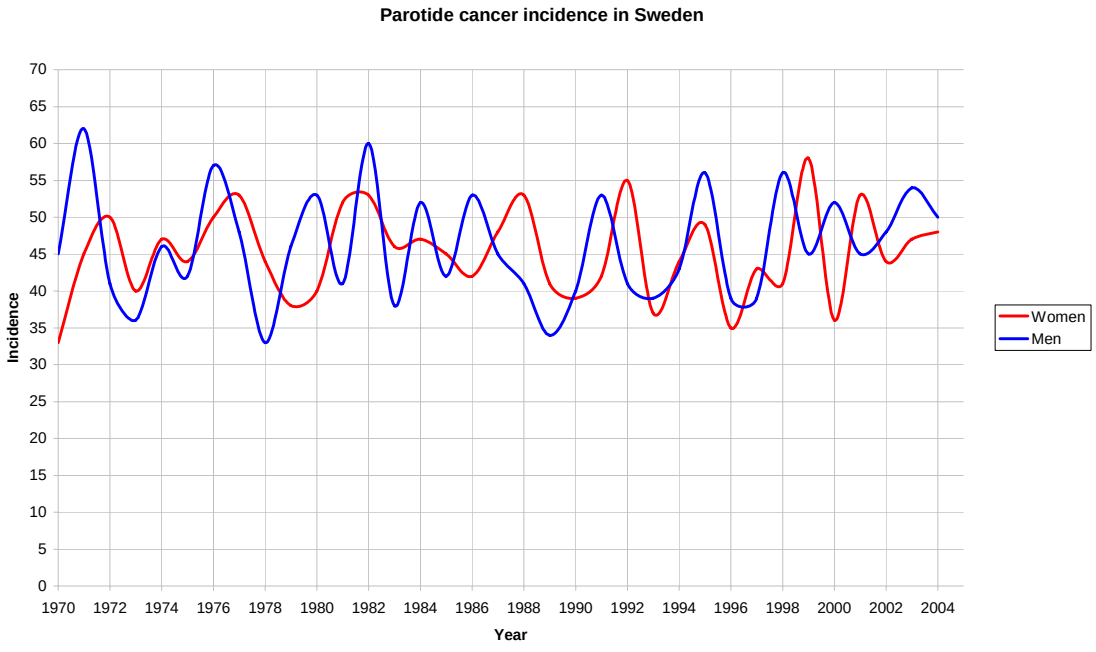

Diagram 8.3 The parotid cancer incidence in Sweden from 1970 to 2004 [Swedish cancer registry, national board of health and welfare]

9 Material and methods

Conventional photon treatment plans, intensity modulated plans with photons (IMXT) and intensity modulated plans with protons (IMPT) were produced and compared. Oncentra MasterPlan (OMP) version 1.5 from Nucletron was used for the IMXT plans while IMPT plans were produced with the research software of RaySearch, Orbit Workstation (version 1.0). This software is not yet released for clinical use.

The same CT-study with identical delineation of structures was used for each case in all treatment plans. Three diagnoses were chosen for the comparative study; breast carcinoma, prostate cancer and parotid cancer. The patient selection was done by the radiation oncologist. The diagnoses were also recommended as eligible for proton therapy in a recent Swedish publication [32].
A total number of seven patient cases were used, all previously treated with conventional photon plans at Lund University Hospital.

In all cases the aim was to treat the entire target with a minimum dose greater than or equal to 95%, and the maximum dose less than or equal to 107% of the prescribed dose to the ICRU reference point. This is in accordance with the recommendations of the International Commission of Radiation Units and Measurements Report no. 50 (ICRU 50) [33]

9.1 Patient groups

In each patient group either two or three cases were studied. Due to lack of time it has not been possible to create and evaluate dose plans in more cases and hence perform statistical evaluation between the outcomes of the different techniques for each diagnosis. The patients should instead be considered as representing a typical case for the majority of all patients with these diagnoses.

In the patient group with breast cancer three cases were selected;
Number 1.1 breast carcinoma stage I and II with no spread to regional lymph nodes
Number 1.2 breast carcinoma stage I and II with spread to the regional nodes
Number 1.3 breast cancer after radical mastectomy
Transversal CT-slices through the center of the PTV for these patients are seen in Figure 9.1 to 9.3 respectively.

The stages that are referred to indicate:
Stage I: The primary tumor is smaller than 2 cm with no spread outside the breast
Stage II : This stage is valid if more than one of the following conditions are fulfilled;
i. The tumor is smaller than 2 cm with spread to the lymph nodes under the arm
ii. The tumor is 2 cm to 5 cm, with or without spread to the lymph nodes under the arm
iii. The tumor is greater than 5 cm with no spread outside the breast [34]

CT-scans were performed with a slice thickness of 5mm for the three breast cancer cases with PTV and relevant organs delineated.

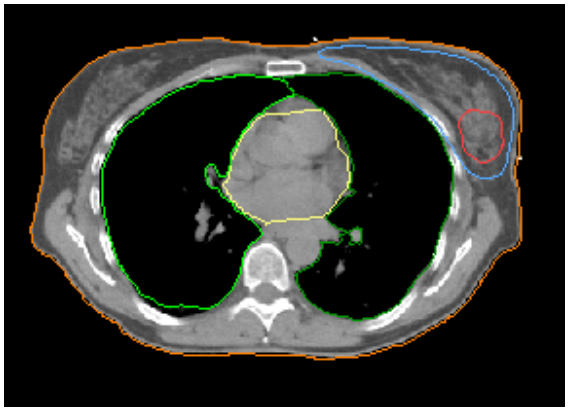

Figure 9.1 Case number 1.1, breast with no spread to the regional lymphnodes

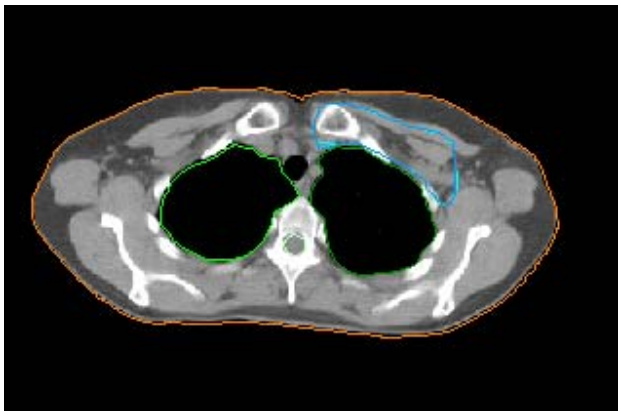

Figure 9.2 Case number 1.2, breast cancer with spread to the lymph nodes.

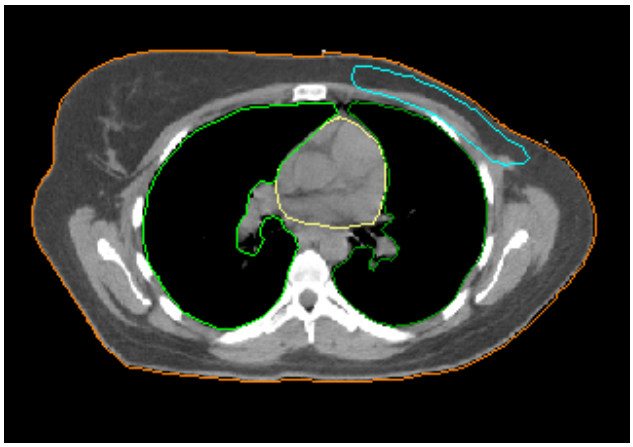

Figure 9.3 Case number 1.3, breast cancer after radical mastectomy

In the patient group with prostate cancer the treatment planning was performed on two patients, number 2.1 and number 2.2 shown in the figures below. Both patients were CT-scanned with a slice thickness of 3 mm, see Figure 9.4 and Figure 9.5.

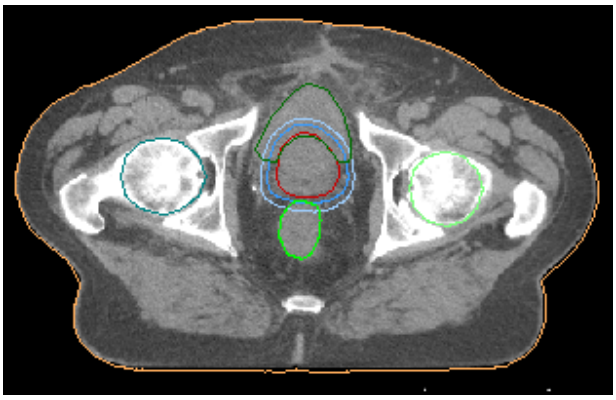

Figure 9.4 A CT-slice of patient number 2.1.

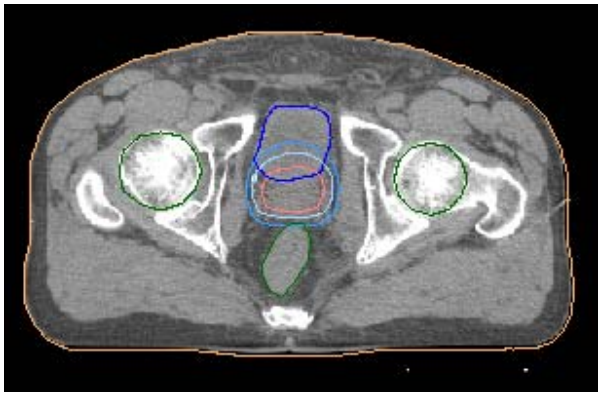

Figure 9.5 A CT-slice of patient number 2.2

Two patients with head and neck tumors were selected and referred to as patient number 3.1 and patient number 3.2. Both cases were diagnosed with parotid cancer. Imaging was performed with 5 mm thick CT slices, see Figure 9.6and Figure 9.7

Figure 9.6. Patient number 3.1 with parotid tumor

Figure 9.7. Patient number 3.2 with parotid tumor.

9.2 Structure delineation

All the patients had been treated with conventional methods and CT images had already been transferred to the treatment planning system (TPS). The basic structure set were taken from the conventional plan. The IMRT method, both with photons and protons, should result in a better dose conformity and in better possibilities to spare organs at risk than conventional treatments. More volumes are therefore worth to be evaluated and hence more structures were needed to be delineated in some of the cases. This was performed by a radiation oncologist at the Radiation Therapy Department in Lund.

For the breast cancer cases the following structures were delineated;
CTV, PTV, heart, right and left lung and patient outline.

In the prostate cancer cases the structures of interest were;
Prostate, prostate boost (3/4 cm margin), prostate + 1 cm margin, bladder, rectum, femoral heads and the patient outline

In the parotid cancer the following structures were delineated;
PTV, brain, right and left eye, right and left optical nerve, chiasm, brain stem, PRV brain stem, mandibular joint, right and left inner ears, oral cavity, parotid, vertebra, mandible, right and left lung and patient outline.

If some of the structures were entirely or partly located inside the target region they were kept like that. When a structure is drawn too close to the skin surface there will not be charge particle equilibrium in the case of the photons and hence the target will not reach the prescribed dose. In an optimal scenario there will be approximately 3 to 5 mm distance between the target and the skin surface and for superficially located tumors a bolus has to be used to reach that space.

9.3 Dose-volume constraints and objectives

Inverse planning systems require that dose constraints, a criteria that must be fulfilled, or objectives, a criteria that guides the optimization, are chosen for each structure of interest. The constraints can either be made on a physical basis or on a radiobiological basis. The most common today is physical criteria, i.e. dose and dose-volume based requirements and this was also used in all plans presented in this study. However, the physical constraints are merely a substitute for the biological effects that will be the result of the treatments. A choice can be made whether to use a dose-volume constraint, which implies that, a part of the irradiated volume might exceed more dose than it is predicted to tolerate without incurring any complications. The dose-volume constraint is generally stated that “no more than q% of the organ may exceed the dose d”.
The DVHs are the bases for change in constraints when optimizing IMRT-plans. The histograms give a good illustration of the dose distribution of each delineated structure and help to decide what kind of changes are necessary to apply in order to achieve the optimal plan.

In this study the dose limitations were based on normal tissue tolerances from Emami et al. [31] and the DAHANCA protocol [35]. If possible, the dose distributions in normal tissue were kept lower than the predicted tolerance doses, performed by a trial and error process with requirement of a remaining acceptable dose distribution in the target. In the paper by Emami et al. TD5/5, the tolerance doses with 5% probability of a specific endpoint within a five-year period, were used. The following parameters, shown in Table 9.1, were thus used as tolerance doses for normal tissue;

Table 9.1 The tolerance doses that guided the choice of objectives and constraints.

Organ	Max tolerance dose [Gy]
Bladder	65 Gy [31]
Brain	45 Gy [31]
Brain stem	54 Gy [35]
Brain stem PRV	60 Gy [35]
Chiasma	54 Gy [35]
Femoral Head	52 Gy [31]
Heart	40 Gy [31]
Inner ear	54 Gy [35]
Inner ear PRV	60 Gy [35]
Joint mandible	60 Gy [31]
Lung	17.50 Gy [31]
Optic nerve	54 Gy [35]
Parotid	32 Gy [31]
Rectum	60 Gy [31]
Spinal cord	45 Gy [35]
Spinal cord PRV	50 Gy [35]

To find a good treatment plan, compromises frequently have to be made between the different structure constraints. To find an optimal solution, all structures have to be considered. Therefore to optimize a solution for only one single DVH at a time, the over all optimal solution may be missed.

9.4 Conventional treatments

9.4.1 Breast carcinoma.

In case 1.1 the patient is treated with two tangential wedged beams, the field parameters are shown in Table 9.2. Wedged fields commonly result in an inhomogeneous dose distribution with hot-or coldspots typically found in the cranial and caudal part of the field [36]. The wedges are placed in a lateral direction. In case 1.1 the aim was to deliver 50 Gy to both CTV and PTV in 25 fractions.

Table 9.2 Field parameters used for conventional planning of Ca mam case 1.1

Field	Energy	Gantry angle (deg)	Collimator angle (deg)	Wedge angle (deg)
1	6 MV	305	94	15
2	6 MV	130	356	8

In the second breast carcinoma case, number 1.2, five fields were used with gantry angles and corresponding energies and wedges as shown in Table 9.3. In all fields the multileaf collimator (MLC) was used to shield adjacent tissue. The dose received by both the CTV and the PTV was intended to be 50 Gy in 25 fractions.

Table 9.3 Field parameters used for conventional planning of Ca mam case 1.2

Field	Energy	Gantry angle (deg)	Collimator angle (deg)	Wedge angle (deg)
1	6 MV	350	90	8
2	10 MV	170	90	
3	6 MV	307	90	15
4	6 MV	307	90	
5	6 MV	135	270	15

In the last case, the patient with radical mastectomy of the breast (number 1.3), six fields were used, see the field parameters in Table 9.4. To avoid the organs at risk two of the beams were tangential beams in opposite directions, but to be able to cover the entire target it was necessary to use other beam directions as well. None of the fields were wedged but all were conformed to the target with MLC. Also in this case the CTV and PTV should to receive 50 Gy in 25 fractions.

Table 9.4 Field parameters used for conventional planning of Ca mam case 1.3

Field	Energy	Gantry angle (deg)	Collimator angle (deg)
1	6 MV	350	0
2	10 MV	180	0
3	10 MV	180	0
4	6 MV	302	0
5	6 MV	129	0
6	6 MV	0	90

9.4.2 Prostate carcinoma

In the first prostate case, six fields with five different angles were used. They were distributed in the following way; one beam from each side of the body, one vertical from the front and then finally two oblique from the front, see Table 9.5. In only the two lateral opposed fields, wedges were used but field shaping was performed with MLC in all fields. In all three target definitions Prostate, prostate boost (3/4 cm margin) and prostate + 1 cm margin 78 Gy was the goal to deliver in 39 fractions.

Table 9.5 Field parameters used for conventional planning of prostate cancer case 2.1

Field	Energy	Gantry angle (deg)	Collimator angle (deg)	Wedge angle (deg)
1	10 MV	0	0	
2	10 MV	320	0	
3	10 MV	270	90	
4	10 MV	90	270	
5	10 MV	90	270	
6	10 MV	42	0	

The second prostate plan, 2.2, consists of five fields in five different angles identical to the former dose plan constructed for case 2.1, see Table 9.6. Like the first prostate plan the two lateral fields were wedged and all fields were shaped with MLC. In all the three target volumes a total dose of 78 Gy was prescribed in 2 Gy fractions.

Table 9.6 Field parameters used for conventional planning of prostate cancer case 2.2

Field	Energy	Gantry angle (deg)	Collimator angle (deg)	Wedge angle (deg)
1	10 MV	0	0	
2	10 MV	320	0	
3	10 MV	270	109	
4	10 MV	90	251	
5	10 MV	43	0	

9.4.3 Parotid cancer

A common radiotherapy technique in conventional treatment is two angled wedged photon fields both impinging on the target side. This method is used in both parotid cases. In the first one (case number 3.1) the left parotid constitutes the target which is irradiated to the dose of 68 Gy in 2 Gy fractions. The field parameters are shown in Table 9.7

Table 9.7 The Field parameters used for conventional planning of parotid cancer case 3.1

Field	Energy	Gantry angle (deg)	Collimator angle (deg)	Wedge angle (deg)
1	4 MV	128	266	38
2	4 MV	36	90	35

In the second parotid plan the tumor is located on the right side, see the field parameters in Table 9.8, and the prescription dose was 60 Gy in 2 Gy fractions.

Table 9.8 Field parameters used for conventional planning of parotid cancer case 3.2

Field	Energy	Gantry angle (deg)	Collimator angle (deg)	Wedge angle (deg)
1	4 MV	310	270	46
2	4 MV	225	90	46

9.5 Intensity modulated photon therapy (IMXT)

In all patient cases, irrespective of diagnoses, the treatment plan was optimized with the step-and-shoot technique using 45 iterations with accurate dose calculations in every 15th iteration. The pencil beam algorithm was chosen for both the accurate dose and the final dose calculation in favor of the collapsed cone, which needs a considerably longer calculation time. The fluence matrix had a resolution of 0.7 cm and the target margin was set to 0.5 cm. The optimization dose grid resolution was; X: 0.4 cm, Y: 0.4 cm and Z: 0.4 cm. The maximum numbers of MLC segments were set to 70, the minimum open field size allowed was 5cm^2 and the minimum number of open leaf pairs was set to 5 pairs. It was decided to put at least 2 monitor units (MU) for each segment to ensure an accurate dose delivery. The collimator angle was set to 2 degrees to decrease problems with any tongue and groove effect. All these parameters have been evaluated clinically at our department and were hence kept constant.

To achieve a clinically acceptable plan the decisions on the beam set-up parameters in each case was based on a trial and error processes. This was done by varying the number of coplanar beams and to adapt every beam angle. Parallel opposing beams were avoided. In several cases it was necessary to adjust the dose-volume objectives in order to find the best solution. The photon energy used in the IMXT optimization was identical to the

energy used in the conventional treatment plan, except for one plan in cases 1.1, 1.2 and 1.3. Lomax et al [37] performed IMRT treatment plans to a breast cancer case consisting of 9 evenly spaced 15-MV coplanar fields. This was also for comparison created in this study, in addition to our optimized plan, but instead of using 15 MV, 10 MV was adopted. Several plans were computed in each case but evaluations and comparisons were only made between the plans judged to be the clinically best in every case.

9.6 Intensity modulated proton therapy (IMPT)

The best IMXT treatment plan from Oncentra Masterplan was imported in the RaySearch Orbit Workstation with all objectives included.
In the current prototype, the user selects the angle of incidence and the maximum and minimum energy for each beam and the number of energies to be used in that range (the energy levels max, min and number of steps will in a later version be automatically generated). Based on these input data, equally spaced energy levels in terms of geometrical depth are selected and the target projections are computed for each energy level. Some target projections may be excluded if it does not hold a spot inside the target at the radiological depth of that specific energy, and are then not included in the optimization. The present version of the target projection algorithm does not account for heterogeneities (this is under development). The value of each bixel (beam "pixel" of rectangular form) in each projection for all beams is registered as an optimization variable. The size of the bixels is currently a parameter selected by the user.

A maximal of 25 iterations were used with an accurate dose calculation every 5th iteration. The optimization dose algorithm and the accurate dose calculation were a "singular value decomposition" (SVD) algorithm. The fluence matrix had the resolution; X: 1cm and Y: 1cm and an upper limit of 50 segments were adopted. These settings were recommended by RaySearch and small variations did not result in any significant changes in the DVHs. The energies used varied between the fields depending on beam angles i.e. how deep the protons had to penetrate to reach the target. Roughly, the energy intervals in the different patient groups were;

- Treatment plans for mammary carcinoma; 20-135 MeV
- Treatment plans for prostate cancer; 145-200 MeV
- Treatment plans for parotid cancer, 20-120 MeV

The objectives were adjusted in the OARs to maintain as low doses as possible while keeping good dose coverage of the targets.
Since the relative biological effect differs between photons (RBE = 1) and protons (RBE = 1.1) the prescribed dose to the targets and the dose limitations to OARs should be lower than those for photons to receive the same cobalt gray equivalent (CGE) dose and also the same biological effect. This RBE correction has not been don explicitly in the present study since it is just a simple scaling with a factor of 1.1. The dose reported should thus all be considered as expressed in CGE units even though we have kept Gy as the dose unit for simplicity.

9.7 Evaluations of the plans

The DVHs of the best clinical treatment plans for all treatments and for each case were exported to Microsoft Excel where they were analyzed and compared, i.e. three plans were participating in the comparison; the conventional plan, the IMXT-plan and the IMPT-plan for each patient case. DVHs, representing the same structure for all three techniques, were plotted in the same diagram. The dose distribution, in the same volume, created with the three different methods could then easily be compared by eye.

The dose distributions were evaluated by calculating the generalized equivalent uniform dose (gEUD), target dose uniformity, radiation conformity index RCI, and irradiated volume IV. The maximum, minimum and average doses in the targets were also recorded, see appendix II. The formula for the target dose uniformity and the RCI are given in Equation 9.1 [29] and Equation 9.2 [38]

$$u = \left(D_{5\%} - D_{95\%}\right)/D_{mean} \qquad \textbf{Equation 9.1}$$

$$RCI_i = V_{PTV}/V_{95\%} \qquad \textbf{Equation 9.2}$$

V_{PTV} is the volume of the planning target and $V_{95\%}$ is the volume receiving 95% of the prescribed target dose. The irradiated volume, IV, is defined as $V_{50\%}$ i.e. the volume that receives 50% of the prescribed target dose.

For all the structures, targets as well as OARs, the generalized equivalent uniform dose (gEUD) were calculated in order to compare the dose distributions. An attempt to calculate the TCP and NTCP was also made.

10 Results and discussion

10.1 DVH

Dose volume histograms (DVHs) for the PTV and the total body are shown below in Figure 10.1 to Figure 10.7. In all cases the IMPT-plans, when compared with both conventional- and IMXT-plans, deliver a highly homogeneous target dose as well as the lowest total dose burden to the patient.

10.1.1 Mammary carcinoma

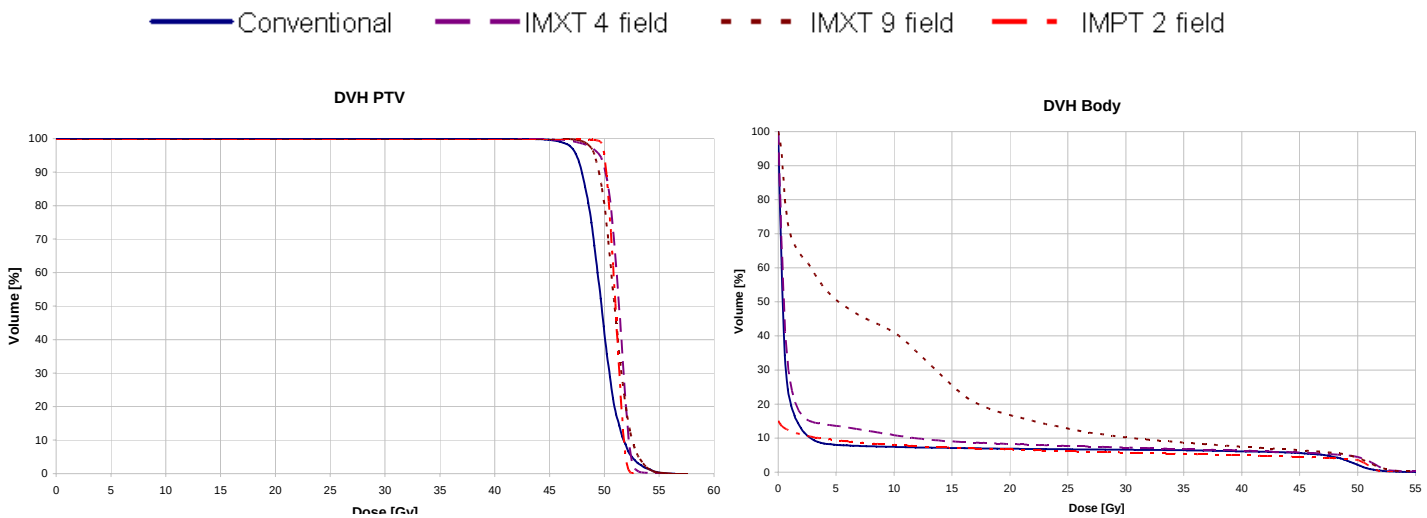

Figure 10.1 Case 1.1 breast carcinoma stage I and II. The prescribed dose was 50 Gy in 2 Gy per fraction

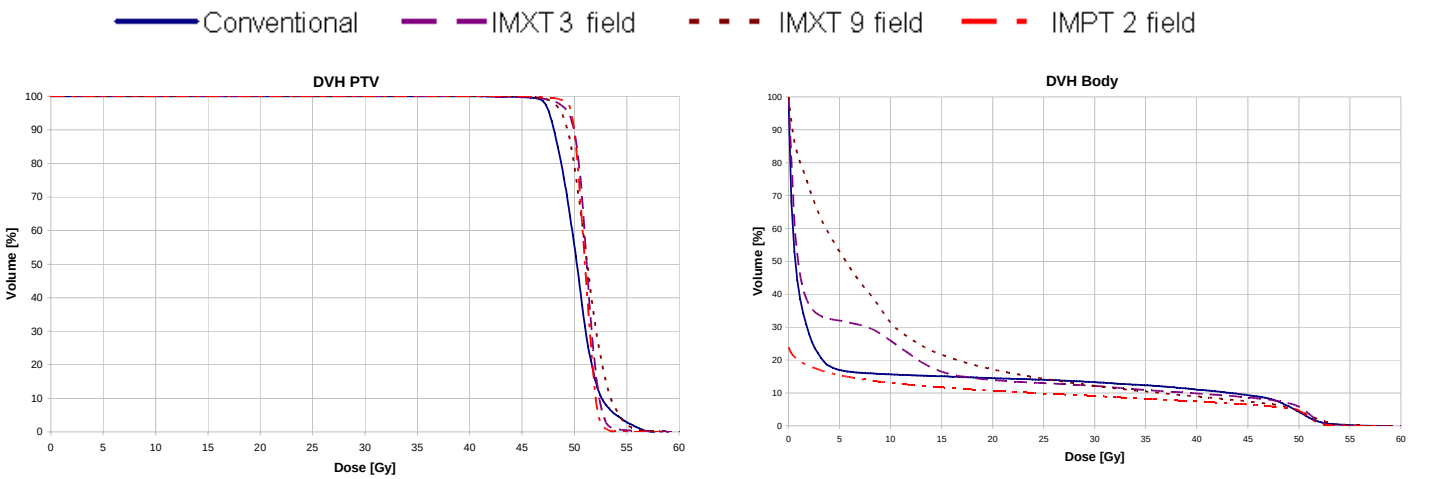

Figure 10.2 Case 1.2 breast carcinoma stage I and II with involved nodes. The prescribed dose was 50 Gy in 2 Gy per fraction

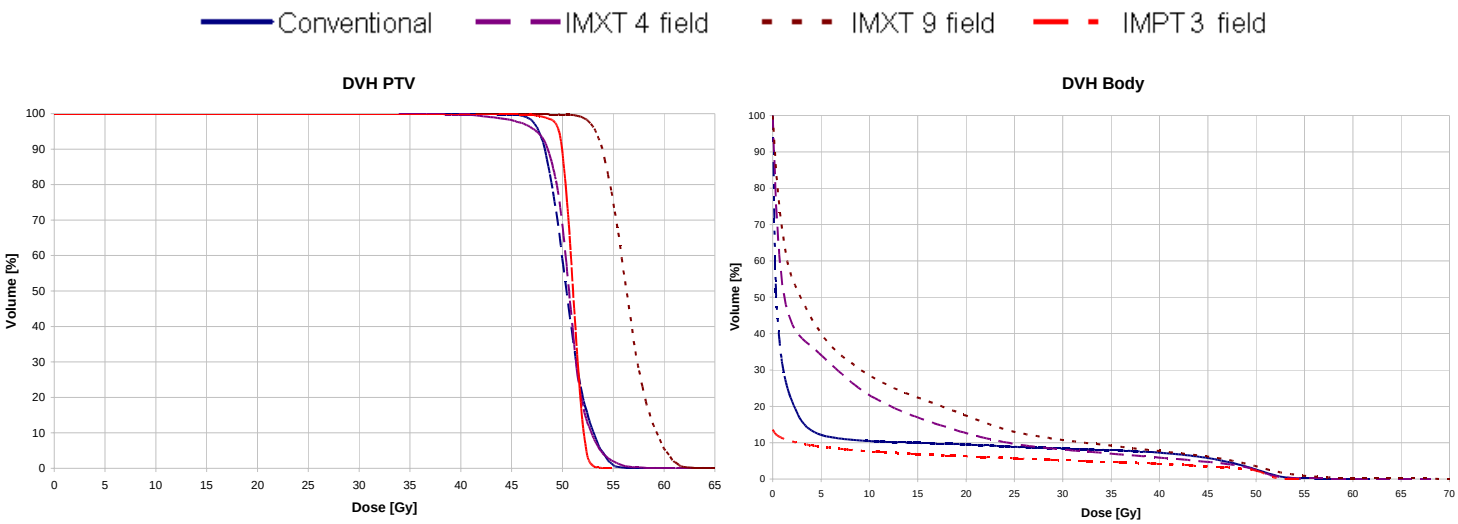

Figure 10.3 Case 1.3 breast with radical mastectomy. The prescribed dose was 50 Gy in 2 Gy per fraction

10.1.2 Prostate carcinoma

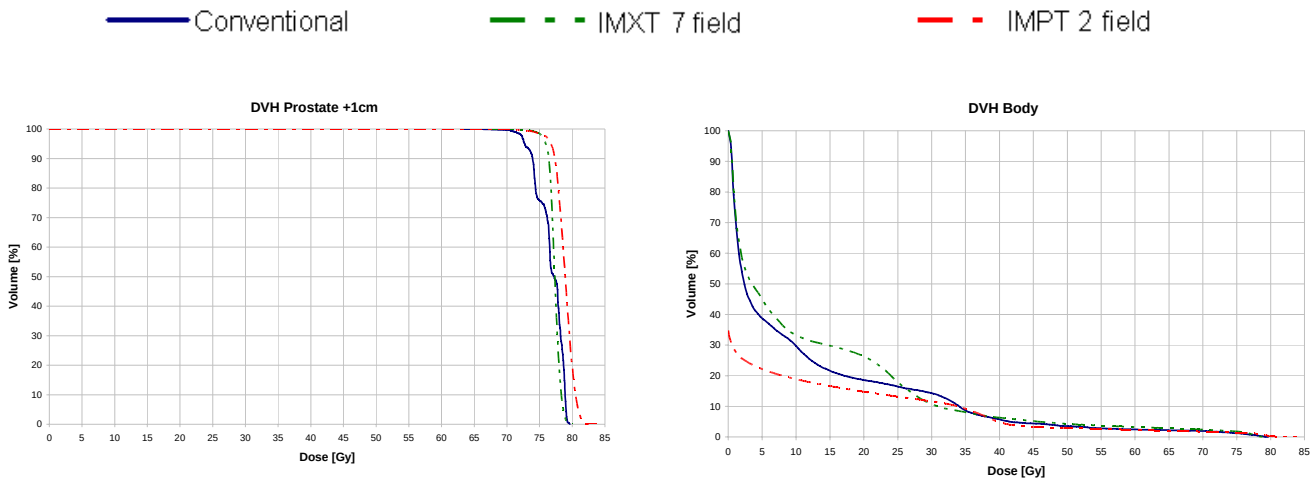

Figure 10.1 Case 2.1, prostate carcinoma. The prescribed dose was 78 Gy in 2 Gy per fraction

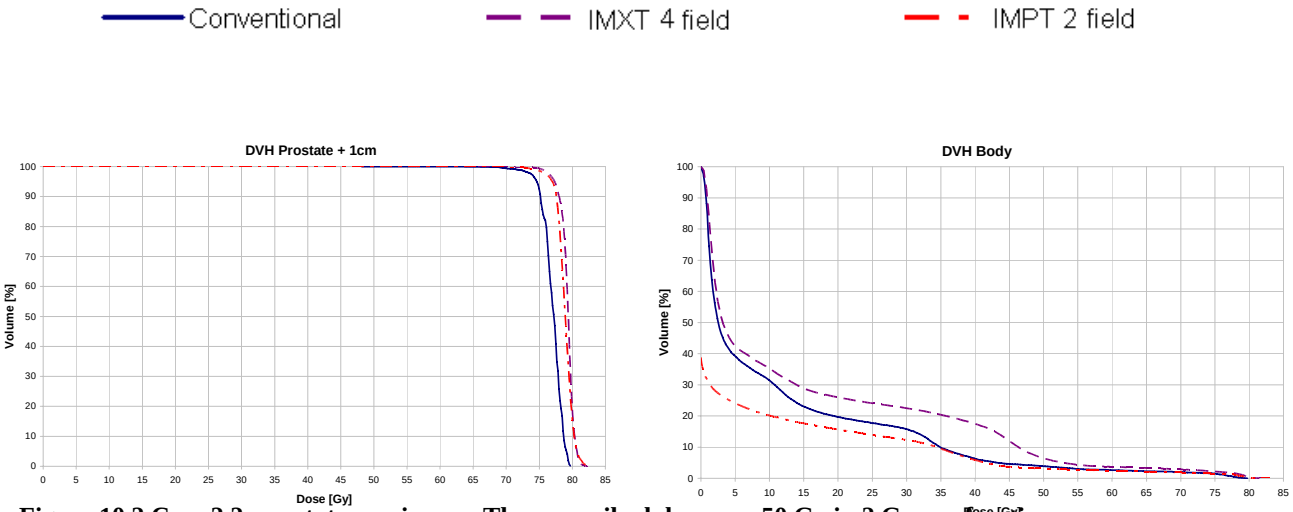

Figure 10.2 Case 2.2, prostate carcinoma. The prescribed dose was 50 Gy in 2 Gy per fraction

10.1.3 Tumor of the parotid

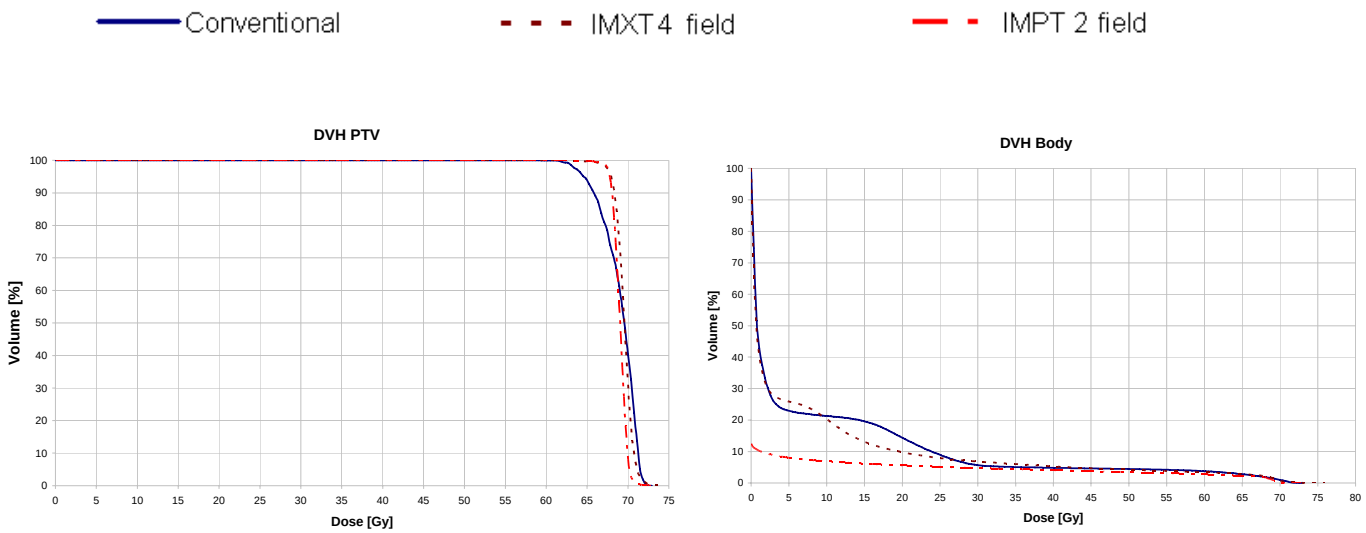

Figure 10.3 Case 3.1, parotid tumor. The prescribed dose was 68 Gy in 2 Gy per fraction

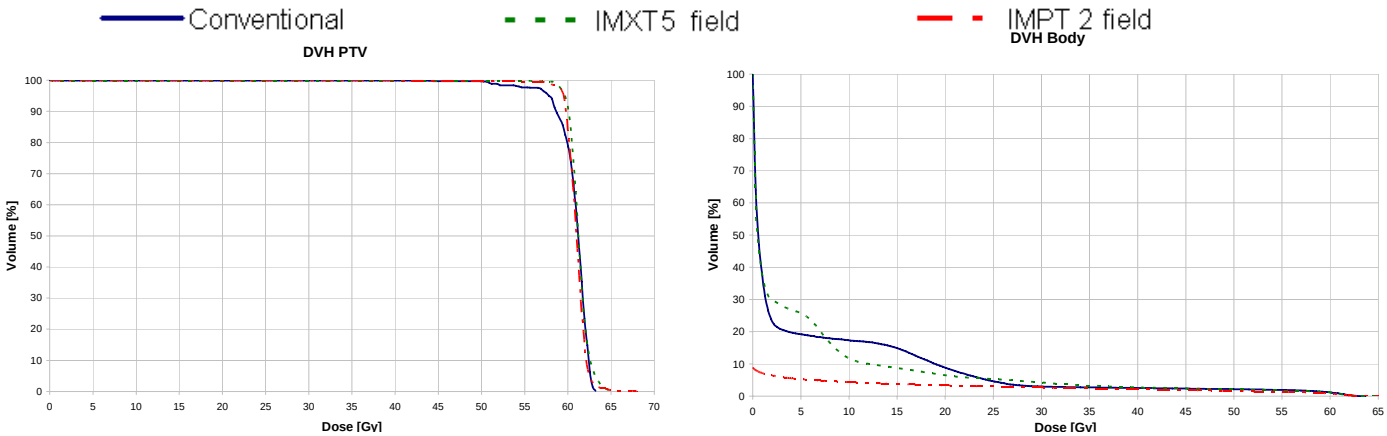

Figure 10.4 Case 3.2, parotid tumor. The prescribed dose was 60 Gy in 2 Gy per fraction

In almost all IMXT-plans the volume of normal tissue irradiated to low and intermediate dose levels were larger compared with conventional plans and IMPT. This can be observed in the DVHs representing the entire body. The dose to the healthy tissue in the IMPT–plans was considerably lower for almost all structures. In healthy tissue adjacent to the target the dose reductions were in all IMPT-plans predominantly observed in the low to medium dose ranges. One example is the dose distribution delivered to the ipsilateral lung in all mammary cases, see Figure 13.4, Figure 13.10 and Figure 13.17 in Appendix 1. For some cases the dose distribution resulted in even higher doses in the IMPT-plans, e.g. for medulla in case 1.2 and 1.3, see Figure 13.12 and Figure 13.19 in Appendix 1. In the more "distal" normal tissue, such as the brain stem in the parotid cases (see Figures 13.41 and 13.61 in Appendix 1) the dose was significantly decreased in the IMPT-plans compared to the photon plans. In the prostate case, the most prominent difference was improvements in target dose uniformity and the reduction in dose distribution in the entire body. All the other dose distributions were quite similar.
In finding a good treatment plan the challenge is to make the accurate compromises. The reduced dose to one OAR is commonly at the expense of higher dose to other OARs or decreased homogeneity in the target. This is especially true for the photon plans, see appendix 1.

For some structures the DVH for the IMPT-plan intersects with the corresponding DVH for the photon plans (see e.g. Figure 13.12, PRV medulla in case 1.2) i.e. a hotspot in the structure. This could have a devastating effect on serial structures if the IMPT-plan exceeds the dose limit and if the conventional plan does not. On the other hand, parallel structures can survive large doses if just a small part is exposed.

10.2 Dose distribution

10.2.1 Mammary carcinoma

The beam arrangements in the breast cases were basically kept tangential for the IMXT plans but to receive acceptable dose homogeneity in the targets other angles were also necessary to use. The transversal dose distribution from the different techniques with corresponding beam directions are shown in Figure 10., Figure 10. and Figure 10.10. Deep lying parts of the targets, i.e. involved lymph nodes, required additional beams which increased the dose to the organs at risk. Case number 1.3 shows poorer dose conformity to the target in comparison to the other two cases, but it still fulfills the dose requirements. In all three cases the IMPT plans have the lowest doses to the normal tissue, especially to the lungs and to the heart. The contralateral lung and the heart receive essentially no radiation. By using multiple fields (2-3) the skin dose is decreased and the risk of acute moist desquamation is reduced [39].

In OMP the angles increase clockwise and in Orbit workstation the angles increase counter clockwise (clockwise in the brackets)

Gantry angles;
IMXT: 133°, 304°, 117°, 317° IMPT: 0° (0°), 270° (90°)

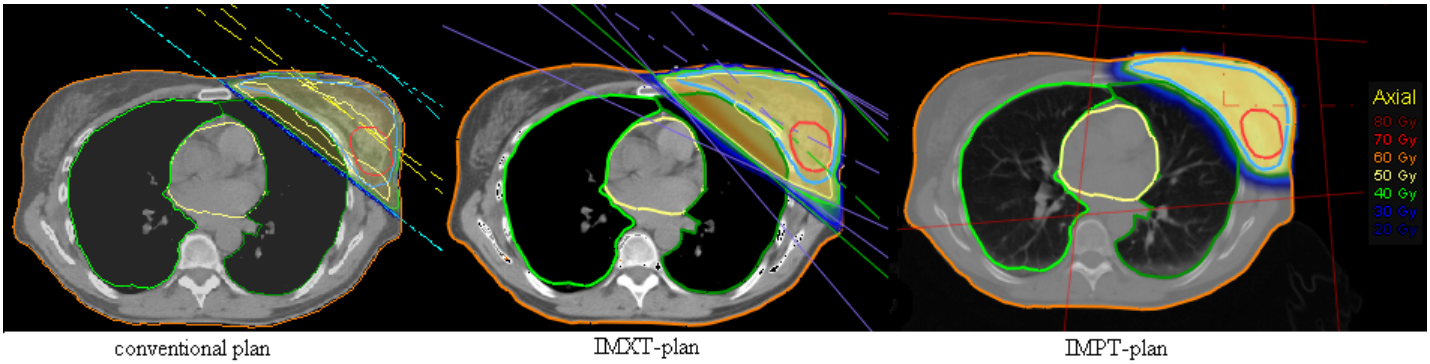

Figure 10.8 Case number 1.1, breast carcinoma stage I and II

Gantry angles;
IMXT: 352°, 133°, 308° IMPT: 0° (0°), 300° (60°)

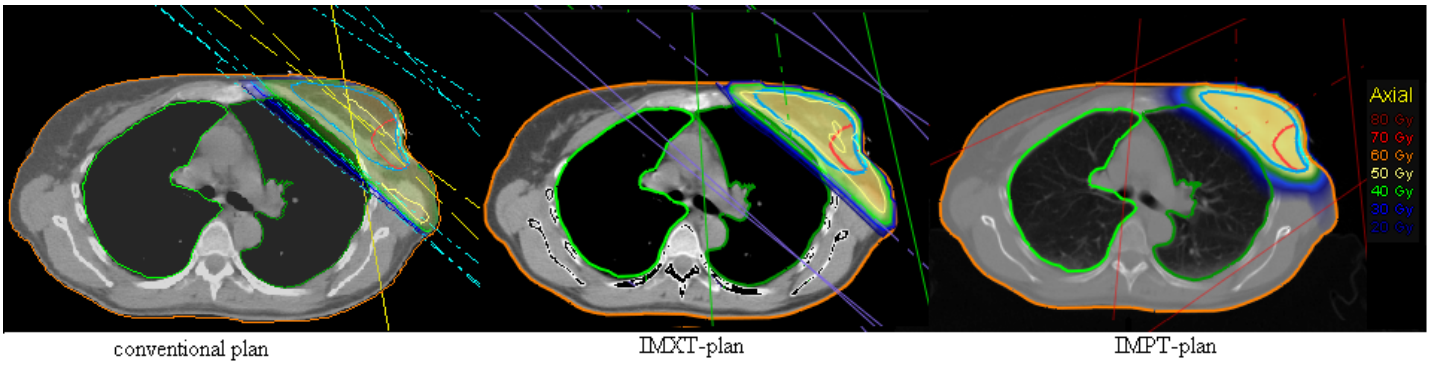

Figure 10.9Case number 1.2, breast carcinoma stage I and II with involved lymph nodes

Gantry angles;
IMXT: 15°, 311°, 339°, 109° IMPT: 348° (12°), 66° (294°), 34° (326°)

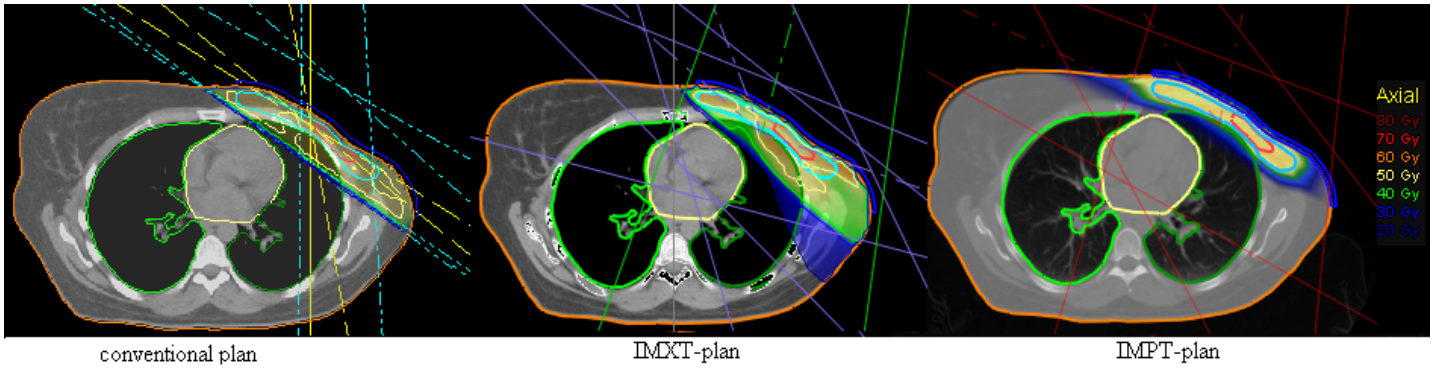

Figure 10.5 Case number 1.3, breast with radical mastectomy

10.2.2 Prostate carcinoma

The dose distribution with corresponding beam directions are shown in Figure 10.11 and Figure 10.12. Good target dose coverage was obtained with all three techniques. The doses to the organs at risk i.e. the rectum and the bladder were not significantly reduced with IMPT compared with the conventional photon and IMXT techniques. It should be stressed that only two fields were used in the proton optimization plan compared with the seven beams used in the photon plans. The choices of beam angles were based on trial and error attempts guided by data from Mock et al. [29]

Gantry angles;
IMXT: 27^o, 79^o, 127^o, 176^o, 233^o, 281^o, 330^o IMPT: 90^o (270^o), 270^o (90^o)

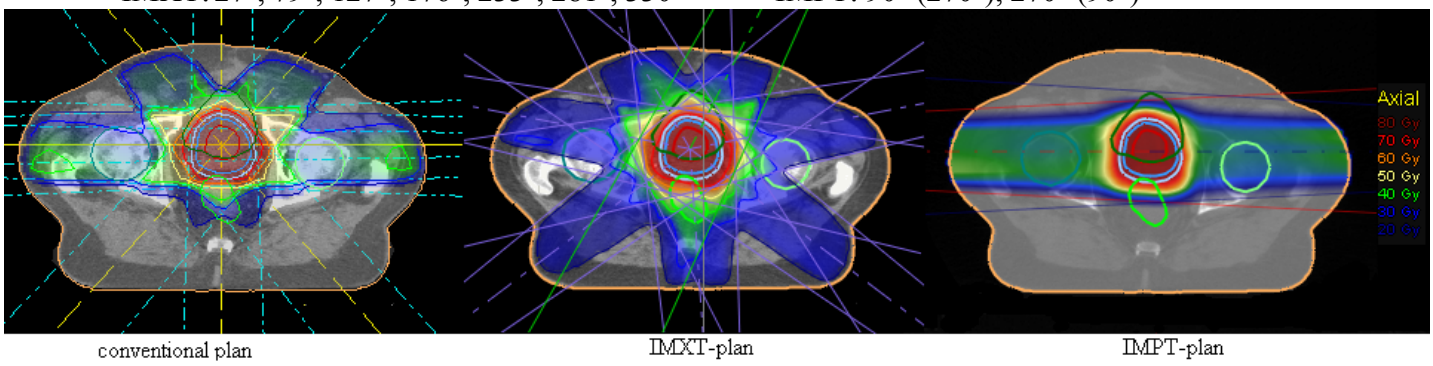

Figure 10.6 Case number 2.1, prostate carcinoma

Gantry angles;
IMXT: 68^o, 118^o, 242^o, 318^o IMPT: 90^o (270^o), 270^o (90^o)

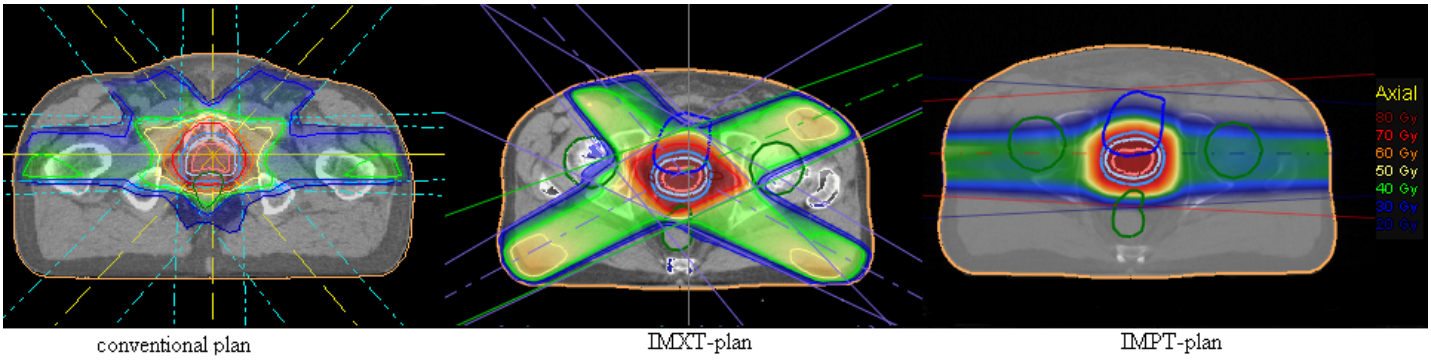

Figure 10.7 Case number 2.1, prostate carcinoma

10.2.3 Tumor of the parotid

The lack of conformity to the PTV in the conventional plans can be clearly seen in Figure 10.13 where the brain receives a significant dose. Both the IMRT plans provide a much better conformity, but especially the IMPT plans. In both cases, Figure 10.13 and Figure 10.14, the IMPT plans reduce the amount of normal tissue receiving high doses. The choice of number of beams and beam orientation in the IMXT plan were guided by an article by Bragg et al. [40]

Gantry angles;
IMXT: 12°, 50°, 131°, 166° IMPT: 135° (315°), 45° (225°), 80° (260°)

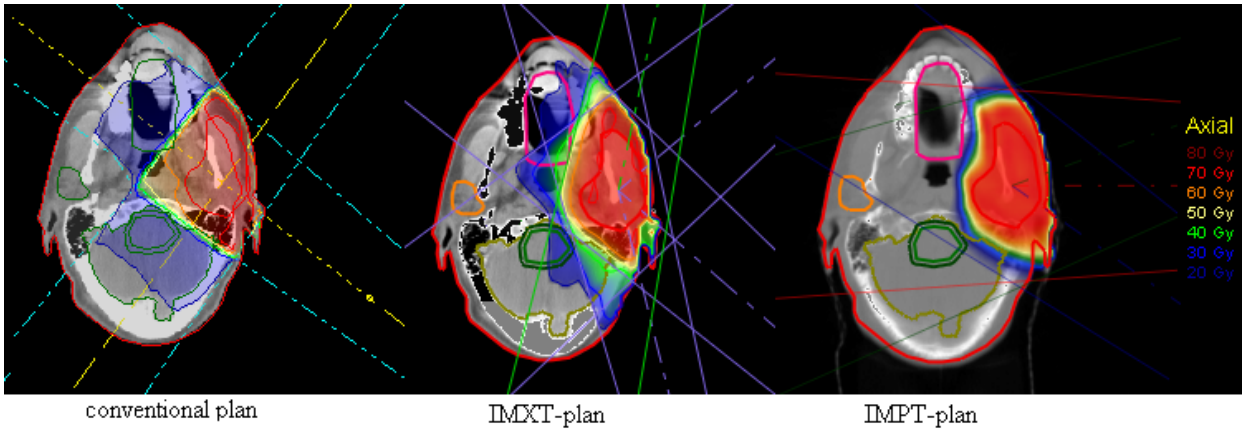

Figure 10.8 Case number 3.1, parotid tumor

Gantry angles;
IMXT: 190°, 230°, 270°, 310°, 350° IMPT: 135° (315°), 45° (225°)

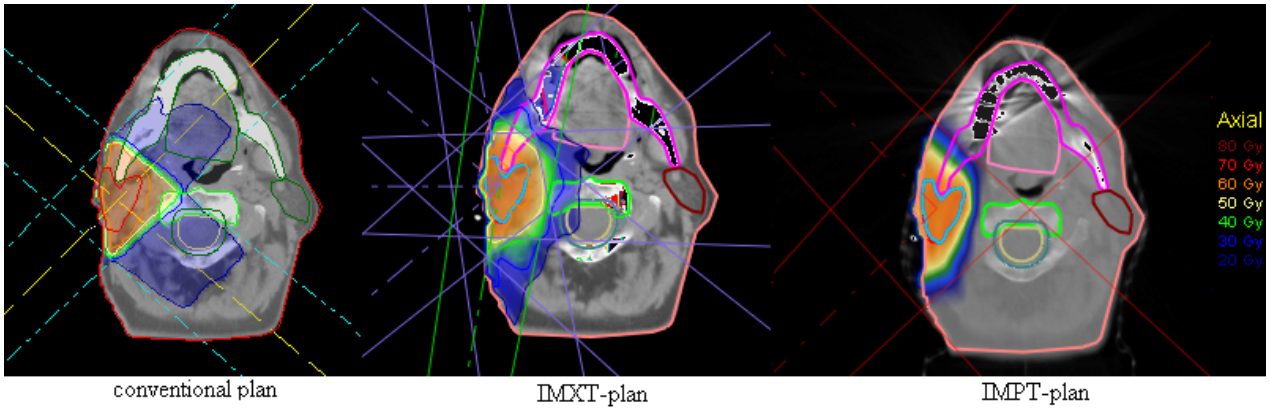

Figure 10.9 Case number 3.2, parotid tumor

10.3 Dose statistics

Dose statistics (maximum, minimum and the average dose) are shown for all cases in Apendix II. The mean dose delivered to all OAR structures in all mammary cases were substantially reduced with IMPT-plans when compared with the conventional plans. They were also better in this respect than all of the IMXT-plans. The best improvement of the dose distribution was in the ipsilateral lung for all three cases. In the prostate cases the average doses to the bladder and the rectum were lower for the proton plan than for both photon plans. In case 2.1 the dose reduction for the IMPT-plan was 2% in the bladder and 16.5% in the rectum when compared with the conventional plan. In case 2.2 the corresponding comparison results in 27% and 18.5%, respectively.
The most significant gain for the two cases with cancer in the parotid was in the structures located at a distance from the target. These structures, such as the medulla, the brain, the inner ear and the healthy parotid received very low doses or no dose at all. All the proton plans produced lower average dose to the body than the photon plans did and the maximum dose were lower for almost all structures, see Appendix II.

10.4 gEUD

The results of the gEUD evaluation are shown in Table 10.1 to Table 10.7 for all the studied cases. For the heart in the three mammary carcinoma cases, the protons reduced the gEUD by a factor of 7.5, 4 and 10 compared with the conventional plans, respectively. The corresponding figures for the ipsilateral lung were 1.5, 2.2 and 2.6.
A comparison of the mammary carcinoma planning technique done in this study with the planning technique performed with 9 fields, as described by Lomax et al. [37], shows a dose advantage in nearly all structures for the plans done in this study.
The gEUD-value for the bladder was almost identical between the proton plan and the conventional plan in the first prostate case and it was only slightly decreased in the second case. For the rectum it was even slightly increased in both cases for the IMPT plans. These high doses in both the bladder and the rectum are due to the fact that both structures are located inside the PTV and also due to the penumbra being similar for protons and photons at that depth. For the parotid tumors the gEUD values are much lower in all OARs in the IMPT plans. In all cases the aim was to treat the entire target with a minimum dose greater than or equal to 95%, and the maximum dose less than or equal to 107% of the prescribed dose and due to that the gEUD value for the PTV slightly can differ between the plans. A lower gEUD value in the PTV could result in better OARs sparing, but in almost all proton plans the gEUD values are slightly higher for the PTV whereas the OARs receive lower gEUD.

Table 10.1 Case 1.1

	Conventional plan	IMXT-plan 4 fields	IMXT-plan 9 fields	IMPT-plan 3 fields
CTV	49.7 Gy	51.5 Gy	50.6 Gy	51.0 Gy
PTV	49.4 Gy	51.0 Gy	50.7 Gy	51.0 Gy
Heart	5.0 Gy	8.1 Gy	15.8 Gy	0.7 Gy
Left lung	6.8 Gy	10.5 Gy	25.7 Gy	4.1 Gy
Right lung	0.4 Gy	0.7 Gy	9.9 Gy	0.0 Gy

Table 10.2 Case 1.2

	Conventional plan	IMXT-plan 3 fields	IMXT-plan 9 fields	IMPT-plan 2 fields
CTV	49.8 Gy	50.9 Gy	50.8 Gy	50.9 Gy
PTV	49.9 Gy	50.9 Gy	51.0 Gy	51.0 Gy
Heart	8.6 Gy	10.5 Gy	7.8 Gy	2.1 Gy
Left lung	15.0 Gy	17.3 Gy	15.6 Gy	6.6 Gy
Right lung	0.6 Gy	0.7 Gy	7.3 Gy	0.0 Gy
Medulla	3.0 Gy	5.2 Gy	6.3 Gy	7.1 Gy

Table 10.3 Case 1.3

	Conventional plan	IMXT-plan 3 fields	IMXT-plan 9 fields	IMPT-plan 2 fields
CTV	50.9 Gy	49.9 Gy	49.8 Gy	51.2 Gy
PTV	49.5 Gy	47.3 Gy	49.6 Gy	51.0 Gy
Heart	10.1 Gy	5.7 Gy	4.1 Gy	1.0 Gy
Left lung	13.5 Gy	14.9 Gy	14.2 Gy	5.1 Gy
Right lung	0.7 Gy	1.1 Gy	1.7 Gy	0.1 Gy
Medulla	5.9 Gy	7.8 Gy	4.5 Gy	5.1 Gy

Table 10.4 Case 2.1

	Conventional plan	IMXT-plan 7 fields	IMPT-plan 2 fields
Prostate	77.2 Gy	77.1 Gy	78.6 Gy
Prostate + 3/4 cm	77.2 Gy	77.4 Gy	78.8 Gy
Prostate + 1cm	76.3 Gy	77.2 Gy	78.8 Gy
Bladder	55.3 Gy	55.7 Gy	55.0 Gy
Femoral head left	32.4 Gy	25.4 Gy	33.1 Gy
Femoral head right	32.3 Gy	24.6 Gy	35.2 Gy
Rectum	62.6 Gy	65.3 Gy	65.3 Gy

Table 10.5 Case 2.2

	Conventional plan	IMXT-plan 4 fields	IMPT-plan 2 fields
Prostate	77.4 Gy	79.7 Gy	78.7 Gy
Prostate + 3/4 cm	77.3 Gy	79.6 Gy	79.0 Gy
Prostate + 1cm	76.7 Gy	79.1 Gy	78.8 Gy
Bladder	56.4 Gy	54.2 Gy	48.1 Gy
Femoral head left	30.2 Gy	36.6 Gy	32.4 Gy
Femoral head right	31.4 Gy	26.5 Gy	36.3 Gy
Rectum	61.9 Gy	67.1 Gy	64.6 Gy

Table 10.6 Case 3.1

	Conventional plan	IMXT-plan 7 fields	IMPT-plan 2 fields
PTV	68.4 Gy	69.3 Gy	69.0 Gy
Brain	21.2 Gy	14.4 Gy	8.4 Gy
Brain stem	21.5 Gy	15.5 Gy	2.7 Gy
Brain stem PRV	21.6 Gy	16.1 Gy	5.1 Gy
Left lung	0.5 Gy	0.3 Gy	0.0 Gy
Medulla	27.2 Gy	27.0 Gy	17.6 Gy
Medulla PRV	41.9 Gy	27.0 Gy	24.3 Gy
Optic chiasm	2.8 Gy	2.3 Gy	0.0 Gy
Optic nerve dx	2.3 Gy	2.5 Gy	0.0 Gy
Optic nerve sin	3.2 Gy	6.6 Gy	0.1 Gy
Parotid dx	2.3 Gy	4.8 Gy	0.0 Gy
Right lung	0.4 Gy	0.3 Gy	0.0 Gy

Table 10.7 Case 3.2

	Conventional plan	IMXT-plan 5 fields	IMPT-plan 2 fields
PTV	60.0 Gy	61.0 Gy	60.9 Gy
Brain	13.1 Gy	11.5 Gy	5.8 Gy
Brain stem	18.2 Gy	12.2 Gy	0.0 Gy
Brain stem PRV	18.4 Gy	12.4 Gy	0.0 Gy
Medulla	25.0 Gy	18.6 Gy	0.0 Gy
Medulla PRV	25.2 Gy	19.1 Gy	0.0 Gy
Optic chiasm	1.4 Gy	1.5 Gy	0.0 Gy
Optic nerve dx	1.5 Gy	1.4 Gy	0.0 Gy
Optic nerve sin	1.4 Gy	0.9 Gy	0.0 Gy
Parotid sin	1.1 Gy	6.5 Gy	0.0 Gy

10.5 RCI, target dose uniformity and irradiated volume

The values of the dose statistics, target dose uniformity (u) radiation conformity index (RCI_i) and the irradiated volume (IV) are shown in Table 10.8 to Table 10.14. In the left sided mammary carcinoma cases, with the left lung and the heart as the primary OARs, the IMPT technique showed the best treatment plans with improved target dose uniformity, RCI and a reduction in the irradiated volumes.
In both prostate cases the target dose uniformity, RCI and irradiated volume differ only slightly between the three techniques.
For the parotid cancer, the IMPT plan shows a great improvement compared with the photon plans. The target dose uniformity, RCI and irradiated volume were all improved with the IMPT technique.
Overall the proton plans generated significantly lower irradiated volumes compared with the photon techniques and improved target dose uniformity in the mammary and parotid cases. In the prostate cases, the only deeply lying tumor, the best target dose uniformity was produced by the IMXT-plans. Case 1.1 shows the most significant decrease in the *u*-

value with a 62.5% lower value in the CTV and 60% lower value in the PTV in comparison with the conventional plan.

Table 10.8 Case 1.1

CTV	D_{max} [Gy]	D_{min} [Gy]	$D_{average}$ [Gy]	$D_{95\%}$ [Gy]	$D_{5\%}$ [Gy]	$TV_{95\%}$	u	RCI_i	$IV_{50\%}$
Conventional plan	53.3	47.3	49.9	48.0	52.2		0.08		1113 cm^3
IMRT-plan 4 fields	53.1	49.8	51.5	50.3	52.6		0.05		1279 cm^3
IMRT-plan 9 fields	53.4	48.8	50.6	49.5	52.3		0.06		2126 cm^3
IMPT-plan 2 fields	53.0	47.0	51.0	50.0	51.8		0.03		1030 cm^3
PTV									
Conventional plan	55.8	44.4	49.8	47.5	52.5	4.7	0.10	0.67	
IMRT-plan 4 fields	55.4	43.5	51.3	49.6	52.4	5.3	0.06	0.59	
IMRT-plan 9 fields	56.0	46.4	51.0	49.1	53.1	5.8	0.08	0.54	
IMPT-plan 2 fields	53.8	42.3	51.1	50.0	51.9	4.2	0.04	0.76	

Table 10.9 Case 1.2

CTV	D_{max} [Gy]	D_{min} [Gy]	$D_{average}$ [Gy]	$D_{95\%}$ [Gy]	$D_{5\%}$ [Gy]	$TV_{95\%}$	u	RCI_i	$IV_{50\%}$
Conventional plan	52.6	47.6	50.1	48.3	51.7		0.07		2325 cm^3
IMRT-plan 3 fields	52.4	49.3	50.9	49.8	51.8		0.04		2142 cm^3
IMRT-plan 9 fields	53.7	48.1	50.8	49.3	52.7		0.07		2375 cm^3
IMPT-plan 2 fields	53.3	48.2	51.0	49.9	52.0		0.04		1628 cm^3
PTV									
Conventional plan	57.4	42.8	50.3	47.6	54.0	7.9	0.13	0.54	
IMRT-plan 3 fields	60.2	36.6	51.2	49.4	52.7	7.7	0.06	0.55	
IMRT-plan 9 fields	59.3	43.6	51.4	48.8	54.3	6.6	0.11	0.65	
IMPT-plan 2 fields	54.3	33.9	51.1	49.7	52.3	5.8	0.05	0.73	

Table 10.10 Case 1.3

CTV	D_{max} [Gy]	D_{min} [Gy]	$D_{average}$ [Gy]	$D_{95\%}$ [Gy]	$D_{5\%}$ [Gy]	$TV_{95\%}$	u	RCI_i	$IV_{50\%}$
Conventional plan	52.5	49.8	50.8	49.9	52.5		0.05		2378 cm^3
IMRT-plan 4 fields	53.9	47.7	50.7	48.6	53.3		0.09		2595 cm^3
IMRT-plan 9 fields	54.5	44.5	50.3	46.3	53.9		0.15		3487 cm^3
IMPT-plan 3 fields	53.4	48.8	51.0	50.4	51.9		0.03		1541 cm^3
PTV									
Conventional plan	56.2	42.9	50.5	47.7	53.9	4.4	0.12	0.48	
IMRT-plan 4 fields	61.1	32.3	50.7	47.4	53.8	3.9	0.12	0.48	
IMRT-plan 9 fields	62.8	34.6	50.7	46.1	55.1	5.0	0.18	0.37	
IMPT-plan 3 fields	55.8	28.3	51.1	49.7	52.4	3.1	0.05	0.62	

Table 10.11 Case 2.1

Prostate	D_{max} [Gy]	D_{min} [Gy]	$D_{average}$ [Gy]	$D_{95\%}$ [Gy]	$D_{5\%}$ [Gy]	$TV_{95\%}$ [%]	u	RCI_i	$IV_{50\%}$
Conventional plan	79.2	72.6	77.6	74.3	79.1		0.06		853 cm^3
IMRT-plan 7 fields	79.2	73.6	77.1	76.5	78.0		0.02		895 cm^3
IMPT-plan 2 fields	81.7	76.0	78.6	77.2	80.0		0.04		771 cm^3
Prostate + 4/6 mm									
Conventional plan	79.3	72.6	77.6	74.2	79.1		0.06		
IMRT-plan 7 fields	80.0	73.6	77.4	76.4	78.7		0.03		
IMPT-plan 2 fields	82.6	75.6	79.1						
Prost + 1cm									
Conventional plan	79.6	72.6	77.1	72.7	79.0	1.4	0.08	0.86	
IMRT-plan 7 fields	80.0	73.2	77.4	75.9	78.6	1.9	0.03	0.63	
IMPT-plan 2 fields	83.3	67.2	79.0	76.8	80.9	1.5	0.05	0.81	

Table 10.12 Case 2.2

Prostate	D_{max} [Gy]	D_{min} [Gy]	$D_{average}$ [Gy]	$D_{95\%}$ [Gy]	$D_{5\%}$ [Gy]	$TV_{95\%}$ [%]	u	RCI_i	$IV_{50\%}$
Conventional plan	79.0	76.0	77.5	76.2	78.7		0.03		835 cm^3
IMRT-plan 4 fields	82.3	78.1	79.7	78.8	81.0		0.03		2191 cm^3
IMPT-plan 2 fields	81.5	76.8	78.8	77.5	80.1		0.03		787 cm^3
Prostate + 4/6 mm									
Conventional plan	79.3	76.0	77.5	76.0	78.9		0.04		
IMRT-plan 4 fields	82.3	77.7	79.7	78.7	80.8		0.03		
IMPT-plan 2 fields	82.8	75.80	79.1	77.6	80.7		0.04		
Prost + 1cm									
Conventional plan	79.7	73.8	77.2	74.6	79.1	1.6	0.06	0.78	
IMRT-plan 4 fields	82.2	70.8	79.4	76.8	80.9	2.3	0.05	0.54	
IMPT-plan 2 fields	83.0	67.0	79.0	77.0	80.7	1.6	0.05	0.81	

Table 10.13 Case 3.1

PTV	D_{max} [Gy]	D_{min} [Gy]	$D_{average}$ [Gy]	$D_{95\%}$ [Gy]	$D_{5\%}$ [Gy]	$TV_{95\%}$	u	RCI_i	$IV_{50\%}$
Conventional plan	72.4	61.5	69.1	64.6	71.5	2.9	0.10	0.50	576 cm^3
IMRT-plan 4 fields	74.2	64.0	69.6	67.9	71.1	2.9	0.05	0.50	701 cm^3
IMPT-plan 3 fields	72.8	51.1	69.1	67.8	70.2	2.3	0.03	0.62	508 cm^3

Table 10.14 Case 3.2

PTV	D_{max} [Gy]	D_{min} [Gy]	$D_{average}$ [Gy]	$D_{95\%}$ [Gy]	$D_{5\%}$ [Gy]	$TV_{95\%}$	u	RCI_i	$IV_{50\%}$
Conventional plan	63.2	51.0	61.0	57.8	62.6	1.7	0.08	0.28	236 cm^3
IMRT-plan 5 fields	65.5	58.5	61.3	59.7	63.1	1.6	0.06	0.30	342 cm^3
IMPT-plan 2 fields	68.1	20.0	61.0	59.5	62.5	1.1	0.05	0.42	220 cm^3

The ability to deliver the required dose varies between different patients and due to the fact that every patient must have a custom made treatment plan. Even if just a few numbers of cases have been evaluated in this study, the tendencies of the different treatment techniques can be noticed. In all of the cases presented in this study, independent of the patient's anatomy, the IMPT treatment technique tends to produce the best treatment plans.
In photon beam radiation therapy, an increase in number of beams often results in a more conformal target dose distribution though this is at the expense of low doses delivered to a larger volume of healthy tissue. The problem to solve when producing treatments plans is to avoid as much of the risk organs as possible and at the same time deliver a uniform dose to the target. The probability of long term complications caused by low doses in tissue, not classified as the primary OARs, is not very well known.
Typically the IMPT technique does not require as many beams as the IMXT technique and hence the amount of irradiated healthy tissue decreases with a maintained tumor control. This effect is shown in the low to intermediate dose range in all the DVHs representing the body, **Error! Reference source not found.** to Figure 10.7.

What must be careful considered in clinical work is the internal organ movements, especially in the case of scanned proton beams. Accurately defined target volumes are also of significant importance due to the finite range of the protons.

Another effect that one must be aware of in proton treatment is the production of secondary neutrons. The neutrons are produced by nuclear interactions in the material, placed in the beam line. In the spot scanned technique the influence of the neutrons to the integral dose distribution are very low and can, in the treatment region, be neglected [41]. In passive scattering systems, the contribution to the integral dose by the neutrons could be much higher [39]. Neutrons have a large biological effect in respect to both photons and protons and this additional dose can increase the risk of radiation induced cancer. Since the spot scanning technique is the technique used in the IMPT the neutrons should not give rise to any serious complications.

It is difficult to compare treatment plans produced in different departments with different patients. There are variations in the dose distribution depending on the patient anatomy but the delineation of the structures can also vary. In one comparative article about prostate treatment by Mock et al. [29] the rectum wall, excluding the PTV, was defined as a separate structure. In this study the rectum and the bladder, both infiltrated in the prostate, received much more dose than it did in that article. A plausible cause of these differences may be the individual differences in the structure delineation between oncologists.

11 Conclusion

This study has shown that proton therapy may have some potential for improving the outcome for patients with any of the studied tumor types. In all cases IMPT produces excellent target dose uniformity and better or equal RCI with significantly lower irradiated volumes compared with the photon techniques.

In the cases with superficial located tumors, the breast carcinoma cases and the parotid tumor cases, substantial lower mean doses in the OARs were obtained for the IMPT-plans. Generally it also shows a decrease in the low to the intermediate dose range delivered to the OARs close to the target. In structures there was a significant dose reduction, and in some volumes no dose at all, in structures located at a distance from the target and not in the primary beam line. This is particularly clear in the cancer of the parotid case.

The results of this study suggest that the IMPT technique is well suitable for tumors located close to critical structures. In this study the most improved plans were obtained in the parotid cancer cases, a tumor in the head and neck region with many critical structures around it.

12 Acknowledgements

I would like to deeply thank the various people who, during the several months in which this project lasted, provided me with all help and assistance.
First I would like to express my gratitude to the supervisors of this project, Per Nilsson and Per Engström for giving me the great opportunity to study proton therapy and for all the help during this project.
I am grateful to Dr Elisabeth Kjellén who provided the necessary delineations in the CT-scans.
I am also pleased to acknowledge Jonas Andersson at Raysearch laboratory who helped me with all the questions concerning Orbit Workstation.

I also owe enormous dept of gratitude to my boyfriend, Gustav Darpö, for all his patience and corrections of the text and for always being willing to help me.
I would also like to forward a special thank you to all my student colleagues during the past 4.5 years.

13 References

[1] Swedish cancer society
Om strålbehandling
http://www.cancerfonden.se/upload/Dokument/Patientbroschyrer/stralbehandling_2005.pdf

[2] *Strålbehandling vid cancer, en systematisk litteraturöversikt*
SBU, The Swedish Council on Technology Assessment in Health Care

[3] Wikipedia
http://en.wikipedia.org

[4] SPTC Swedish Proton Therapy Center
Val av utrustning för strålbehandling med protoner
http://www.brainstorming.se/Bild/val_av_utrustning.pdf 2003

[5] Q. Wu, R. Mohan, A. Niemierko, R Schmidt-Ullrich
Optimization of intensity-modulated radiotherapy plans based on the equivalent uniform dose
Int J Radiat Oncol Biol Phys (2002) Vol.52 pp. 224-235

[6] J. Johansson
Comparative treatment planning in radiotherapy and clinical impact of proton relative biological effectiveness
Thesis, Uppsala University

[7] *The December 1962 report of the RBE committee to the ICRP and ICRU in it's implications for the assessment of proton radiation exposure in space*
Bureau of Medicine and Surgery, Report no.26

[8] A. Brown. H. Suit
The centenary of the discovery of the Bragg peak
Radiother Oncol (2004) Vol.73 pp. 265-268

[9] Massachusetts General Hospital Cancer Center
Northeast Proton Therapy Centre
http://neurosurgery.mgh.harvard.edu/ProtonBeam/NPTCbrochure.pdf

[10] OncoLinc™ Abramson Cancer Center of the University of Pennsylvania
Differences between Protons and X-rays
http://www.oncolink.org/treatment/article.cfm?c=9&s=70&id=210

[11] Synthesis, UC Davis Cancer Center
History of proton beam therapy
http://www.ucdmc.ucdavis.edu/synthesis/features/history.html

[12] R. R. Wilson
Radiological Use of Fast Protons

[13] OncoLinc™ Abramson Cancer Center of the University of Pennsylvania
History of Proton Therapy
http://www.oncolink.org/treatment/article.cfm?c=9&s=70&id=209

[14] PARTICLES, Newsletter number 36 July 2005
http://ptcog.web.psi.ch/ptcentres.html

[15] E. Keil., D. Trbojevic
Fixed field alternating gradient accelerators (FFAG) for hadron cancer therapy
Proceedings of 2005 Particle Accelerator Conference. Knoxville. Tennessee

[16] Proton Therapy In Russia, ITEP Medical Physics Department official site
http://www.protontherapy.itep.ru/intro.html

[17] E.Pedroni
Will we need proton therapy in the future?
Europhysics News (2000) Vol. 31 No. 6

[18] M. Steneker, A. Lomax, U. Schneider
Intensity modulated photon and proton therapy for the treatment of head and neck tumors
Radiother Oncol (2006) Vol.80 pp. 263–267

[19] A. Brahme, J-E. Roos, I. Lax
Solution of an Integral Equation Encountered in Rotation Therapy
Phys. Med. Biol. (1982) Vol. 27 pp. 1221-1229

[20] T. Bortfeld
IMRT; a review and preview
Institute of Physics (2006) Vol.51 pp. 363-379

[21] Welch Cancer Center, Sheridan Memorial Hospital
Multileaf collimator (MLC)
http://welchcancercenter.org/Radiation%20Therapy%20Equip/multileaf%20collimator.htm

[22] L. Xing. A. Boyer. T. Pawlicki, G. Luxton
Overview of IMRT Treatment Planning System
Department of Radiation Oncology. Stanford University

[23] T. Knöös, W. Wieslander, L. Cozzi, C. Brink, A. Fogliata, D. Albers, H. Nyström, S. Lassen
Comparison of dose calculation algorithms for treatment planning in external photon beam therapy for clinical situations
Phys. Med. Biol. (2006) Vol. 51 pp. 5785-5807

[24] G.Gordon Steel
Basic clinical radiobiology, 3rd edition
ISBN-10: 0 340 80783 0

[25] A. Niemierko
Reporting and analyzing dose distributions: A concept of equivalent uniform dose
Medical Physics (1997) Vol.24 pp. 103-110

[26] A. Niemierko
A generalized concept of equivalent uniform dose (EUD)
Medical Physics (1999) Vol.26 pp. 1101 (Abstract)

[27] Swedish cancer society
Om bröstcancer
http://www.cancerfonden.se/upload/Dokument/Patientbroschyrer/Bröstcancer%20WEBB%20050927.pdf

[28] Swedish cancer society
Om prostatacancer
http://www.cancerfonden.se/upload/Dokument/Patientbroschyrer/prostatacancer_050822.pdf

[29] U. Mock, J. Bogner, D. Georg, T. Auberger, R. Pötter
Comparative Treatment Planning on Localized Prostate Carcinoma
Strahlenther Onkol (2005) Vol.181 pp. 448–455

[30] Martin Paulsson
Pleomorft Adenom i Parotis (Mixed tumor):
http://huweb.hu.liu.se/utb/program/lp/terminer/t6/oron/fall-martin-paulsson-pleomorft.pdf

[31] B. Emami. J. Lyman. A. Brown. L. Coia. M. Goitein. J.E. Munzenrider. B. Shank. L.J Solin, M. Wesson
Tolerance of normal tissue to therapeutic irradiation
Int J Radiat Oncol Biol Phys (1999) Vol.21. pp. 109-122

[32] B. Glimelius, A. Ask, G. Bjelkengren, T. Björk-Eriksson, E. Blomquist, B. Johansson, M. Karlsson, B. Zackrisson
Number of patients potentially eligible for proton therapy
Acta Oncologica (2005) Vol.44 pp. 836-849

[33] International Commission of Radiation Units and Measurements.
ICRU Report 50: Prescribing, recording, and reporting photon beam therapy, 1993

[34] OncoLinc™ Abramson Cancer Center of the University of Pennsylvania
Breast Cancer: The Basics
http://www.oncolink.org/types/article.cfm?c=3&s=5&ss=33&id=8320

[35] Danish Head and Neck Cancer Group (DAHANCA)
Retningslinier for strålebehandling af hoved-hals cancer (cavum oris. pharynx. larynx) inklusiv IMRT vejledning
http://conman.au.dk/dahanca/get_media_file.php?mediaid=57

[36] A. Bhatnagar, E. Brandner, D. Sonnik, A. Wu, S. Kalnicki, M. Deutsch, D. Heron
Intensity modulated radiation therapy (IMRT) reduces the dose to the contralateral breast when compared to conventional tangential fields for primary breast irradiation
Breast Cancer Research and Treatment (2006) Vol.96 pp. 41–46

[37] A. Lomax, L. Cella, D. Weber, J. Kurtz, R. Miralbell
Potential role of intensity-modulated photons and protons in the treatment of breast and regional nodes
Int J Radiat Oncol Biol Phys (2003) Vol.55 pp. 785-792

[38] Tommy Knöös. Ingrid Kristensen, Per Nilsson
Volumetric and dosimetric evaluation of radiation treatment plans: radiation conformity index
Int J Radiat Oncol Biol Phys (1998) Vol.42 No. 5. pp. 1169-1176

[39] D. Weber, C. Ares, A. Lomax, J. Kurtz
Radiation therapy planning with photons and protons for early and advanced breast cancer: an overview
Radiation Oncology (2006) Vol.1 pp. 22

[40] C. Bragg, J. Conway, M. Robinson
The role of intensity-modulated radiotherapy in the treatment of parotid tumors
Int J Radiat Oncol Biol Phys (2002) Vol.52 pp. 729-738

[41] U. Schneider, S. Agosteo, E. Pedroni, J. Besserer
Secondary neutron dose during proton therapy using spot scanning
Oncology Biol. Phys (2002) Vol.53 pp. 244-255

14 Appendix 1, DVH

14.1.1 Case 1.1, breast carcinoma with no affected nodes

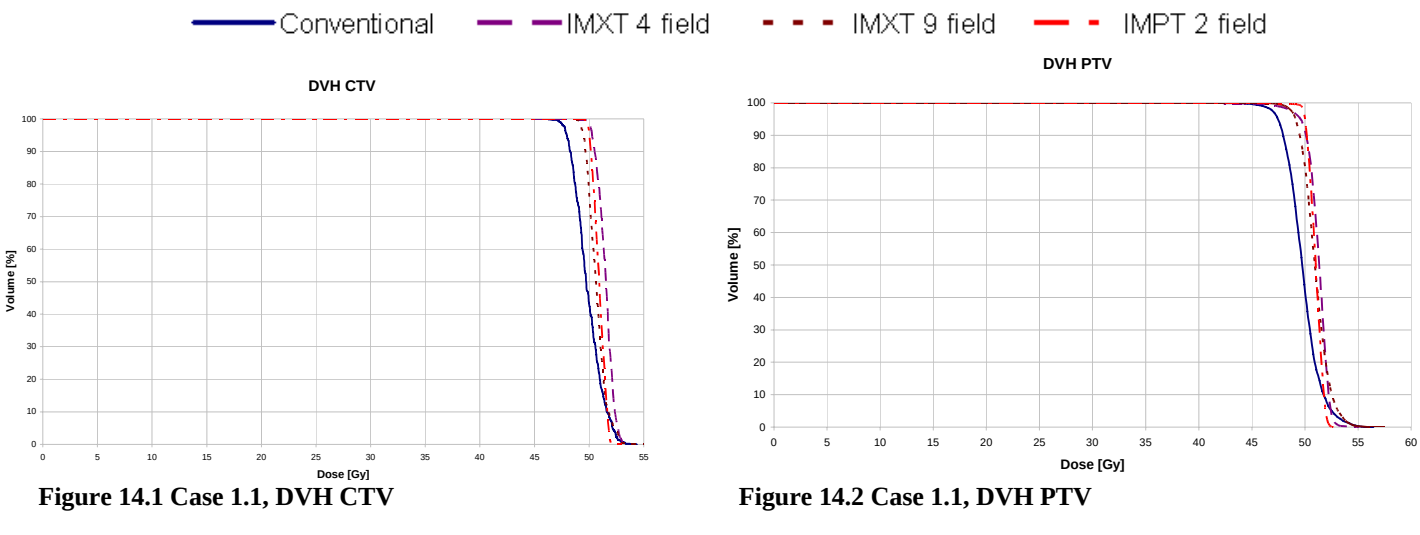

Figure 14.1 Case 1.1, DVH CTV

Figure 14.2 Case 1.1, DVH PTV

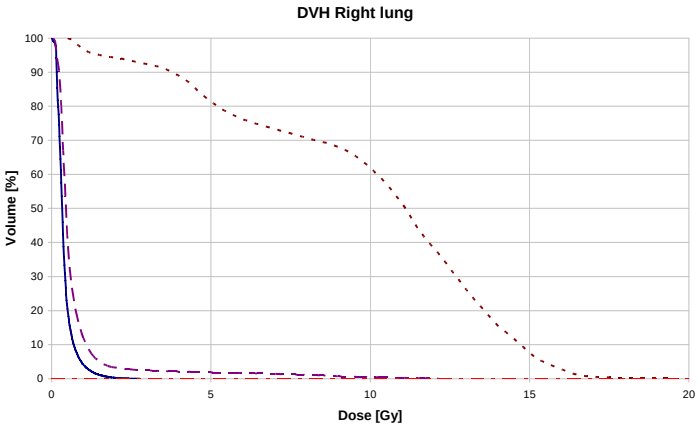

Figure 14.3 Case 1.1, DVH right lung

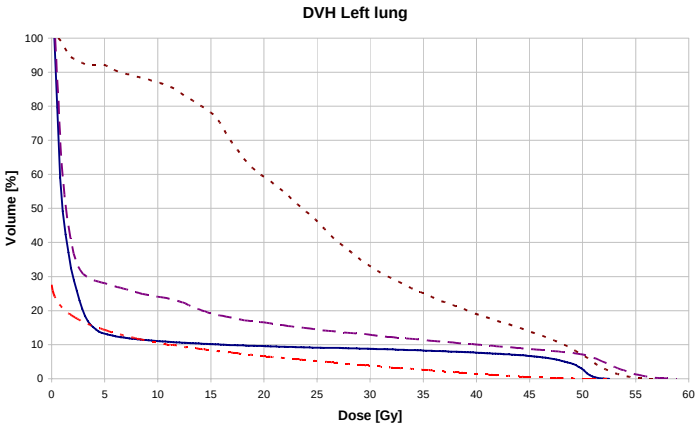

Figure 14.4 Case 1.1, DVH left lung

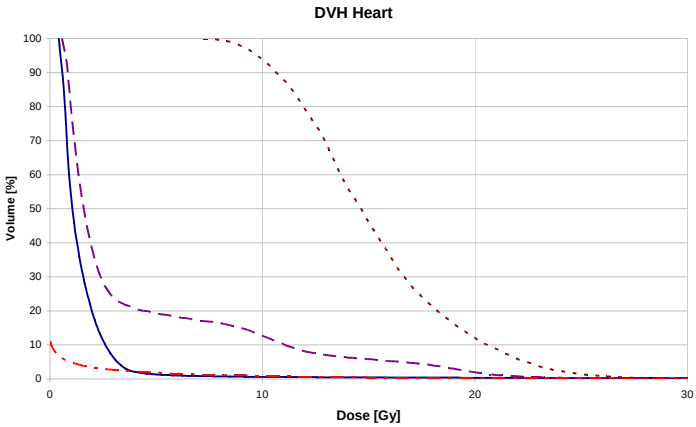

Figure 14.5 Case 1.1, DVH heart

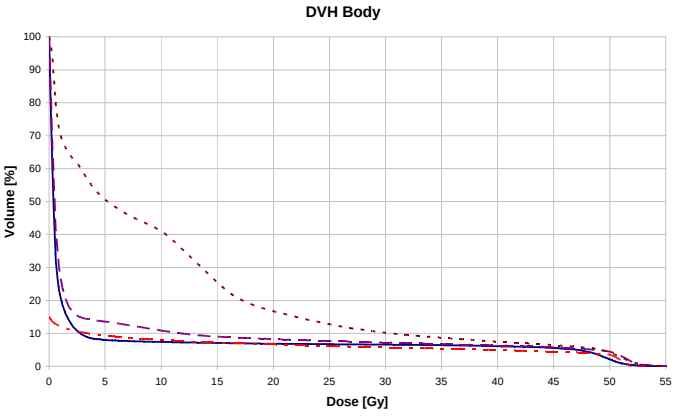

Figure 14.6 Case 1.1, DVH irradiated body

14.1.2 Case 1.2, breast carcinoma with affected nodes

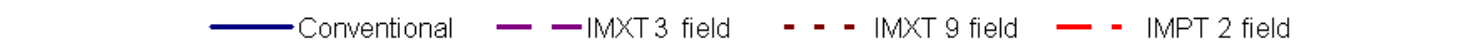

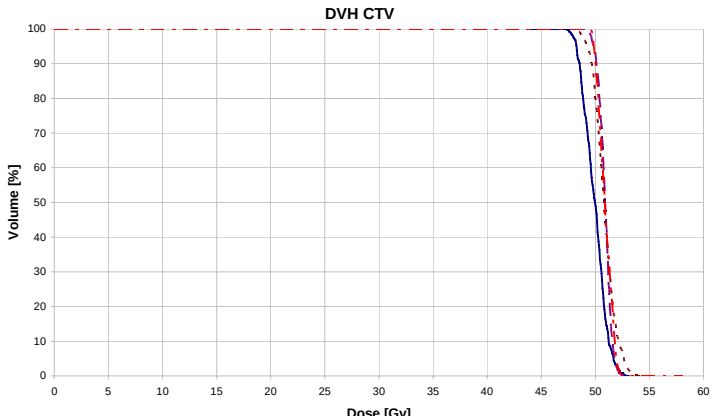

Figure 14.7 Case 1.2, DVH CTV

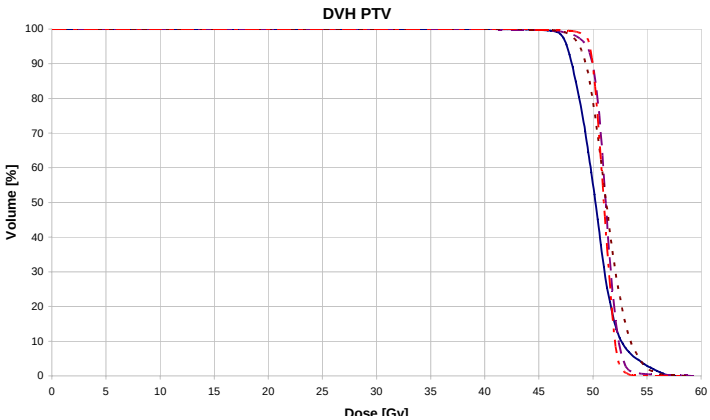

Figure 14.8 Case 1.2, DVH PTV

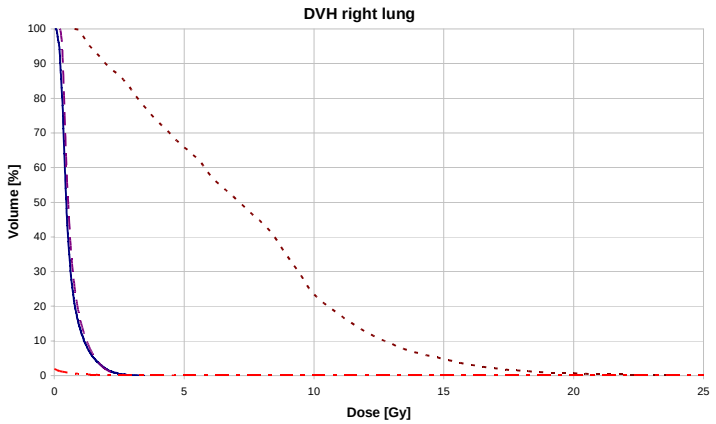

Figure 14.9 Case 1.2, DVH right lung

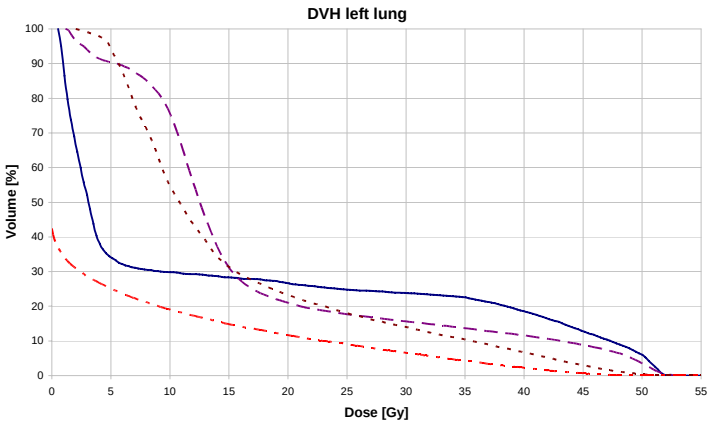

Figure 14.10 Case 1.2, DVH left lung

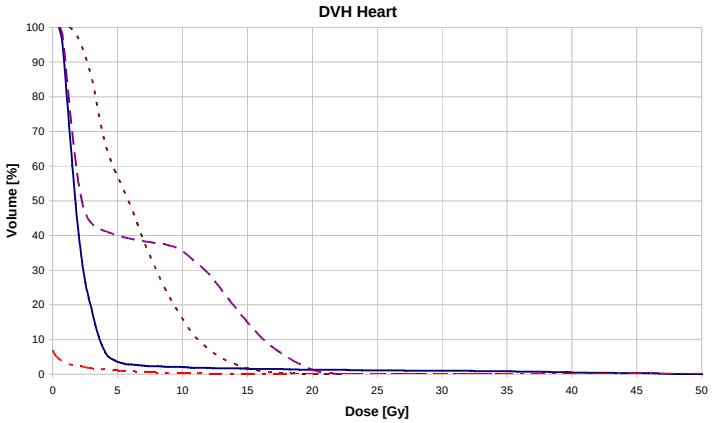

Figure 14.11 Case 1.2, DVH heart

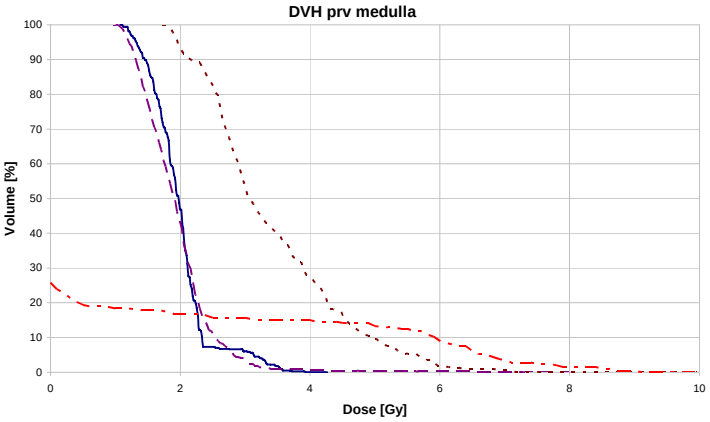

Figure 14.12 Case 1.2, DVH PRVmedulla

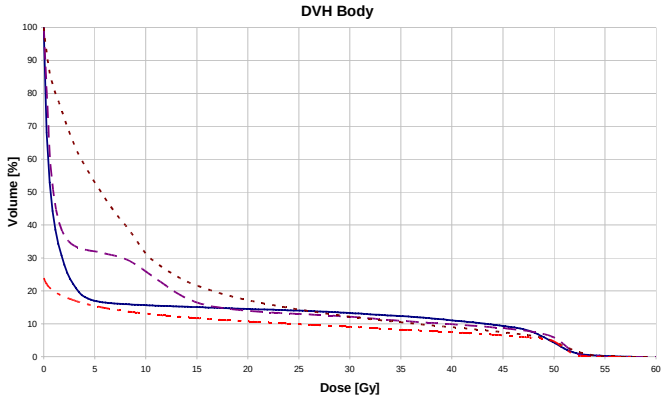

Figure 14.13 Case 1.2, DVH irradiated body

14.1.3 Case 1.3, breast cancer after radical mastectomy

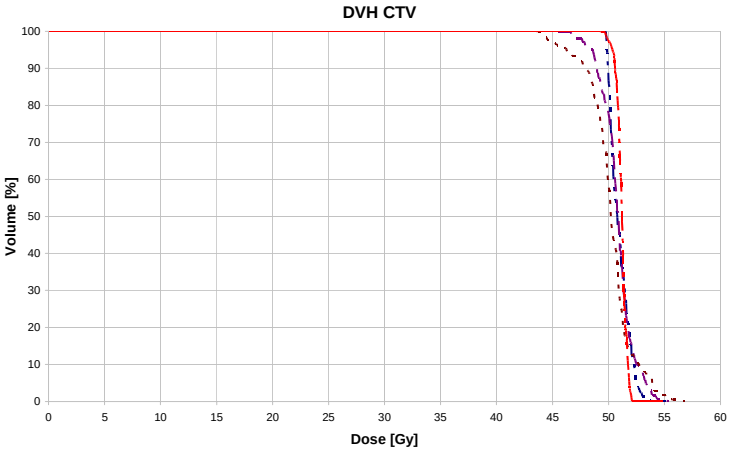

Figure 14.14 Case 1.3, DVH CTV

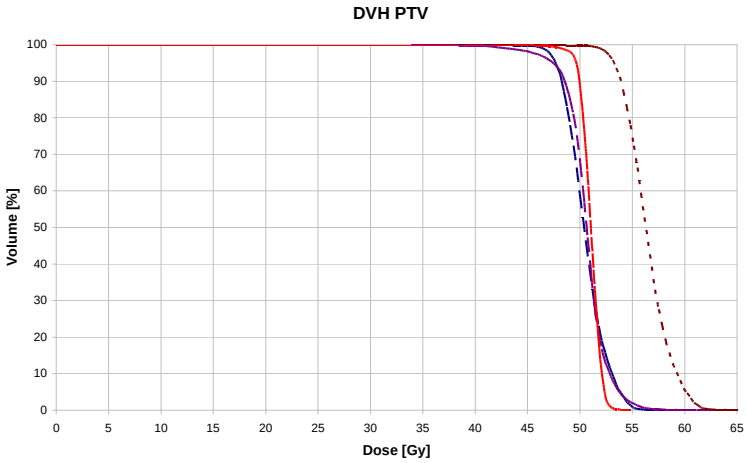

Figure 14.15 Case 1.3, DVH PTV

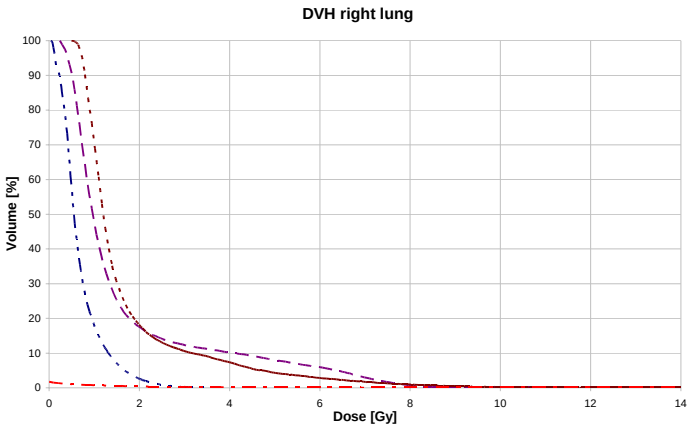

Figure 14.16 Case 1.3, DVH right lung

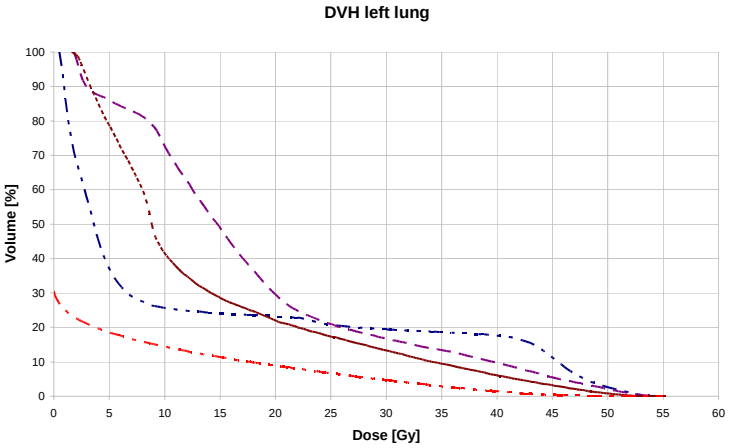

Figure 14.17 Case 1.3, DVH left lung

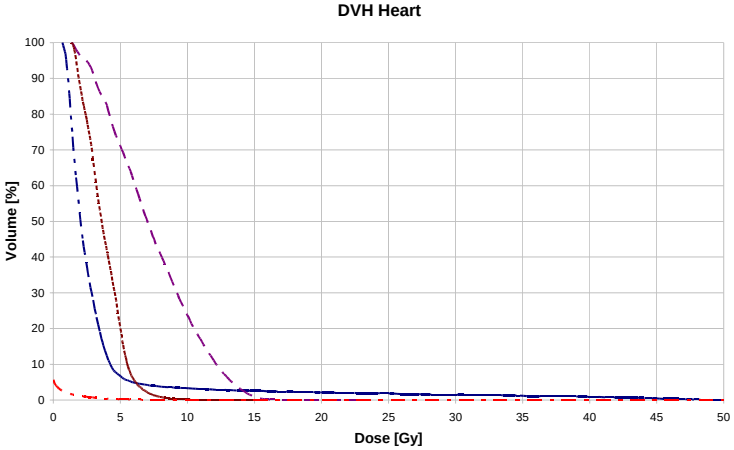

Figure 14.18 Case 1.3, DVH heart

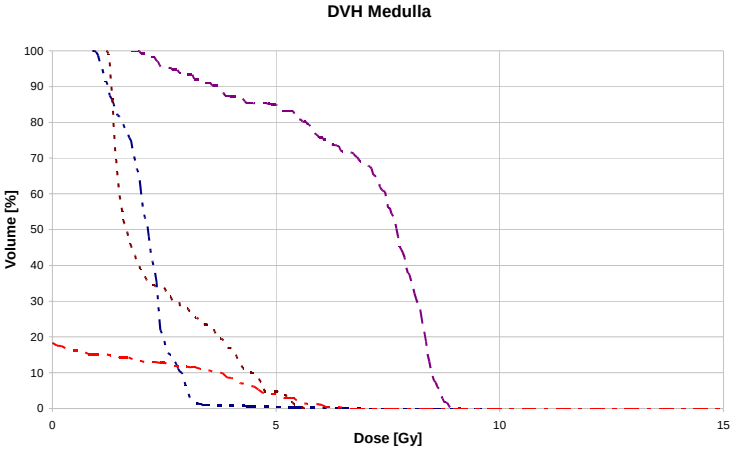

Figure 14.19 medulla

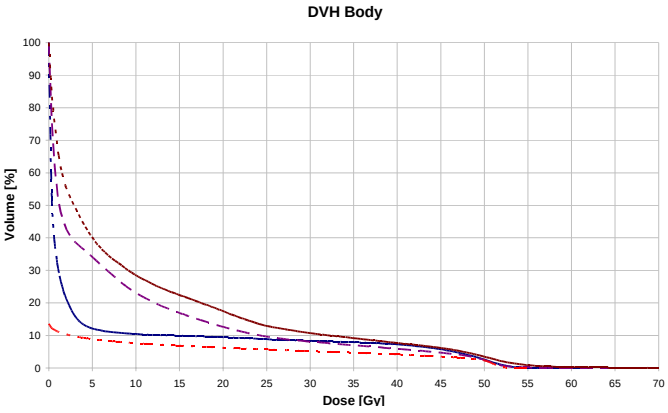

Figure 14.20 Case 1.3, DVH irradiated body

14.1.4 Case 2.1, prostate cancer

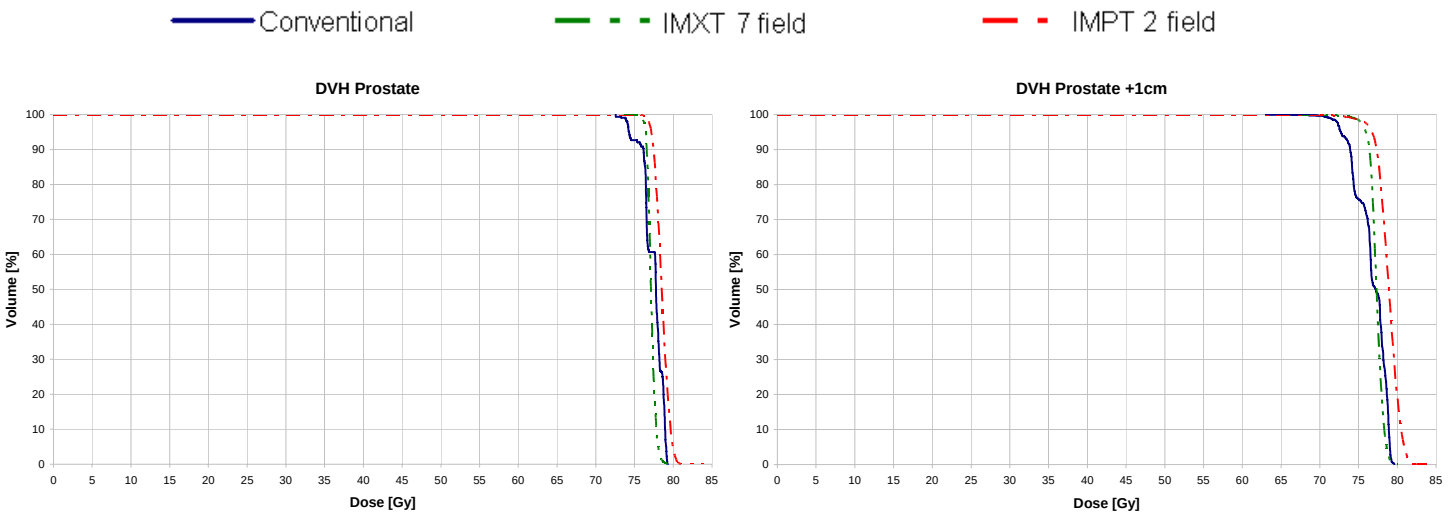

Figure 14.21 Case 2.1, DVH prostate

Figure 14.22 Case 2.1, DVH prostate + 1cm

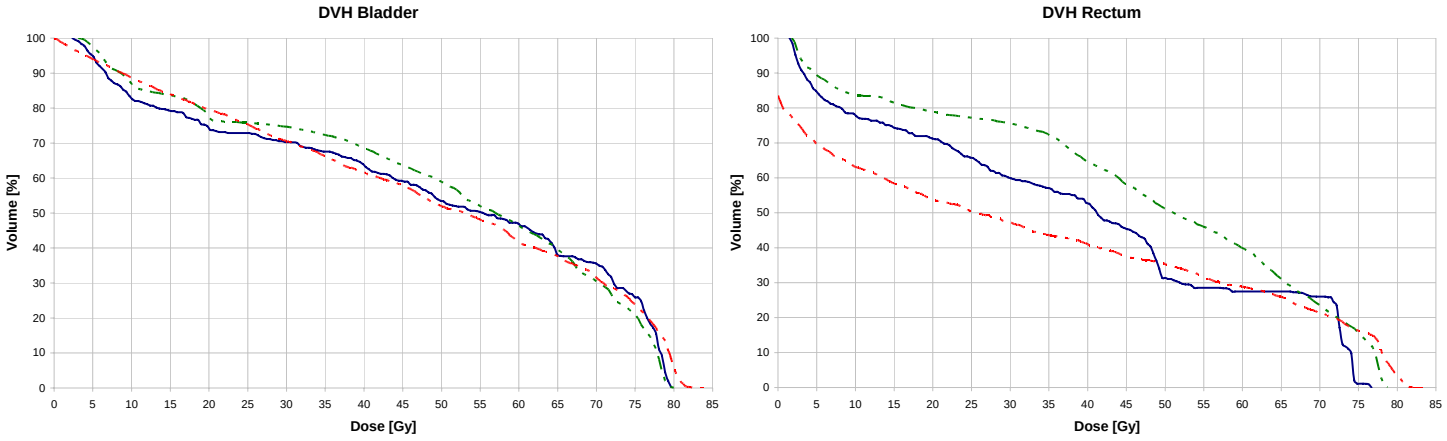

Figure 14.23 Case 2.1, DVH bladder

Figure 14.24 Case 2.1, DVH rectum

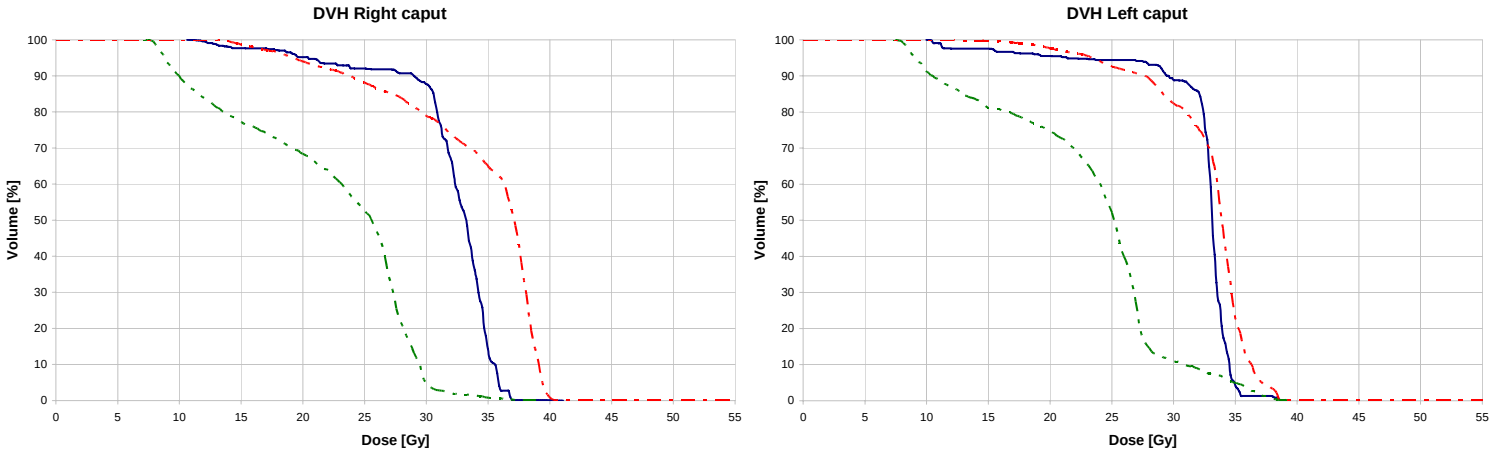

Figure 14.25 Case 2.1, DVH right caput

Figure 14.26 Case 2.1, DVH left caput

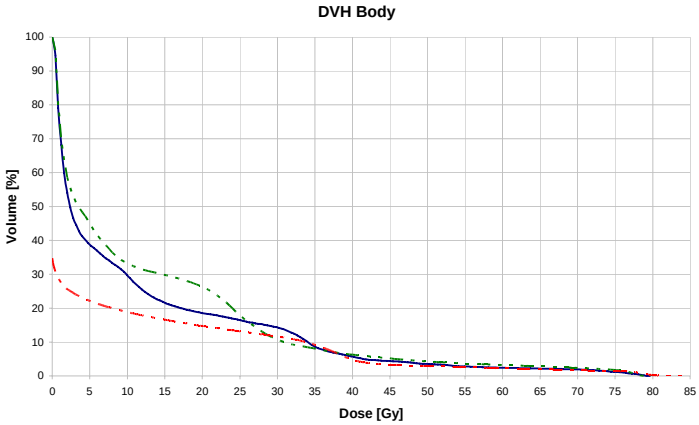

Figure 14.27 Case 2.1, DVH irradiated volume

14.1.5 Case 2.2, prostate cancer

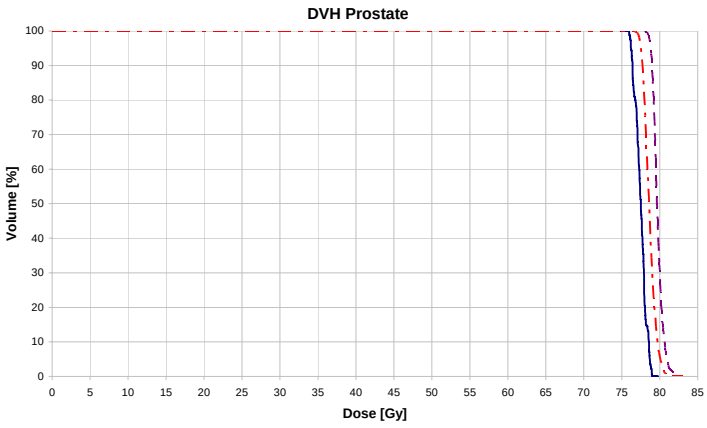

Figure 14.28 Case 2.2, DVH prostate

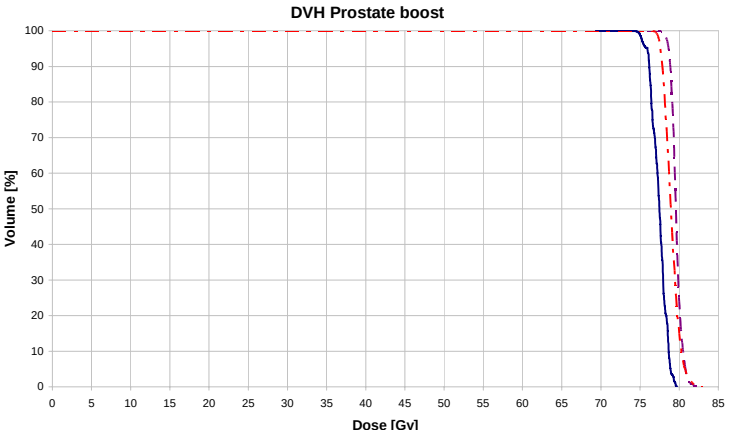

Figure 14.29 Case 2.2, DVH prostate boost

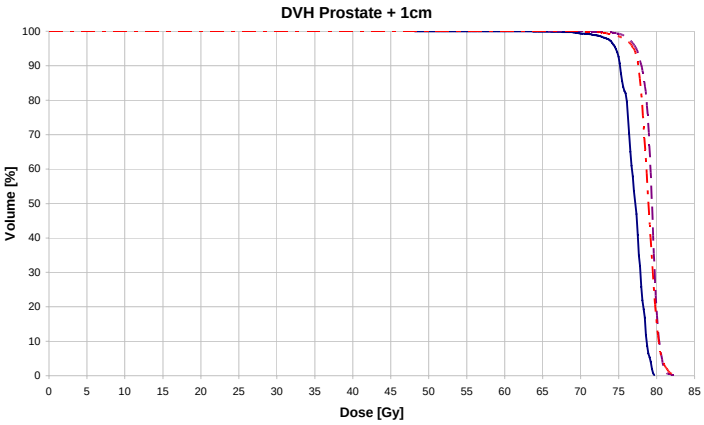

Figure 14.30 Case 2.2, DVH prostate + 1 cm

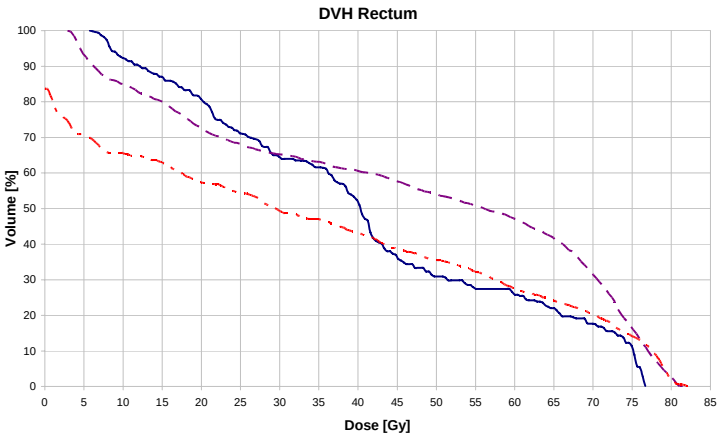

Figure 14.31 Case 2.2, DVH rectum

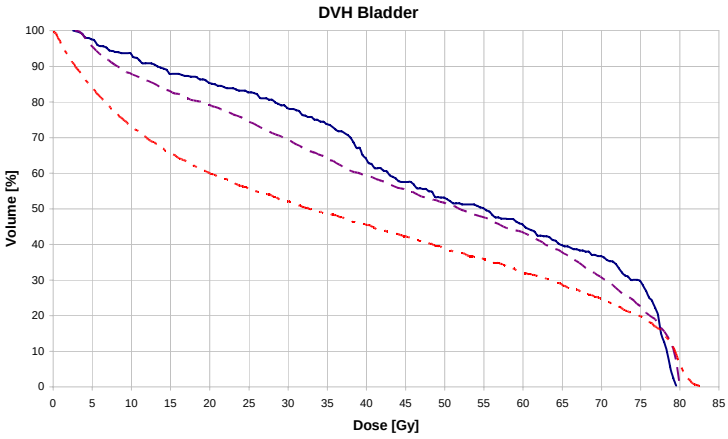

Figure 14.32 Case 2.2, DVH bladder

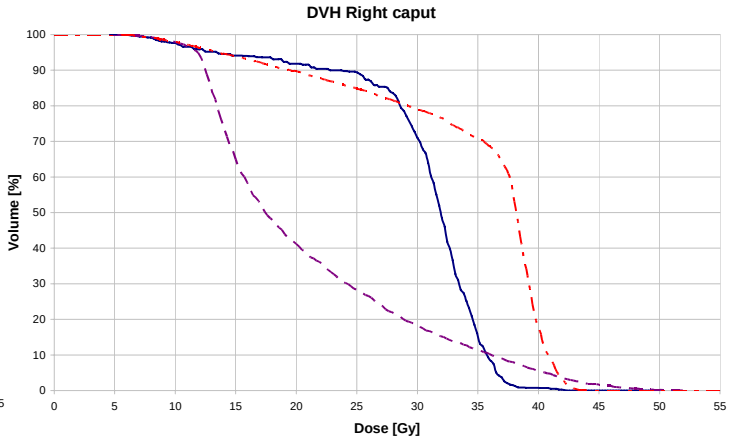

Figure 14.33 Case 2.2, DVH right caput

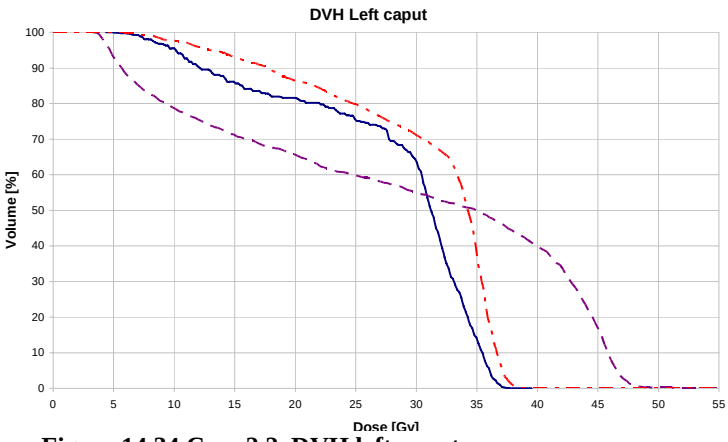

Figure 14.34 Case 2.2, DVH left caput

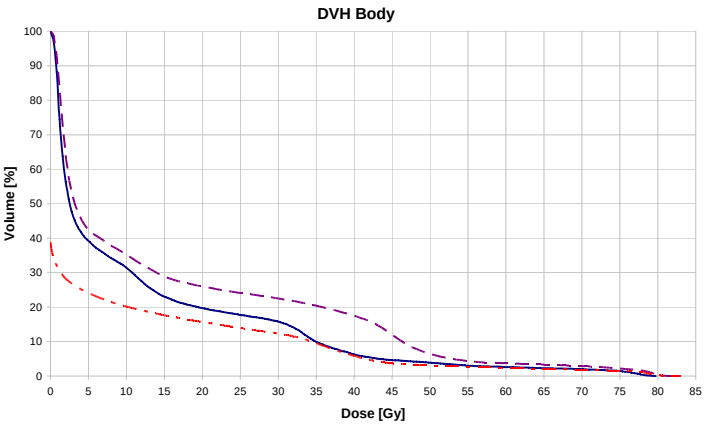

Figure 14.35 Case 2.2, DVH irradiated body

14.1.6 Case 3.1, parotid cancer

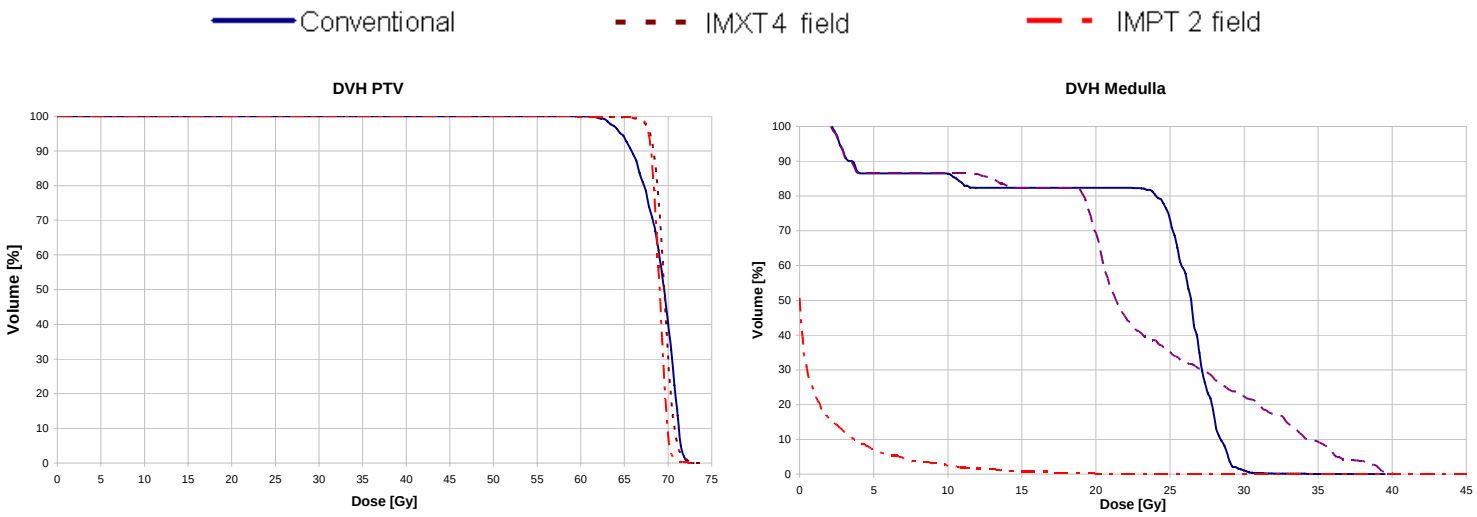

Figure 14.36 Case 3.1, DVH PTV

Figure 14.37 Case 3.1, DVH bladder

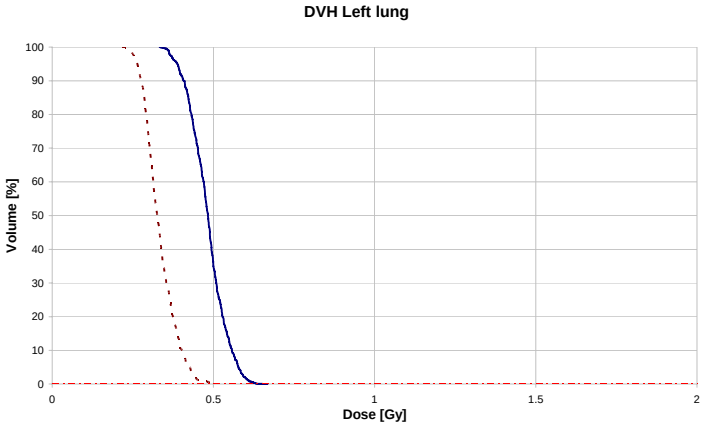

Figure 14.38 Case 3.1, DVH left lung

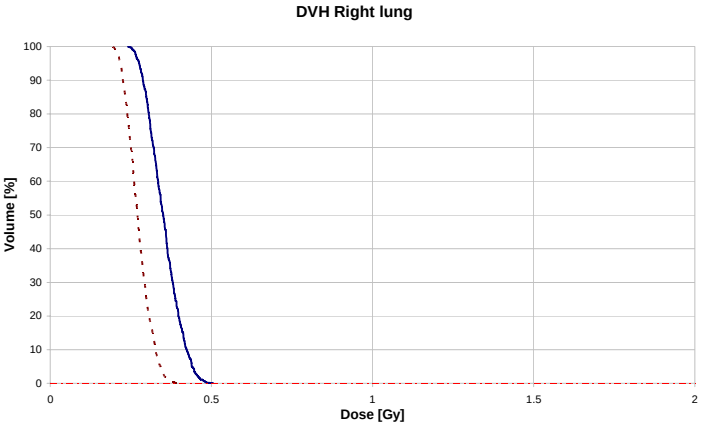

Figure 14.39 Case 3.1, right lung

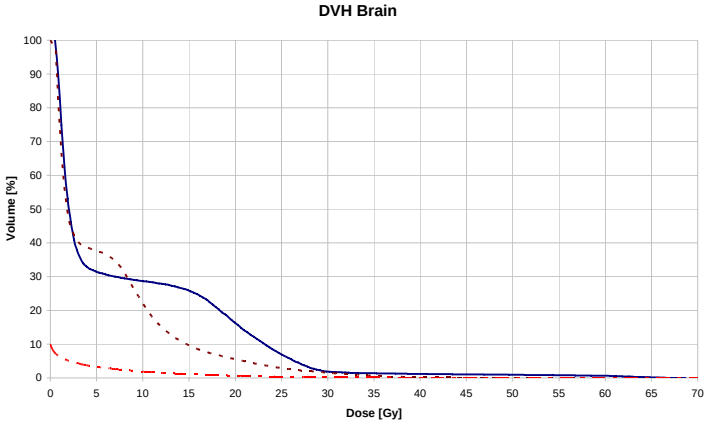

Figure 14.40 Case 3.1, DVH brain

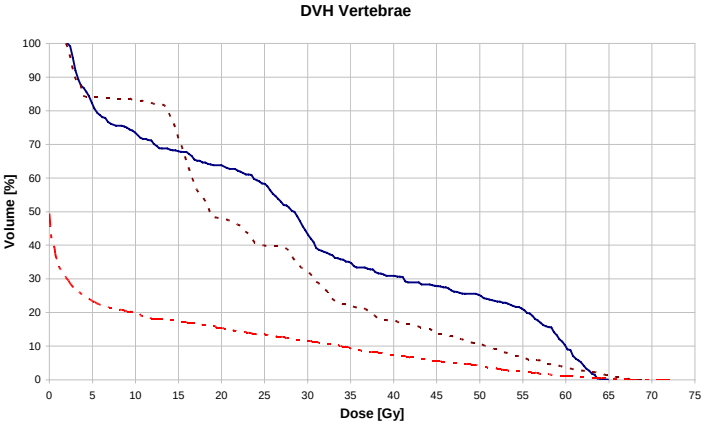

Figure 14.41 Case 3.1, DVH vertebrae

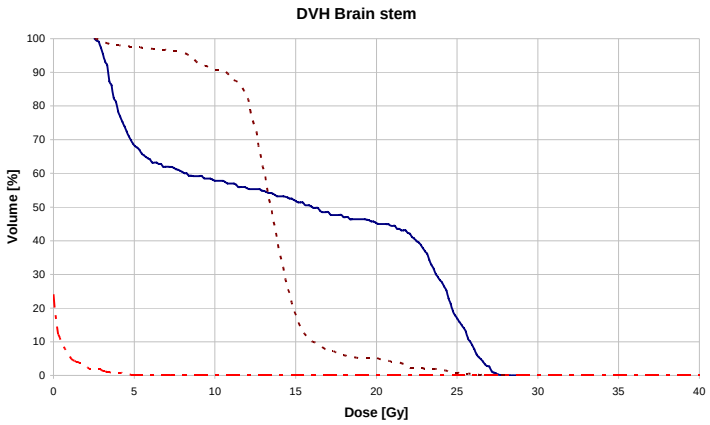

Figure 14.42 Case 3.1, DVH brain stem

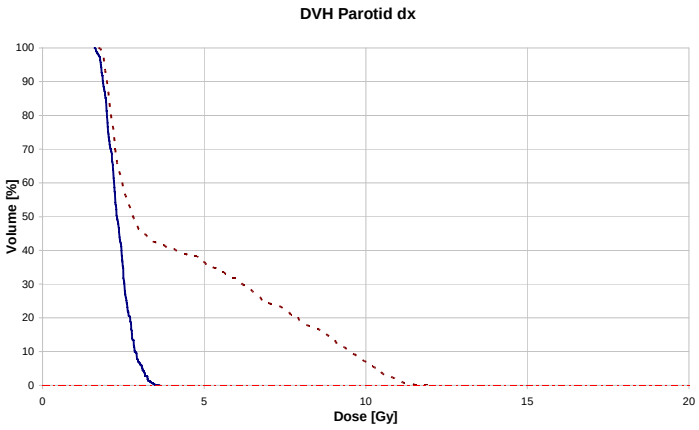

Figure 14.43 Case 3.1, DVH parotid dx

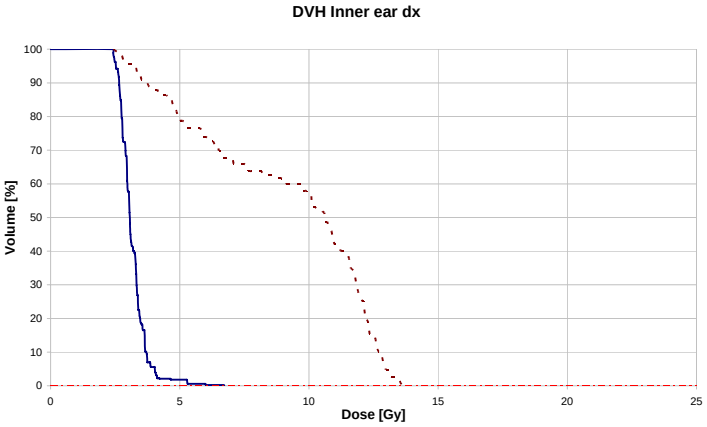

Figure 14.44 Case 3.1, DVH inner ear dx

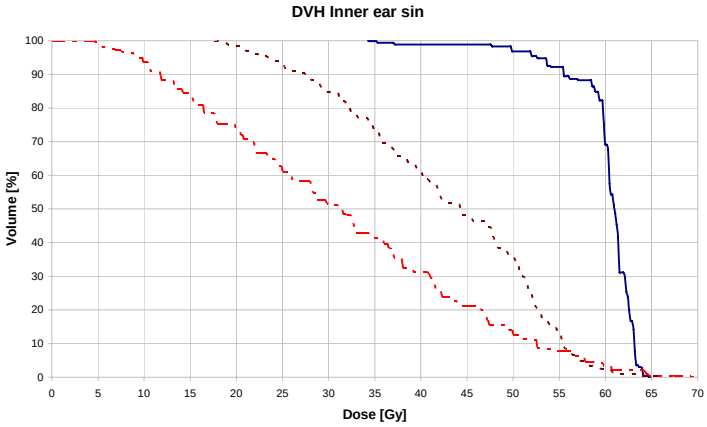

Figure 14.45 Case 3.1, DVH inner ear sin

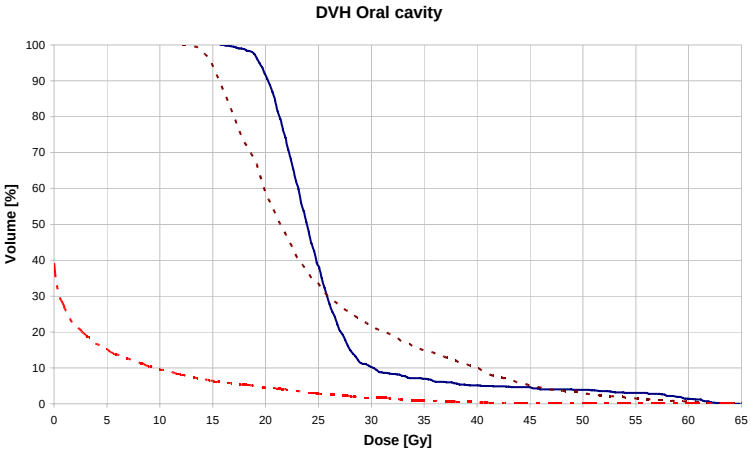

Figure 14.46 Case 3.1, DVH oral cavity

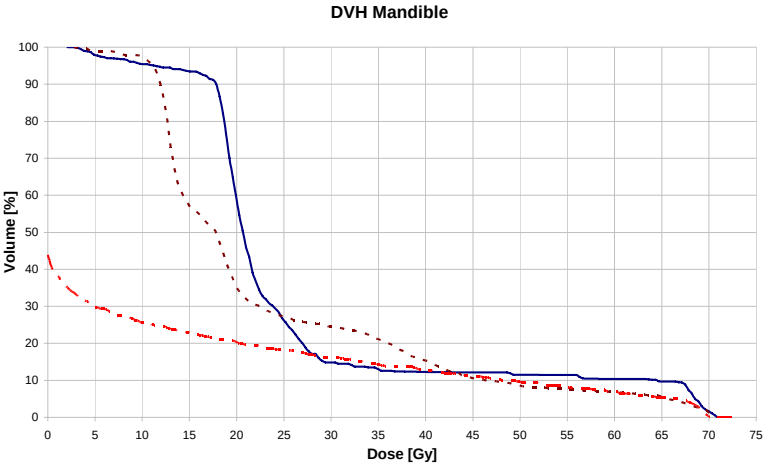

Figure 14.47 Case 3.1, DVH mandible

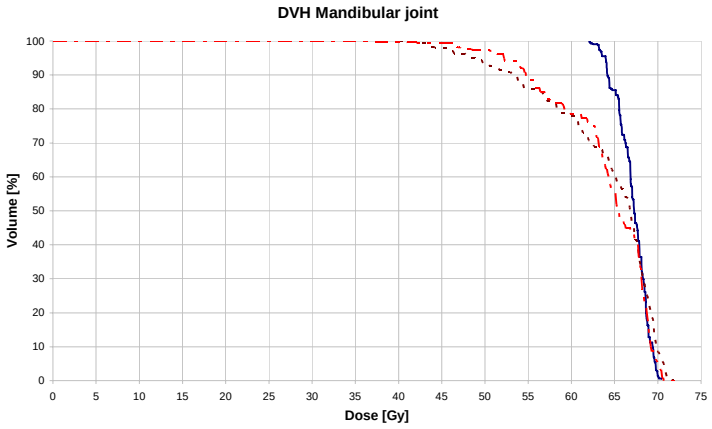

Figure 14.48 Case 3.1, DVH mandibular joint

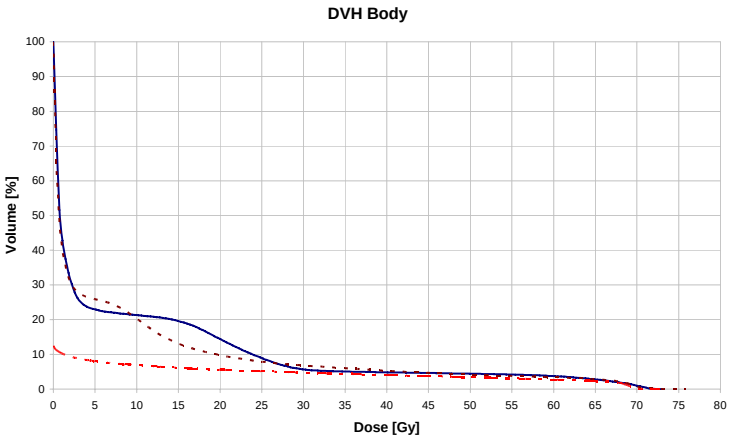

Figure 14.49 Case 3.1, DVH irradiated body

14.1.7 Case 3.2, parotid tumor

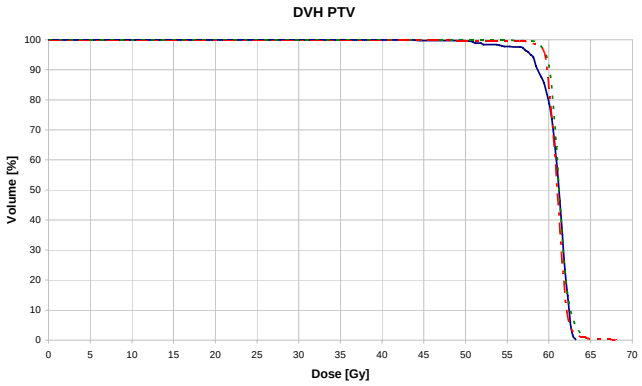

Figure 14.50 Case 3.2, DVH PTV

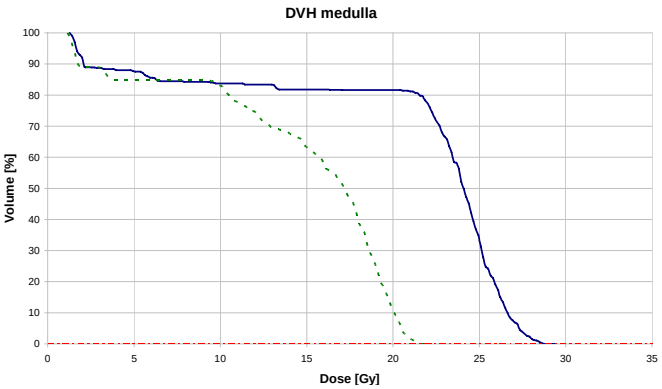

Figure 14.51 Case 3.2, DVH medulla

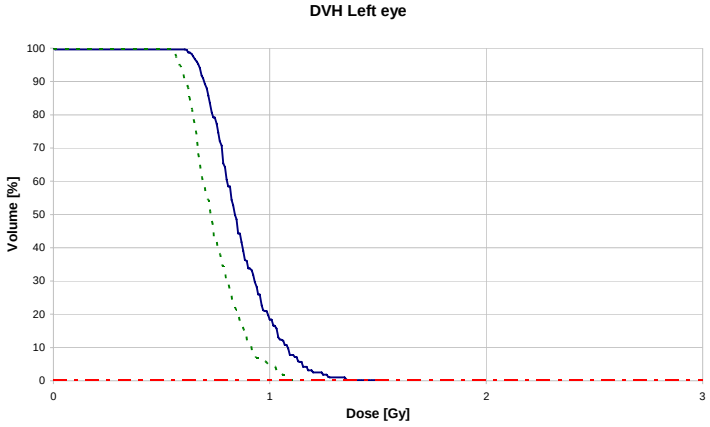

Figure 14.52 Case 3.2, DVH left eye

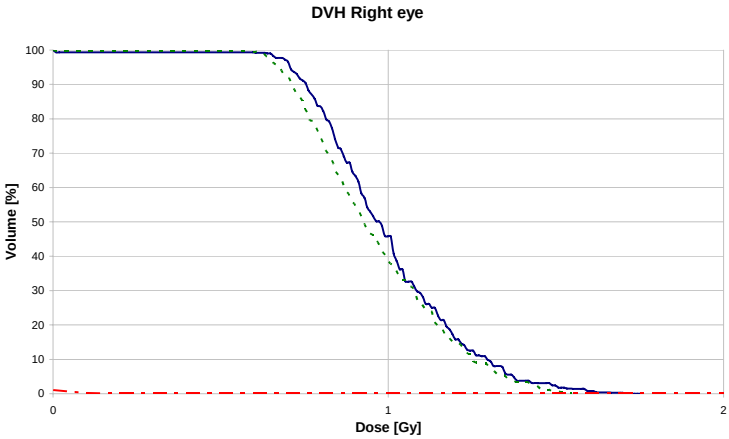

Figure 14.53 Case 3.2, DVH right eye

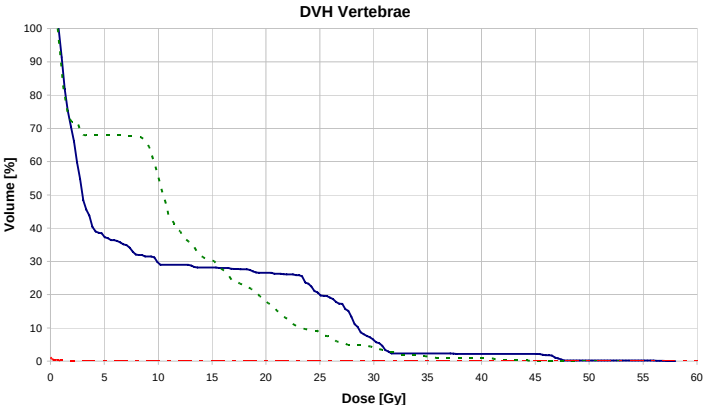

Figure 14.54 Case 3.2, DVH vertebrae

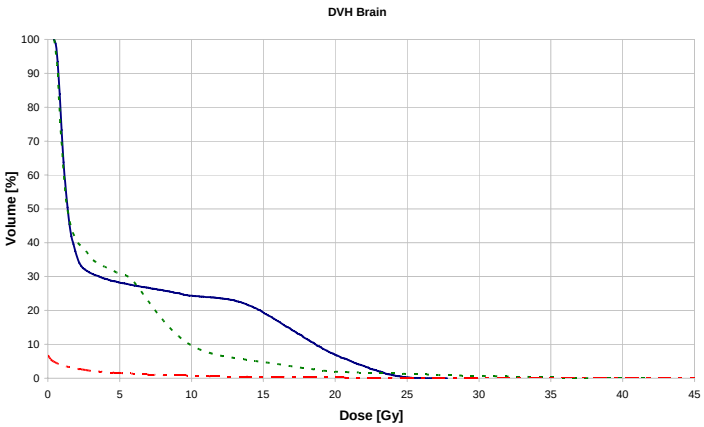

Figure 14.55 Case 3.2, DVH brain

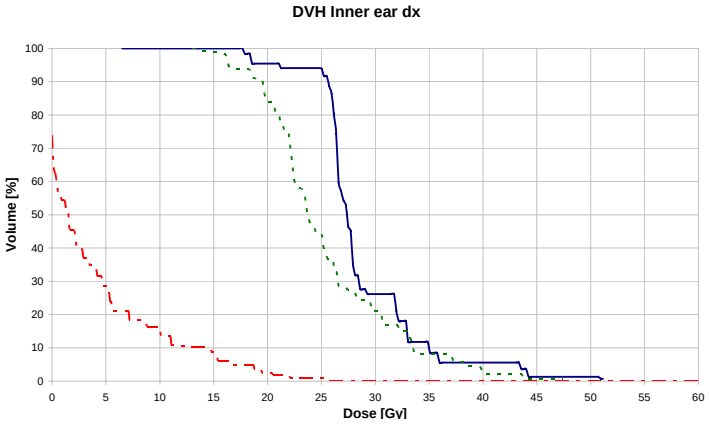

Figure 14.56 Case 3.2, DVH inner ear dx

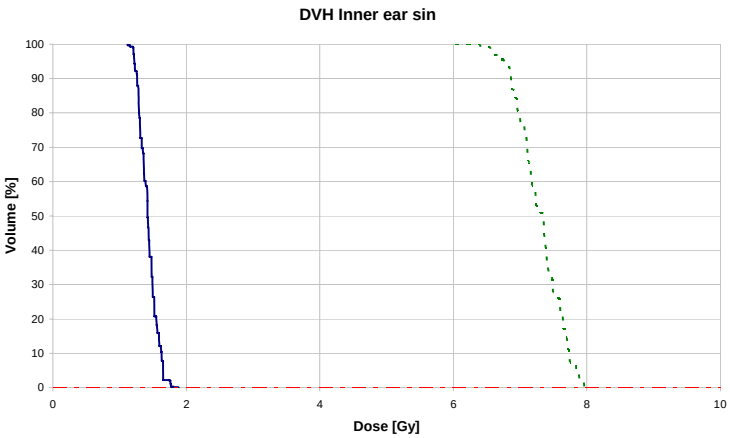

Figure 14.57 Case 3.2, DVH inner ear sin

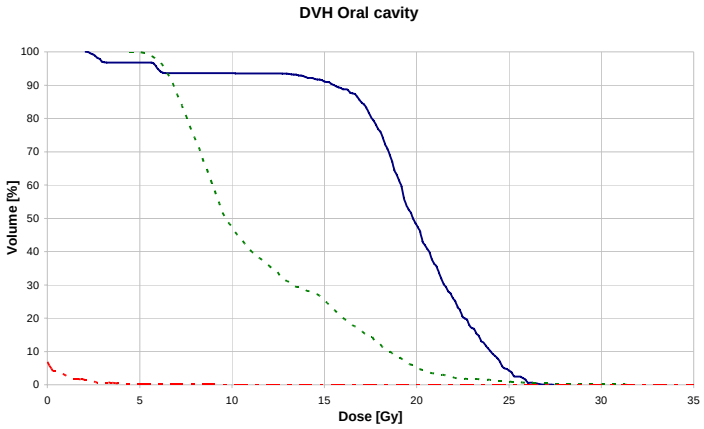

Figure 14.58 Case 3.2, DVH oral cavity

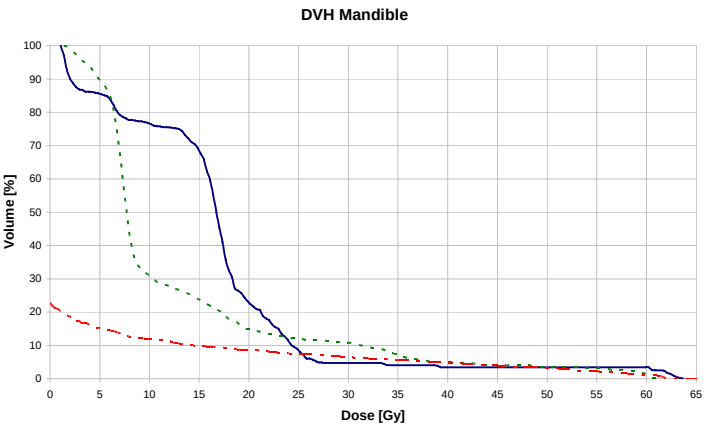

Figure 14.59 Case 3.2, DVH mandible

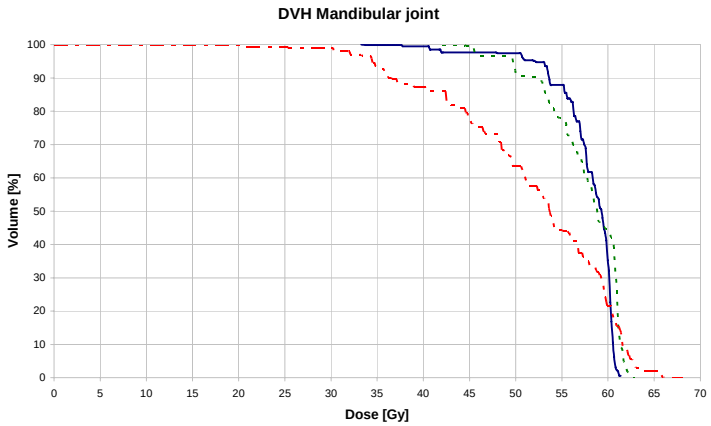

Figure 14.60 Case 3.2, DVH mandibular joint

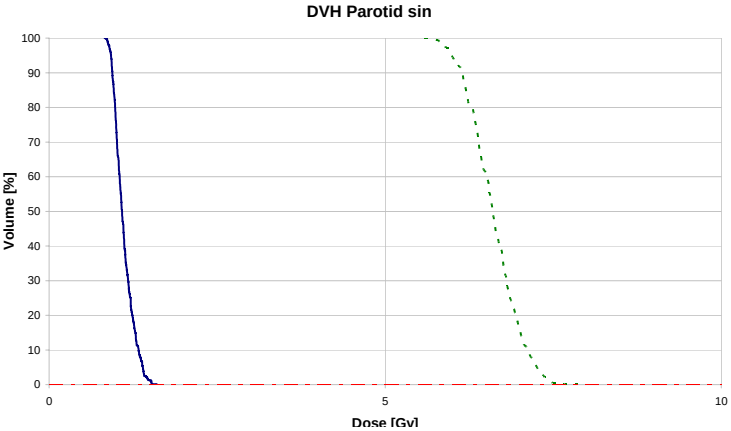

Figure 14.61 Case 3.2, DVH parotid sin

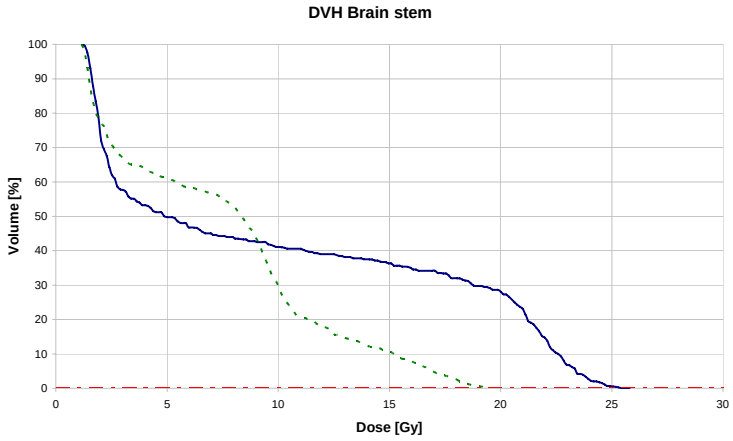

Figure 14.62 Case 3.2, DVH brain stem

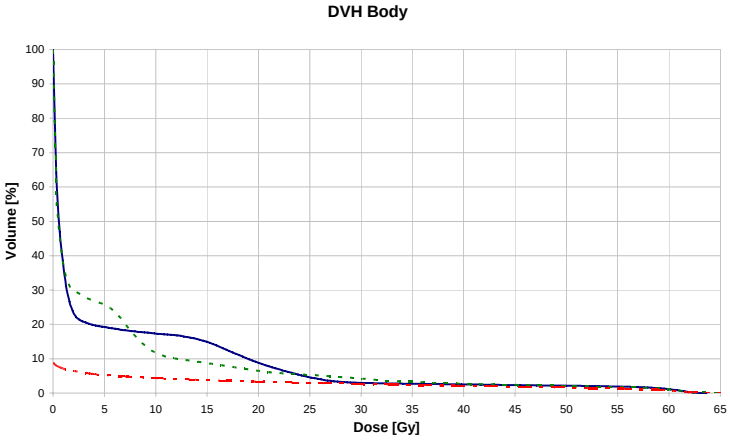

Figure 14.63 Case 3.2, DVH irradiated body

15 Appendix II

15.1.1 Case 1.1, breast carcinoma with no affected nodes

Table 15.1 CTV mammary carcinoma stage I and II

CTV	D_{max} [Gy]	D_{min} [Gy]	$D_{average}$ [Gy]
Conventional	53.3	47.3	49.9
IMXT 4 fields	53.1	49.8	51.5
IMXT 9 fields	53.4	48.8	50.6
IMPT 2 fields	53.0	47.0	51.0

Table 15.2 PTV mammary carcinoma stage I and II

PTV	D_{max} [Gy]	D_{min} [Gy]	$D_{average}$ [Gy]
Conventional	55.7	44.4	49.8
IMXT 4 fields	55.4	43.5	51.3
IMXT 9 fields	56.0	46.4	51.0
IMPT 2 fields	53.8	42.2	51.1

Table 15.3 Entire body mammary carcinoma stage I and II

Body	D_{max} [Gy]	D_{min} [Gy]	$D_{average}$ [Gy]
Conventional	56.4	0.0	3.9
IMXT 4 fields	58.8	0.0	4.9
IMXT 9 fields	57.7	0.0	11.2
IMPT 2 fields	53.8	0.0	3.3

Table 15.4 Right lung mammary carcinoma stage I and II

Right lung	D_{max} [Gy]	D_{min} [Gy]	$D_{average}$ [Gy]
Conventional	2.5	0.0	0.4
IMXT 4 fields	12.2	0.1	0.7
IMXT 9 fields	21.1	0.5	10.0
IMPT 2 fields	12.7	0.0	0.0

Table 15.5 Left lung mammary carcinoma stage I and II

Left lung	D_{max} [Gy]	D_{min} [Gy]	$D_{average}$ [Gy]
Conventional	52.1	0.3	5.6
IMXT 4 fields	58.8	0.3	9.2
IMXT 9 fields	57.0	0.6	25.5
IMPT 2 fields	52.2	0.0	4.0

Table 15.6 Heart mammary carcinoma stage I and II

Heart	D_{max} [Gy]	D_{min} [Gy]	$D_{average}$ [Gy]
Conventional	45.5	0.5	1.5
IMXT 4 fields	36.5	0.6	3.7
IMXT 9 fields	29.2	7.4	15.1
IMPT 2 fields	38.0	0.0	0.4

15.1.2 Case 1.2, breast carcinoma with affected nodes

Table 15.7 CTV mammary carcinoma with involved lymph nodes

CTV	D_{max} [Gy]	D_{min} [Gy]	$D_{average}$ [Gy]
Conventional	52.6	47.6	50.1
IMRT 3 fields	52.4	49.3	50.9
IMXT 9 fields	53.7	48.1	50.8
IMPT 2 fields	53.3	48.2	51.0

Table 15.8 PTV mammary carcinoma with involved lymph nodes

PTV	D_{max} [Gy]	D_{min} [Gy]	$D_{average}$ [Gy]
Conventional	57.4	42.8	50.3
IMRT 3 fields	60.2	36.6	51.2
IMXT 9 fields	59.3	43.6	51.4
IMPT 2 fields	54.3	33.9	51.1

Table 15.9 Entire body mammary carcinoma with involved lymph nodes

Body	D_{max} [Gy]	D_{min} [Gy]	$D_{average}$ [Gy]
Conventional	57.7	0.0	7.5
IMRT 3 fields	60.2	0.0	8.8
IMXT 9 fields	59.3	0.0	11.3
IMPT 2 fields	58.0	0.0	5.3

Table 15.10 Heart mammary carcinoma with involved lymph nodes

Heart	D_{max} [Gy]	D_{min} [Gy]	$D_{average}$ [Gy]
Conventional	48.6	0.6	2.5
IMRT 3 fields	22.5	0.6	6.5
IMXT 9 fields	20.4	1.3	6.3
IMPT 2 fields	30.6	0.0	0.2

Table 15.11 Left lung mammary carcinoma with involved lymph nodes

Left lung	D_{max} [Gy]	D_{min} [Gy]	$D_{average}$ [Gy]
Conventional	53.8	0.5	13.4
IMRT 3 fields	53.5	1.2	16.8
IMXT 9 fields	53.3	2.1	15.1
IMPT 2 fields	53.3	0.0	5.6

Table 15.12 Right lung mammary carcinoma with involved lymph nodes

Right lung	D_{max} [Gy]	D_{min} [Gy]	$D_{average}$ [Gy]
Conventional	3.2	0.0	0.6
IMRT 3 fields	2.7	0.2	0.7
IMXT 9 fields	27.6	0.8	7.3
IMPT 2 fields	14.7	0.0	0.0

Table 15.13 PRV medulla mammary carcinoma with involved lymph nodes

PRV medulla	D_{max} [Gy]	D_{min} [Gy]	$D_{average}$ [Gy]
Conventional	3.6	1.2	2.0
IMRT 3 fields	3.2	1.1	1.9
IMXT 9 fields	7.1	1.8	3.3
IMPT 2 fields	10.2	0.0	1.1

15.1.3 Case 1.3 breast carcinoma after radical mastectomy

Table 15.14 CTV, mammary carcinoma after radical mastectomy

CTV	D_{max} [Gy]	D_{min} [Gy]	$D_{average}$ [Gy]
Conventional	52.5	49.8	50.8
IMXT 4 fields	53.9	47.7	50.7
IMXT 9 fields	54.5	44.5	50.3
IMPT 3 fields	53.4	48.8	51.0

Table 15.15 PTV, mammary carcinoma after radical mastectomy

PTV	D_{max} [Gy]	D_{min} [Gy]	$D_{average}$ [Gy]
Conventional	56.2	42.9	50.5
IMXT 4 fields	61.1	32.3	50.7
IMXT 9 fields	62.8	34.6	50.7
IMPT 3 fields	55.8	28.3	51.1

Table 15.16 Entire body, mammary carcinoma after radical mastectomy

Body	D_{max} [Gy]	D_{min} [Gy]	$D_{average}$ [Gy]
Conventional	61.7	0.0	5.1
IMXT 4 fields	68.1	0.0	7.7
IMXT 9 fields	76.1	0.0	9.8
IMPT 3 fields	57.5	0.0	3.3

Table 15.17 Heart, mammary carcinoma after radical mastectomy

Heart	D_{max} [Gy]	D_{min} [Gy]	$D_{average}$ [Gy]
Conventional	48.9	0.7	3.1
IMXT 4 fields	16.0	1.4	7.3
IMXT 9 fields	9.7	1.4	3.7
IMPT 3 fields	19.1	0.0	1.6

Table 15.18 Left lung, mammary carcinoma after radical mastectomy

Left lung	D_{max} [Gy]	D_{min} [Gy]	$D_{average}$ [Gy]
Conventional	54.1	0.5	12.0
IMXT 4 fields	55.2	1.8	17.7
IMXT 9 fields	55.2	1.7	13.5
IMPT 3 fields	52.9	0.0	5.0

Table 15.19 Right lung, mammary carcinoma after radical mastectomy

Right lung	D_{max} [Gy]	D_{min} [Gy]	$D_{average}$ [Gy]
Conventional	3.5	0.0	0.6
IMXT 4 fields	10.2	0.2	1.6
IMXT 9 fields	11.3	0.5	1.6
IMPT 3 fields	14.0	0.0	0.1

Table 15.20 PRV medulla, mammary carcinoma after radical mastectomy

PRV medulla	D_{max} [Gy]	D_{min} [Gy]	$D_{average}$ [Gy]
Conventional	3.1	1.1	2.1
IMXT 4 fields	8.9	2.3	7.0
IMXT 9 fields	5.6	1.3	2.4
IMPT 3 fields	2.5	0.0	0.1

15.1.4 Case 2.1, prostate cancer

Table 15.21 Prostate, case 2.1 prostate cancer

Prostate	D_{max} [Gy]	D_{min} [Gy]	$D_{average}$ [Gy]
Conventional	79.2	72.6	77.6
IMXT 7 fields	79.2	73.6	77.1
IMPT 2 fields	81.7	76.0	78.6

Table 15.22 Prostate 4/6 mm, case 2.1 prostate cancer

Prostate 4/6 mm	D_{max} [Gy]	D_{min} [Gy]	$D_{average}$ [Gy]
Conventional	79.3	72.6	77.6
IMXT 7 fields	80.0	73.6	77.4
IMPT 2 fields	82.6	75.6	79.1

Table 15.23 Prostate + 1cm, case 2.1 prostate cancer

Prostate + 1cm	D_{max} [Gy]	D_{min} [Gy]	D_{averge} [Gy]
Conventional	79.6	72.6	77.1
IMXT 7 fields	80.0	73.2	77.4
IMPT 2 fields	83.3	67.2	79.0

Table 15.24 Entire body, case 2.1 prostate cancer

Body	D_{max} [Gy]	D_{min} [Gy]	$D_{average}$ [Gy]
Conventional	79.6	0.0	10.6
IMXT 7 fields	80.0	0.0	12.0
IMPT 2 fields	83.9	0.0	7.2

Table 15.25 Bladder, case 2.1 prostate cancer

Bladder	D_{max} [Gy]	D_{min} [Gy]	$D_{average}$ [Gy]
Conventional	79.6	2.7	49.7
IMXT 7 fields	80.0	3.3	50.5
IMPT 2 fields	83.3	0.0	48.6

Table 15.26 Rectum, case 2.1 prostate cancer

Rectum	D_{max} [Gy]	D_{min} [Gy]	$D_{average}$ [Gy]
Conventional	74.5	1.7	40.3
IMXT 7 fields	78.7	1.9	47.6
IMPT 2 fields	82.1	0.0	33.6

Table 15.27 Right capu, case 2.1 prostate cancer

Right caput	D_{max} [Gy]	D_{min} [Gy]	$D_{average}$ [Gy]
Conventional	36.8	12.2	32.4
IMXT 7 fields	37.6	7.9	22.4
IMPT 2 fields	40.9	12.9	34.2

Table 15.28 Left caput, case 2.1 prostate cancer

Left caput	D_{max} [Gy]	D_{min} [Gy]	$D_{average}$ [Gy]
Conventional	35.4	17.1	33.0
IMXT 7 fields	38.2	8.0	23.2
IMPT 2 fields	39.1	11.7	32.9

15.1.5 Case 2.2, prostate cancer

Table 15.29 Prostate, case 2.2 prostate cancer

Prostate	D_{max} [Gy]	D_{min} [Gy]	$D_{average}$ [Gy]
Conventional	79.0	76.0	77.5
IMXT 4 fields	82.3	78.1	79.7
IMPT 2 fields	81.5	76.8	78.8

Table 15.30 Prostate boost, case 2.2 prostate cancer

Prostate boost	D_{max} [Gy]	D_{min} [Gy]	$D_{average}$ [Gy]
Conventional	79.3	76.0	77.5
IMXT 4 fields	82.3	77.7	79.7
IMPT 2 fields	82.8	75.8	79.1

Table 15.31 Prostate + 1cm, case 2.2 prostate cancer

Prostate + 1cm	D_{max} [Gy]	D_{min} [Gy]	$D_{average}$ [Gy]
Conventional	79.7	73.8	77.2
IMXT 4 fields	82.3	73.3	79.3
IMPT 2 fields	83.0	67.0	79.0

Table 15.32 Entire body, case 2.2 prostate cancer

Body	D_{max} [Gy]	D_{min} [Gy]	$D_{average}$ [Gy]
Conventional	79.7	0.0	11.4
IMXT 4 fields	82.3	0.0	14.9
IMPT 2 fields	83.0	0.0	7.7

Table 15.33 Bladder, case 2.2 prostate cancer

Bladder	D_{max} [Gy]	D_{min} [Gy]	$D_{average}$ [Gy]
Conventional	79.5	3.4	52.2
IMXT 4 fields	80.3	3.2	48.2
IMPT 2 fields	82.8	0.1	38.2

Table 15.34 Rectum, case 2.2 prostate cancer

Rectum	D_{max} [Gy]	D_{min} [Gy]	$D_{average}$ [Gy]
Conventional	76.4	6.6	42.3
IMXT 4 fields	81.0	3.4	47.3
IMPT 2 fields	83.0	0.0	34.4

Table 15.35 Right caput, case 2.2 prostate cancer

Right caput	D_{max} [Gy]	D_{min} [Gy]	$D_{average}$ [Gy]
Conventional	38.2	8.1	30.7
IMXT 4 fields	50.2	6.5	20.9
IMPT 2 fields	44.5	5.3	34.5

Table 15.36 Left caput, case 2.2 prostate cancer

Left caput	D_{max} [Gy]	D_{min} [Gy]	$D_{average}$ [Gy]
Conventional	37.0	7.5	28.8
IMXT 4 fields	51.3	3.6	29.1
IMPT 2 fields	38.9	5.6	30.8

15.1.6 Case 3.1, parotid cancer

Table 15.37 PTV, case 3.1 cancer of the parotid

PTV	D_{max} [Gy]	D_{min} [Gy]	$D_{average}$ [Gy]
Conventional.	72.4	61.5	69.1
IMXT 4 fields	74.2	64.0	69.6
IMPT 3 fields	72.8	51.1	69.1

Table 15.38 Entire body, case 3.1 cancer of the parotid

Body	D_{max} [Gy]	D_{min} [Gy]	$D_{average}$ [Gy]
Conventional.	72.9	0.0	7.5
IMXT 4 fields	75.9	0.0	7.0
IMPT 3 fields	72.8	0.0	3.3

Table 15.39 Left lung, case 3.1 cancer of the parotid

Left lung	D_{max} [Gy]	D_{min} [Gy]	$D_{average}$ [Gy]
Conventional.	0.6	0.4	0.5
IMXT 4 fields	0.5	0.2	0.3
IMPT 3 fields	0.0	0.0	0.0

Table 15.40 Right lung, case 3.1 cancer of the parotid

Right lung	D_{max} [Gy]	D_{min} [Gy]	$D_{average}$ [Gy]
Conventional.	0.5	0.3	0.4
IMXT 4 fields	0.4	0.2	0.3
IMPT 3 fields	0.0	0.0	0.0

Table 15.41 Medulla, case 3.1 cancer of the parotid

Medulla	D_{max} [Gy]	D_{min} [Gy]	$D_{average}$ [Gy]
Conventional.	29.2	2.3	23.0
IMXT 4 fields	30.3	2.1	16.5
IMPT 3 fields	26.2	0.0	1.2

Table 15.42 Vertebrae, case 3.1 cancer of the parotid

Vertebrae	D_{max} [Gy]	D_{min} [Gy]	$D_{average}$ [Gy]
Conventional.	63.7	2.4	29.4
IMXT 4 fields	67.9	2.0	24.3
IMPT 3 fields	69.2	0.0	7.5

Table 15.43 Left eye, case 3.1 cancer of the parotid

Left eye	D_{max} [Gy]	D_{min} [Gy]	$D_{average}$ [Gy]
Conventional.	3.0	1.6	2.1
IMXT 4 fields	6.5	1.3	2.2
IMPT 3 fields	2.1	0.0	0.1

Table 15.44 Right eye, case 3.1 cancer of the parotid

Right eye	D_{max} [Gy]	D_{min} [Gy]	$D_{average}$ [Gy]
Conventional.	5.8	1.3	1.9
IMXT 4 fields	8.9	1.1	2.6
IMPT 3 fields	0.0	0.0	0.0

Table 15.45 Brain, case 3.1 cancer of the parotid

Brain	D_{max} [Gy]	D_{min} [Gy]	$D_{average}$ [Gy]
Conventional.	68.6	0.6	7.7
IMXT 4 fields	44.0	0.0	5.7
IMPT 3 fields	51.9	0.0	0.6

Table 15.46 Optical nerve dx, case 3.1 cancer of the parotid

Optical nerve dx	D_{max} [Gy]	D_{min} [Gy]	$D_{average}$ [Gy]
Conventional.			
IMXT 4 fields	2.1	1.8	2.0
IMPT 3 fields	0.0	0.0	0.0

Table 15.47 Optical nerve sin, case 3.1 cancer of the parotid

Optical nerve sin	D_{max} [Gy]	D_{min} [Gy]	$D_{average}$ [Gy]
Conventional.			
IMXT 4 fields	2.6	2.6	2.6
IMPT 3 fields	0.2	0.0	0.0

Table 15.48 Chiasm, case 3.1 cancer of the parotid

Chiasm	D_{max} [Gy]	D_{min} [Gy]	$D_{average}$ [Gy]
Conventional.	2.7	2.7	2.7
IMXT 4 fields	2.5	2.4	2.5
IMPT 3 fields	0.0	0.0	0.0

Table 15.49 Inner ear dx, case 3.1 cancer of the parotid

Inner ear dx	D_{max} [Gy]	D_{min} [Gy]	$D_{average}$ [Gy]
Conventional.	4.0	2.5	3.2
IMXT 4 fields	12.5	2.8	9.3
IMPT 3 fields	0.0	0.0	0.0

Table 15.50 Inner ear sin, case 3.1 cancer of the parotid

Inner ear sin	D_{max} [Gy]	D_{min} [Gy]	$D_{average}$ [Gy]
Conventional.	63.3	53.6	60.8
IMXT 4 fields	59.3	20.8	43.1
IMPT 3 fields	69.8	4.8	31.7

Table 15.51 Brain stem, case 3.1 cancer of the parotid

Brain stem	D_{max} [Gy]	D_{min} [Gy]	$D_{average}$ [Gy]
Conventional.	27.5	2.8	14.7
IMXT 4 fields	26.3	2.9	13.5
IMPT 3 fields	8.7	0.0	0.2

Table 15.52 Oral cavity, case 3.1 cancer of the parotid

Oral cavity	D_{max} [Gy]	D_{min} [Gy]	$D_{average}$ [Gy]
Conventional.	64.3	16.2	25.5
IMXT 4 fields	63.5	12.6	24.6
IMPT 3 fields	55.3	0.0	2.8

Table 15.53 Mandible, case 3.1 cancer of the parotid

Mandible	D_{max} [Gy]	D_{min} [Gy]	$D_{average}$ [Gy]
Conventional.	70.7	3.6	25.8
IMXT 4 fields	70.6	3.1	23.4
IMPT 3 fields	70.4	0.0	11.2

Table 15.54 Mandible joint sin, case 3.1 cancer of the parotid

Mandible joint sin	D_{max} [Gy]	D_{min} [Gy]	$D_{average}$ [Gy]
Conventional.	69.8	64.0	67.2
IMXT 4 fields	71.5	43.7	64.7
IMPT 3 fields	70.7	32.6	64.1

Table 15.55 Brain stem porv, case 3.1 cancer of the parotid

Brain stem PRV	D_{max} [Gy]	D_{min} [Gy]	$D_{average}$ [Gy]
Conventional.	28.7	2.5	14.8
IMXT 4 fields	27.5	2.6	13.4
IMPT 3 fields	20.2	0.0	0.4

Table 15.56 Medulla porv, case 3.1 cancer of the parotid

Medulla PRV	D_{max} [Gy]	D_{min} [Gy]	$D_{average}$ [Gy]
Conventional.	38.4	2.3	22.2
IMXT 4 fields	46.9	2.0	16.8
IMPT 3 fields	41.5	0.0	1.7

Table 15.57 Parotid dx, case 3.1 cancer of the parotid

Parotid dx	D_{max} [Gy]	D_{min} [Gy]	$D_{average}$ [Gy]
Conventional.	3.47	1.78	2.36
IMXT 4 fields	11.37	1.82	4.56
IMPT 3 fields	0.00	0.00	0.00

15.1.7 Case 3.2, parotid cancer

Equation 15.58 PTV, case 3.2 cancer of the parotid

PTV	D_{max} [Gy]	D_{min} [Gy]	$D_{average}$ [Gy
Conventional.	63.2	51.0	61.0
IMXT 5 fields	65.5	58.5	61.3
IMPT 2 fields	68.1	20.0	61.0

Equation 15.59 Entire body, case 3.2 cancer of the parotid

Body	D_{max} [Gy]	D_{min} [Gy]	$D_{average}$ [Gy
Conventional.	63.7	0.0	5.1
IMXT 5 fields	65.5	0.0	4.9
IMPT 2 fields	68.1	0.0	1.8

Equation 15.60 Left eye, case 3.2 cancer of the parotid

Left eye	D_{max} [Gy]	D_{min} [Gy]	$D_{average}$ [Gy
Conventional.	1.3	0.7	0.9
IMXT 5 fields	1.1	0.6	0.7
IMPT 2 fields	0.0	0.0	0.0

Equation 15.61 Right eye, case 3.2 cancer of the parotid

Right eye	D_{max} [Gy]	D_{min} [Gy]	$D_{average}$ [Gy
Conventional.	1.5	0.7	1.0
IMXT 5 fields	1.5	0.6	1.0
IMPT 2 fields	0.4	0.0	0.0

Equation 15.62 Medulla, case 3.2 cancer of the parotid

Medulla	D_{max} [Gy]	D_{min} [Gy]	$D_{average}$ [Gy
Conventional.	28.7	1.4	21.2
IMXT 5 fields	21.3	1.2	14.9
IMPT 2 fields	0.0	0.0	0.0

Equation 15.63 Vertebrae, case 3.2 cancer of the parotid

Vertebrae	D_{max} [Gy]	D_{min} [Gy]	$D_{average}$ [Gy
Conventional.	47.5	0.8	9.6
IMXT 5 fields	43.8	0.7	11.1
IMPT 2 fields	3.8	0.0	0.0

Equation 15.64 Brain, case 3.2 cancer of the parotid

Brain	D_{max} [Gy]	D_{min} [Gy]	$D_{average}$ [Gy
Conventional.	26.2	0.4	5.6
IMXT 5 fields	38.0	0.5	4.0
IMPT 2 fields	38.9	0.0	0.3

Equation 15.65 Optical nerve dx, case 3.2 cancer of the parotid

Optical nerve dx	D_{max} [Gy]	D_{min} [Gy]	$D_{average}$ [Gy
Conventional.	1.5	1.4	1.4
IMXT 5 fields	1.3	1.2	1.3
IMPT 2 fields	0.0	0.0	0.0

Equation 15.66 Optical nerve sin, case 3.2 cancer of the parotid

Optical nerve sin	D_{max} [Gy]	D_{min} [Gy]	$D_{average}$ [Gy]
Conventional.	0.9	0.9	0.8
IMXT 5 fields	0.9	0.8	0.9
IMPT 2 fields	0.0	0.0	0.0

Equation 15.67 Chiasm, case 3.2 cancer of the parotid

Chiasm	D_{max} [Gy]	D_{min} [Gy]	$D_{average}$ [Gy]
Conventional.	1.5	1.5	1.5
IMXT 5 fields	1.6	1.4	1.5
IMPT 2 fields	0.0	0.0	0.0

Equation 15.68 Inner ear dx, case 3.2 cancer of the parotid

Inner ear dx	D_{max} [Gy]	D_{min} [Gy]	$D_{average}$ [Gy]
Conventional.	32.9	26.0	28.5
IMXT 5 fields	37.1	18.4	24.8
IMPT 2 fields	25.8	0.0	4.1

Equation 15.691 Inner ear sin, case 3.2 cancer of the parotid

Inner ear sin	D_{max} [Gy]	D_{min} [Gy]	$D_{average}$ [Gy]
Conventional.	1.7	1.3	1.4
IMXT 5 fields	7.8	6.9	7.3
IMPT 2 fields	0.0	0.0	0.0

Equation 15.70 Oral cavity, case 3.2 cancer of the parotid

Oral cavity	D_{max} [Gy]	D_{min} [Gy]	$D_{average}$ [Gy]
Conventional.	26.7	2.3	19.5
IMXT 5 fields	30.0	5.1	11.4
IMPT 2 fields	11.2	0.0	0.1

Equation 15.71 Mandible, case 3.2 cancer of the parotid

Mandible	D_{max} [Gy]	D_{min} [Gy]	$D_{average}$ [Gy]
Conventional.	63.2	1.2	16.8
IMXT 5 fields	60.6	1.6	12.4
IMPT 2 fields	62.2	0.0	4.5

Equation 15.72 Mandible joint dx, case 3.2 cancer of the parotid

Mandible joint dx	D_{max} [Gy]	D_{min} [Gy]	$D_{average}$ [Gy
Conventional.	61.1	53.5	58.5
IMXT 5 fields	61.9	45.5	57.6
IMPT 2 fields	66.2	12.1	52.1

Equation 15.73 Parotid sin, case 3.2 cancer of the parotid

Parotid sin	D_{max} [Gy]	D_{min} [Gy]	$D_{average}$ [Gy
Conventional.	1.5	0.9	1.1
IMXT 5 fields	7.5	5.8	6.6
IMPT 2 fields	0.0	0.0	0.0

Equation 15.74 Medulla PRV, case 3.2 cancer of the parotid

Medulla PRV	D_{max} [Gy]	D_{min} [Gy]	$D_{average}$ [Gy
Conventional.	29.5	1.3	19.8
IMXT 5 fields	22.3	1.2	14.0
IMPT 2 fields	0.1	0.0	0.0

Equation 15.75 Brain stem, case 3.2 cancer of the parotid

Brain stem	D_{max} [Gy]	D_{min} [Gy]	$D_{average}$ [Gy]
Conventional.	25.3	1.3	10.0
IMXT 5 fields	19.3	1.2	7.5
IMPT 2 fields	0.0	0.0	0.0

Equation 15.76 Brain stem PRV, case 3.2 cancer of the parotid

Brain stem PRV	D_{max} [Gy]	D_{min} [Gy]	$D_{average}$ [Gy
Conventional.	25.8	1.3	10.6
IMXT 5 fields	20.3	1.2	7.7
IMPT 2 fields	0.0	0.0	0.0